AD A136 667 LIQUEFACTION POTENTIAL OF PROPOSED FILLS LOS ANGELES HARBOR APPENDIX D LOS ANGELES-LONG BEACH HARBORS(U) ARMY ENGINEER DISTRICT LOS ANGELES CA L A KNUPPEL 1974 1/2

UNCLASSIFIED F/G 8/13 NL

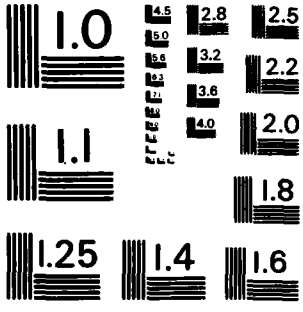

MICROCOPY RESOLUTION TEST CHART
NATIONAL BUREAU OF STANDARDS - 1963 - A

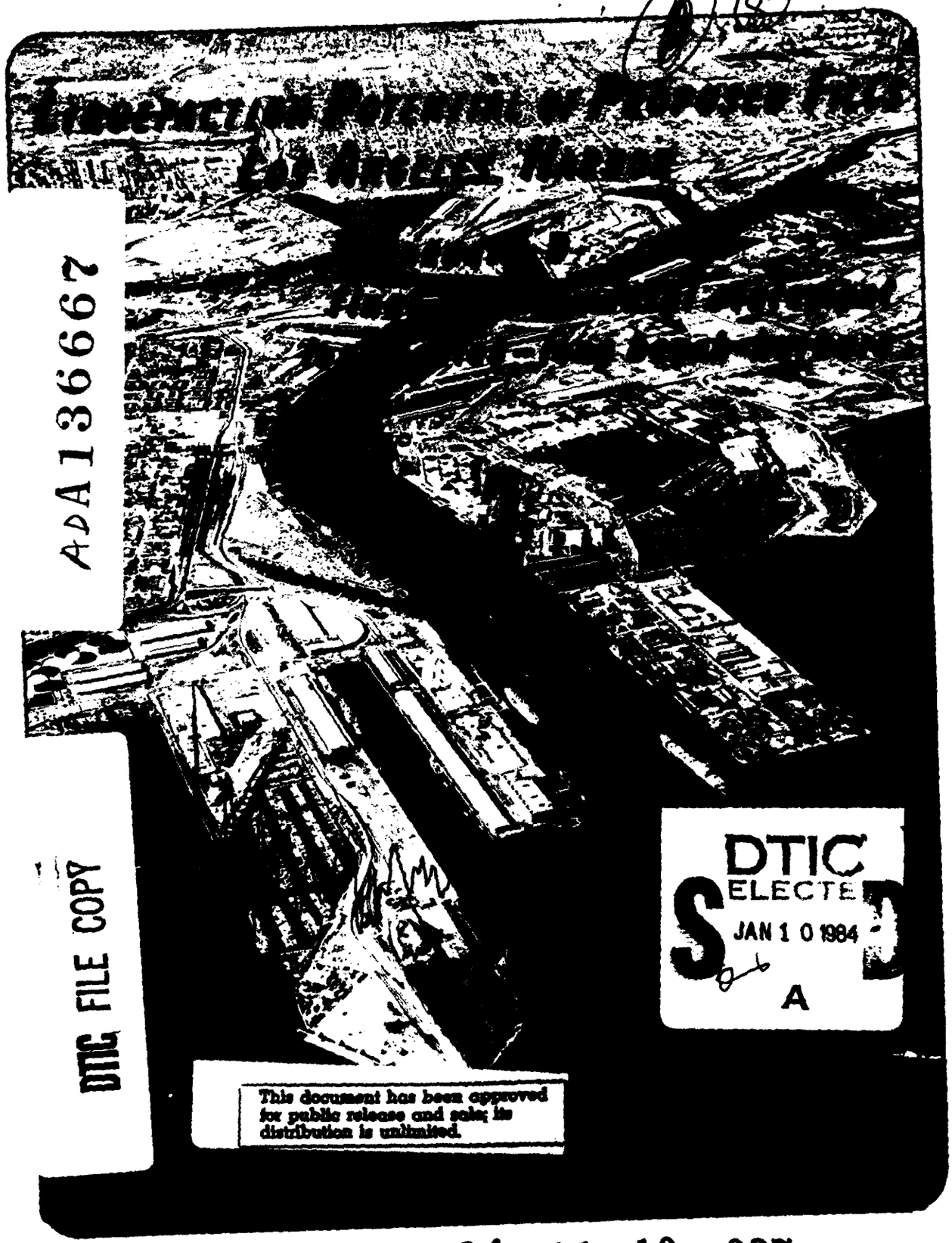

AD-A136667

DTIC FILE COPY

DTIC
ELECTE
JAN 10 1984
S D
A

This document has been approved for public release and sale; its distribution is unlimited.

84 01 10 037

REPORT DOCUMENTATION PAGE		READ INSTRUCTIONS BEFORE COMPLETING FORM
1. REPORT NUMBER	2. GOVT ACCESSION NO. AD-A136667	3. RECIPIENT'S CATALOG NUMBER
4. TITLE (and Subtitle) LIQUEFACTION POTENTIAL OF PROPOSED FILLS LOS ANGELES HARBOR APPENDIX D FINAL ENVIRONMENTAL STATEMENT LOS ANGELES-LONG BEACH HARBORS		5. TYPE OF REPORT & PERIOD COVERED 6. PERFORMING ORG. REPORT NUMBER
7. AUTHOR(s) LEE ALAN KNUPPEL		8. CONTRACT OR GRANT NUMBER(s)
9. PERFORMING ORGANIZATION NAME AND ADDRESS US ARMY CORPS OF ENGINEERS LOS ANGELES DISTRICT P.O. BOX 2711, LOS ANGELES, CA 90053		10. PROGRAM ELEMENT, PROJECT, TASK AREA & WORK UNIT NUMBERS
11. CONTROLLING OFFICE NAME AND ADDRESS US ARMY CORPS OF ENGINEERS LOS ANGELES DISTRICT P.O. BOX 2711, LOS ANGELES, CA 90053		12. REPORT DATE 1974 13. NUMBER OF PAGES
14. MONITORING AGENCY NAME & ADDRESS(if different from Controlling Office)		15. SECURITY CLASS. (of this report) UNCLASSIFIED 15a. DECLASSIFICATION/DOWNGRADING SCHEDULE

16. DISTRIBUTION STATEMENT (of this Report)

Approved for public release; distribution unlimited.

17. DISTRIBUTION STATEMENT (of the abstract entered in Block 20, if different from Report)

18. SUPPLEMENTARY NOTES

Copies are obtainable from the National Technical Information Services, Springfield, VA 22151

19. KEY WORDS (Continue on reverse side if necessary and identify by block number)

20. ABSTRACT (Continue on reverse side if necessary and identify by block number)

Consideration is being given by the Corps of Engineers to dredge the ship channels and turning basins in the Los Angeles Harbor and to hydraulically dispose of the dredged material in parts of the harbor where new land areas are desired. This thesis studies the stability of the porposed hydraulic fill under seismic stress conditions. The soil design parameters assumed, were based on available soil properties of existing hydraulic fills in the harbor area. Generally, these fills consist of materials similar to

those found in the proposed dredge area.

UNIVERSITY OF CALIFORNIA
Los Angeles

Liquefaction Potential of Proposed Fills Los Angeles Harbor

A thesis submitted in partial satisfaction of the requirements for the degree Master of Science in Engineering

by

Lee Alan Knuppel

1974

The thesis of Lee Alan Knuppel is approved.

Poul Lade

Poul V. Lade

C. Martin Duke

C. Martin Duke

Kenneth L. Lee

Kenneth L. Lee, Committee Chairman

University of California, Los Angeles

1974

DEDICATION

To the memory of:

Wesley F. Knuppel
Robert C. Kennedy

TABLE OF CONTENTS

TABLE OF CONTENTS (Continued)

TABLES

TABLES (Continued)

FIGURES

FIGURES (Continued)

FIGURES (Continued)

FIGURES (Continued)

PLATES

ACKNOWLEDGEMENTS

The author wishes to express his gratitude to the many people of the U.S. Army Corps of Engineers and the University of California who have helped in bringing this project to a successful completion.

Foremost among these is his major advisor Professor Kenneth L. Lee, who has provided continual guidance and encouragement over the past two years.

Thanks are also due to the other members of the author's committee, Professor C. Martin Duke and Professor Poul V. Lade, for their support and assistance.

Special thanks are due to Messrs. John Bird, Chief, Foundations and Materials Branch, Lawrence Lauro, Chief, Soil Design Section, Samuel Ackerman, Chief, Navigation Section and Hugh Converse, Los Angeles Harbor Project Engineer, of the Los Angeles District, U.S. Army Corps of Engineers. Without their support, this project could not have been undertaken.

The assistance of Lawrence Anderson and Elmer Guillermo, Engineering Division, Port of Los Angeles in obtaining the extensive amounts of soil data used in this thesis is gratefully acknowledged.

The author would also like to thank Miss Agnes Matosian for her help in the preparation of the many plates and figures in this thesis.

Finally, the author would like to express his profound gratitude to his wife, Kathleen, whose support and understanding has made this thesis possible at the expense of delays in her own education and graduation.

ABSTRACT OF THE THESIS

Liquefaction Potential of Proposed Fills
Los Angeles Harbor
by
Lee Alan Knuppel

Master of Science in Engineering
University of California, Los Angeles, 1974

Professor Kenneth L. Lee, Chairman

Consideration is being given by the Corps of Engineers to dredge the ship channels and turning basins in the Los Angeles Harbor and to hydraulically dispose of the dredged material in parts of the harbor where new land areas are desired.

This thesis studies the stability of the proposed hydraulic fill under seismic stress conditions. The soil design parameters assumed, were based on available soil properties of existing hydraulic fills in the harbor area. Generally, these fills consist of materials similar to those found in the proposed dredge area.

The maximum probable design earthquake was determined to be a magnitude 7.0 occuring on the Newport-Inglewood Fault with an epicentral distance of approximately 6.5 miles from the site. The maximum rock acceleration at the site for this earthquake would be approximately 0.5g.

The proposed fill response to seismic excitation was evaluated using the motions developed by two highly probable earthquakes that may be expected to affect the site. These earthquakes were a magnitude 5.25 occuring on the Newport-Inglewood Fault with a maximum site rock acceleration of 0.11g, and a magnitude 8.25 occuring on the San Andreas Fault with a maximum site rock acceleration of 0.13g. These two probable earthquakes have lower site rock accelerations than the maximum probable design

earthquake. Since the studies conducted herein showed that the fill would not be stable under these earthquakes, the effect of even stronger shaking developed by the maximum probable earthquake was not analyzed.

The proposed fill was also analyzed assuming that a modified construction procedure could be developed allowing the fill to be constructed at a higher density than is typical of existing hydraulic fills in the area.

The results of the laboratory testing and dynamic analysis indicate that the proposed fill, constructed by present procedures, would liquefy when subjected to the stresses of the earthquakes studied. If the same materials were to be placed at the higher density, corresponding to the modified placement procedure, it would be stable against the stresses induced by the magnitude 5.25 earthquake, but would liquefy under the higher stress levels of the magnitude 8.25 earthquake and the magnitude 7.0 maximum probable design earthquake.

CHAPTER 1

INTRODUCTION

Purpose and Scope

Consideration is being given by the Corps of Engineers to dredge the ship channels and turning basins in the Los Angeles Harbor and to hydraulically dispose of the dredged material in parts of the harbor where new land areas are desired. The exact plans for the proposed project have not been finalized, but the recommended dimensions of the waterways and proposed disposal areas are presented in figure 1-1.

The purpose of this thesis is to analyze the liquefaction potential of the proposed hydraulic fill under various magnitudes of seismic activity. To conduct this study it was necessary to gather all the available soil data on the proposed dredging areas, fill site, and several existing hydraulic fills of various soil compositions, in order to establish soil parameters which could be expected to exist in the future hydraulic fill.

This report presents the available harbor geologic and soil data, static and dynamic soil parameters and the liquefaction potential of the proposed fill.

Sources of Information

Information on the geology and soils in the Los Angeles Harbor was obtained from the Los Angeles Harbor Department, Southern California Gas Company, Los Angeles District Corps of Engineers, and various private engineering companies. The cyclic loading data was obtained by direct testing at the University of California, Los Angeles (UCLA) soils laboratory.

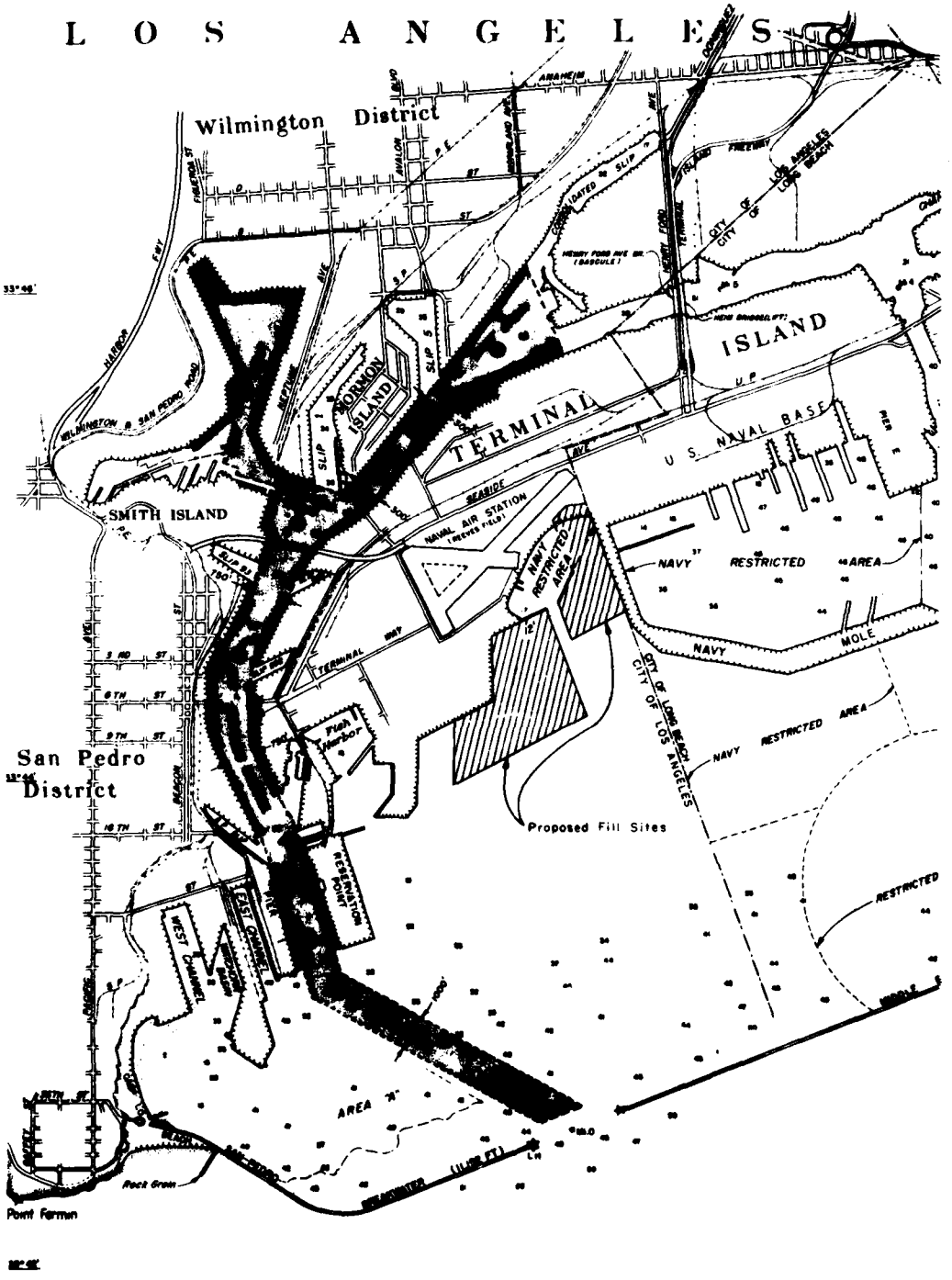

FIG. 1-1 LOCATION OF PROPOSED DREDGE AND FILL AREAS IN THE LOS ANGELES HARBOR

Background

The Los Angeles Harbor occupies a major part of the San Pedro Bay. It is located approximately 25 miles south of the civic center of Los Angeles and with reference to other California harbors, it is 370 nautical miles southeast of San Francisco Bay and 95 nautical miles northwest of San Diego Bay. In its natural state, San Pedro Bay was a half moon shaped body of water protected on the west by the Palos Verdes Hills and entirely exposed on the southeast.

The manmade harbor is protected by stone breakwaters extending eastward from Point Fermin. There is a 1,000 foot-wide entrance channel to the Los Angeles Harbor and a 800 foot-wide entrance channel to the Long Beach Harbor. Various small islands, which once clustered about the estuarial complex of tidal sloughs, lagoons and marshlands in the western part of the bay, have been obliterated by the intermittent dredging and filling operations which have created the existing inner harbor channels and parts of Terminal Island.

The Los Angeles inner harbor is still the disposal point for floodwaters drained from an 80 square mile area by the Dominquez Channel. Because of the urbanized nature of the drainage area and the fact that the channel itself is concrete lined, large amounts of sediment are no longer deposited in the various basins and channels of the harbor complex. In the outer harbor, some parts of the original San Pedro Bay sea floor may still remain in its natural state. Much of the floor of the main channel and basins, however, are covered with a layer of organic and non-organic silt and clay with varing degrees of chemical pollution. The approximate known distribution of the healthy and polluted zones are shown in figure 1-2. It is this degree of pollution in the channels and basins which will determine the order that the materials will be dredged and placed at the proposed fill site to meet Los Angeles Regional Water Quality Control Board requirements (ref. 1.) For the purposes of this report, the area to be dredged is divided into three subareas based on the degree of pollution.

The area extending from the breakwater to the turning basin will be referred to as the main channel and has the least degree of bottom pollution. The areas extending from the turning basin to the back of the east and west basins will be referred to as the east and west basins respectively. These latter two areas have a somewhat higher degree of pollution than the main channel. The three areas are discussed in more detail in Chapter 2.

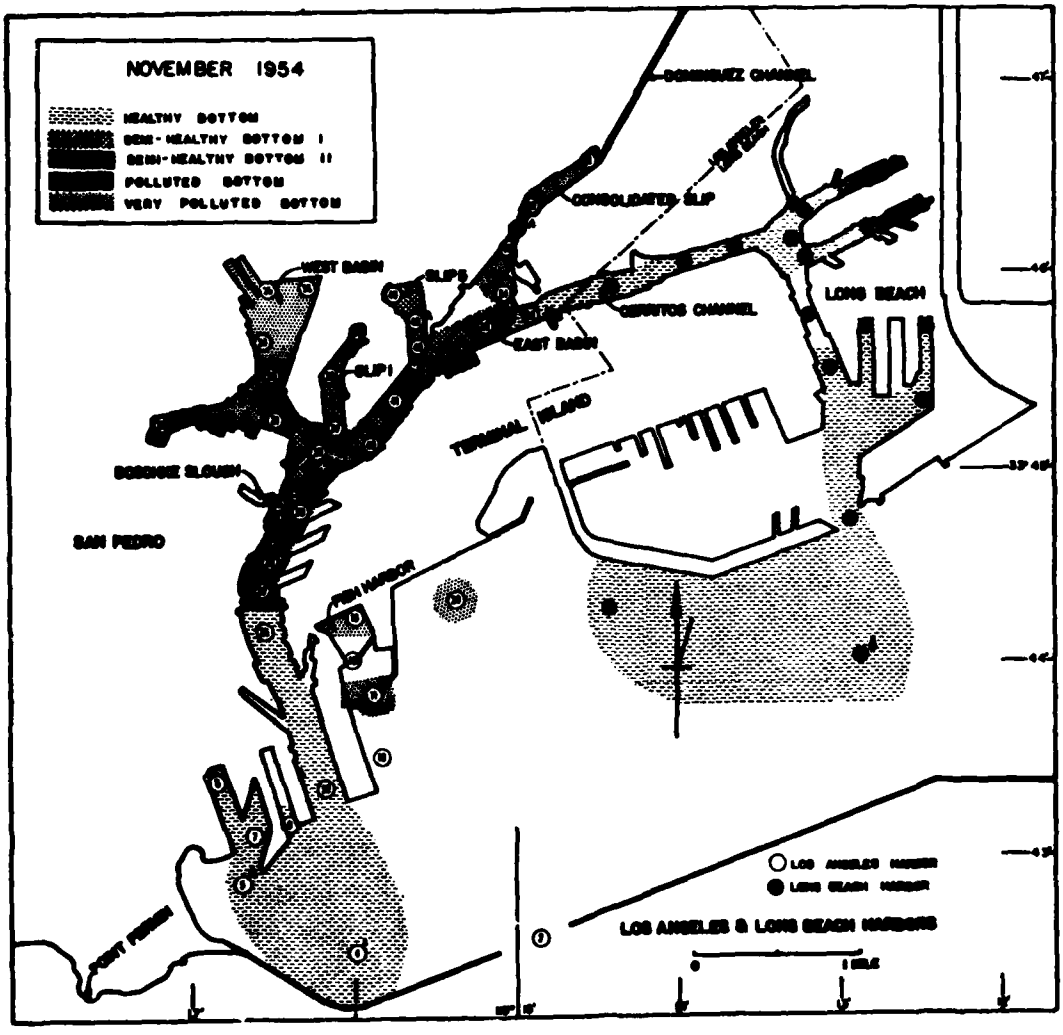

FIG. 1-2

Biological characterization of the harbor bottom indicating areas of healthy and polluted bottom sediments. The present condition of the West Basin bottom sediment is not known due to a dredging project conducted in 1964. However, the condition of most bottom sediments has greatly improved since 1954 when the last detailed survey was made. The circled numbers indicate station locations where water samples have been collected monthly since 1952, (1).

CHAPTER 2

GEOLOGY AND SOILS

Previous Explorations

The soil explorations in the Los Angeles Harbor Main Channel, east and west basins have been conducted primarily by the Corps of Engineers, Port of Los Angeles (prior to channel dredging) and by several private engineering firms conducting environmental studies and subsurface investigations for wharfs or piers.

The hydraulic fill areas studied were investigated by private engineering firms which had conducted foundations investigations for the Port of Los Angeles and U.S. Coast Guard. The three sites, identified on plate 2-1, were selected for analysis in this report primarily because they contained materials similar to those found in the areas to be dredged and a large amount of soil data was available.

The soil data, for the future dredging areas and existing hydraulic fill areas, was obtained from 148 test holes and core holes and consists of soil logs, grain size distribution curves, Atterberg Limits, dry densities, moisture contents, static cone resistance values, shear strengths, water table locations and depth soundings. The locations of these testholes are shown on plates 2-1 and 2-2.

The geology of the harbor area was established from references 2, 3, 4 and 5 which contain good geological studies of the Los Angeles Basin. These references were used to establish a detailed stratigraphic column and a geologic cross section of the proposed fill site. The locations of the stratigraphic column and cross section are shown on plate 2-1.

Quality of Data

The available soil data was readily usable, in that most firms classified soil in accordance with the Unified Soil Classification System, and usually provide typical soil gradation curves for materials in a given area. All data was referenced with respect to mean lower low water (MLLW).

There was no way to check on the validity of an individual soil report, but when comparing various reports of a given area, good correlations were indicated regarding the type of soils and the soil parameters. It should be noted that standard penetration tests were not conducted for most projects and that only limited data were available on the Atterberg Limits of the fine grained soils.

The geologic information on the Los Angeles Harbor area, most of which was extracted from published and nonpublished geologic reports on the Wilmington Oil Fields, exhibited a high degree of correlation regardless of its source. However, there is a lack of detailed geologic information on the actual areas under study and, for this reason, a small degree of error may have been introduced into the geologic cross section as a result of projecting the depths of the geologic formations to the proposed fill site.

General Geology

The Los Angeles Basin is divided into four subbasins or "blocks" on the basis of rock type and major zones of faulting in the basement complex. These four subbasins are informally designated the southwestern, northwestern, central and northeastern blocks. This report is concerned only with the southwestern block in which the harbor area is located. The surface of this southwestern block is a low flat plain that extends from the Santa Monica-Hollywood fault zone south to Long Beach with little topographic relief except for the Palos Verdes Hills. The Newport-Inglewood Fault Zone extends from the northwest to the southeast along the inland margins of the plain (refs. 2, 5). The southwestern block is an exposed part of the much more extensive continental shelf, most of which is beneath the Pacific Ocean.

The Los Angeles harbor is bisected by the major northwest-trending Palos Verdes Fault Zone. The abrupt changes in configuration of the basement rock surface, as well as changes in the lithology and thickness of middle miocene, upper miocene and pliocene sedimentary rock units is problably the result of right-lateral strike-slip movement along the fault. The faulting along this zone probably occured in the middle to late Pleistocene age (ref. 5). After the anticlinal folding, the vicinity of the present Palos Verdes Hills was uplifted at least 1,300 feet and the down thrown block depressed approximately 500 to 11,000 feet relative to present sea level (ref. 5). A geologic cross section taken through the proposed fill site and crossing the Palos Verdes Fault Zone is shown on plate 2-3.

Stratigraphy of the Harbor Area

The following is a brief discussion of the various rock formations shown in the stratigraphic column in figure 2-1.

Basement Rocks. The basement rock in the harbor area is Catalina Schist. This Cataline Schist is exposed on the mainland only in a small area of the Palos Verdes Hills where it is chiefly fine-grained chlorite-quartz schist and blue glaucophane or crossite-bearing schist. Neither the age nor the stratigraphic position of the schist is known (ref. 5).

Paleocene, Eocene and Oligocene. Rocks of the Paleocene, Eocene and Oligocene ages are not present in the southwestern block.

Miocene. Rocks of the Early Miocene age are absent and there is approximately 15 feet of Middle Miocene age schist conglomerate present in the southwestern block. Since the thickness of this middle miocene material is relatively negligible, both the early and middle miocene age rocks are omitted from this study. The Late Miocene age rock is the Puente Formation. Lithologically this formation includes marine shales and fine to coarse grained sandstone (ref. 5).

Pliocene. Rocks of the Pliocene age have been divided into two formations; Repetto (Early Pliocene) and Pico (Late Pliocene). The Repetto Formation consists of marine siltstone, shale and sandstone, and the Pico Formation is marine siltstone and sandstone (refs. 2, 5).

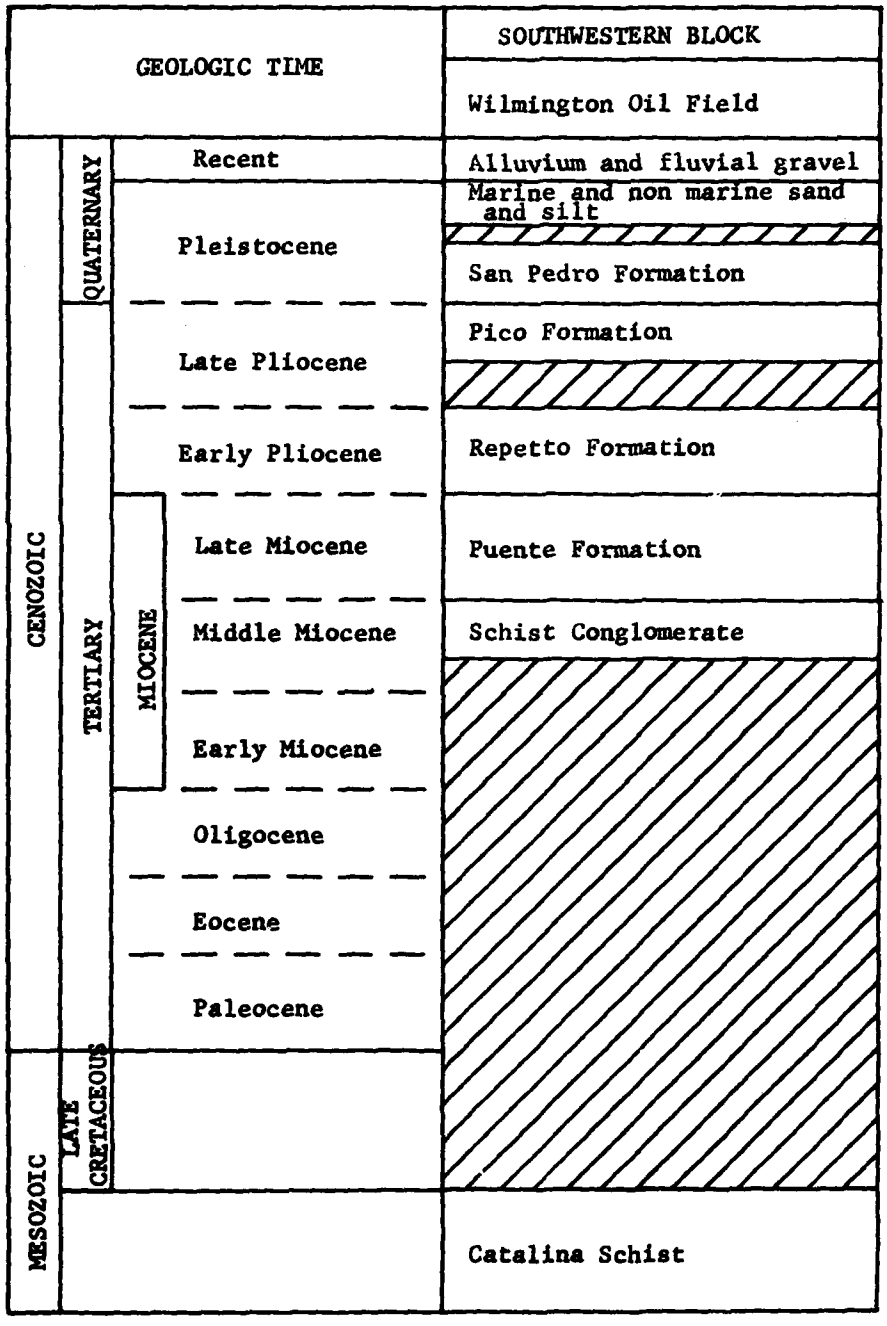

FIG. 2-1 STRATIGRAPHIC COLUMN OF THE AREA EAST OF THE PALOS VERDES FAULT ZONE AND WEST OF THE NEWPORT-INGLEWOOD FAULT ZONE

Pleistocene. Rocks of the Pleistocene age consist of the silts, sands and gravels of the San Pedro Formation, which is overlaid by older alluvium. This older alluvium consists of marine fine to medium grained sand, gravel and silt (refs. 2, 5).

Recent. Recent alluvium deposits consist of marine fine to medium grained sand, clay and silt. These materials are discussed in more detail in the following sections.

Channel and Basin Soil Conditions

Prior to construction of the harbor, the shallow bottom of the San Pedro Bay was covered with an unconsolidated sand which contained very little silt or clay. The sediments in the wetlands to the north of what is now Terminal Island were largely estuarine muds. The bay floor sands and the finer marsh sediments rested on thick sections of consolidated sands, shales and sandstone (Quaternary and Tertiary Sediments) which outcrop in small areas at the western end of the harbor (ref. 1).

The bottom of the main channel and basins have been dredged to a depth of 35 feet below MLLW and, under the proposed project, would be dredged to a depth of 45 feet. The channel and basin soil profiles, locations of drill holes, abbreviated soil logs, and soil classifications for an approximate depth of 20 feet below the existing bottom surface are shown on plates 2-4 and 2-5.

These explorations indicate that the materials are predominantly nonplastic sands and silty sands, with zones and strata of sandy silt or sandy clay with a Plasticity Index (PI) ranging from 3 to 50 and a Liquid Limit (LL) range of 28 to 83. Deposits of silt and clay together with a variety of wastes discharged into the harbor, have created a layer of mud or sludge which covers considerable parts of the harbor floor. This dark gray surface sludge ranges in depth from 1 to 3 feet and will make up approximately 6 percent of the dredged materials composition.

The gradation ranges of the fine sand, silty sands and silts or clays are shown in figures 2-2 through 2-4. It should be noted, that through direct comparison there is no distinct difference in grain size distribution, for a given soil type, between the three dredge

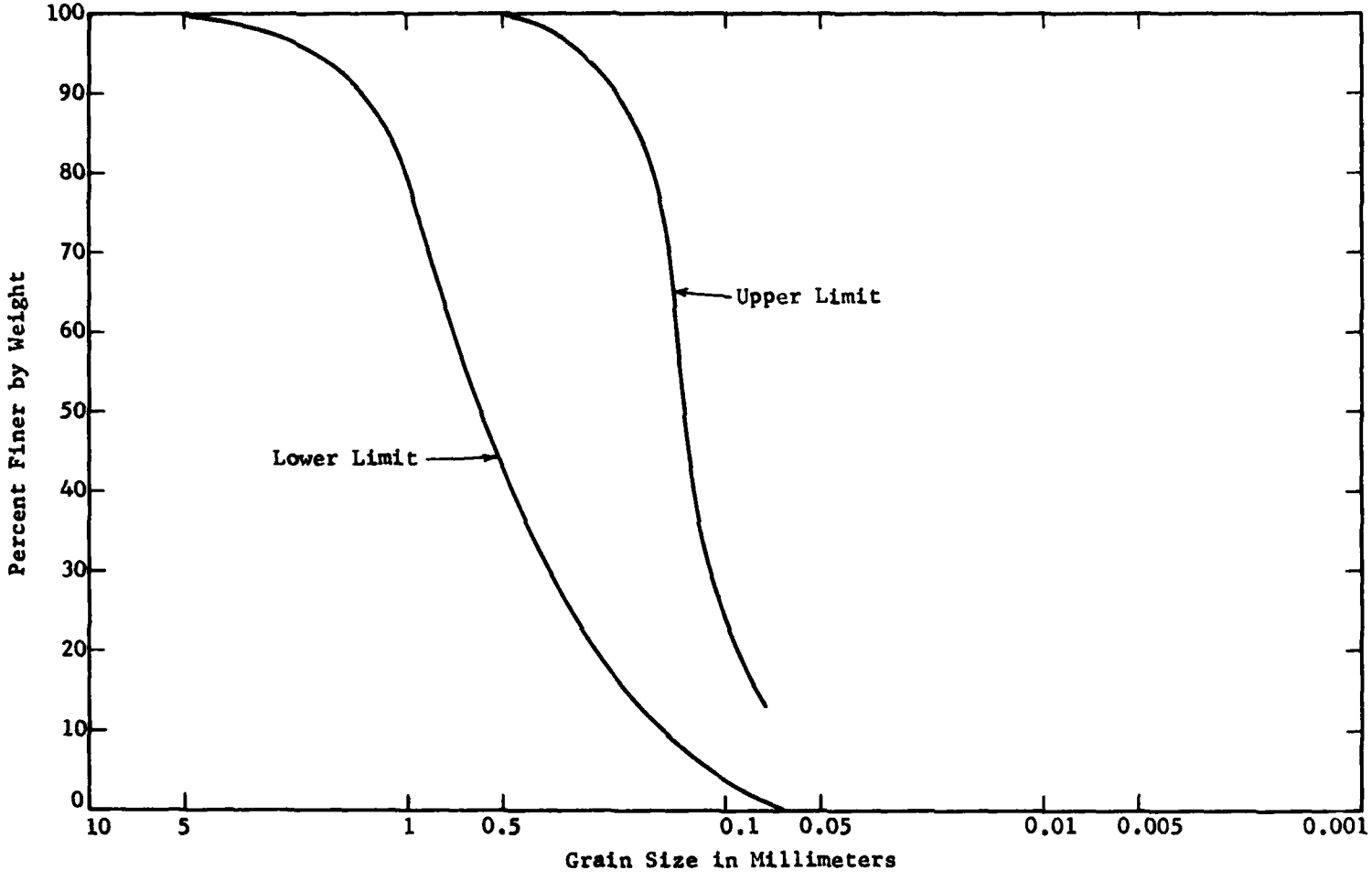

FIG. 2-2 UPPER AND LOWER LIMITS OF SAND IN THE PROPOSED DREDGE AREAS OF THE LOS ANGELES H RBOR

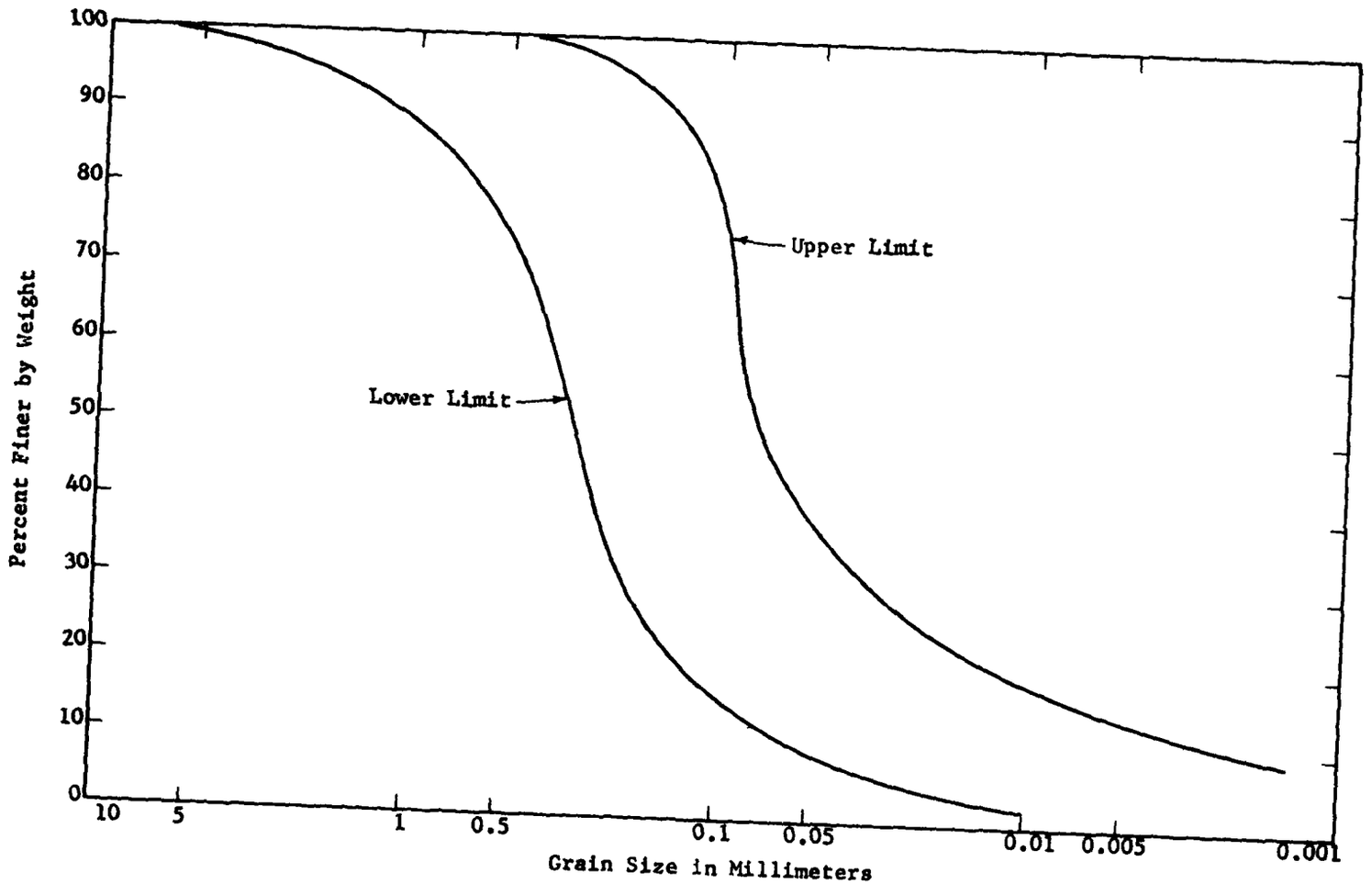

FIG. 2-3 UPPER AND LOWER LIMITS OF SILTY SAND IN THE PROPOSED DREDGE AREAS OF THE LOS ANGELES HARBOR

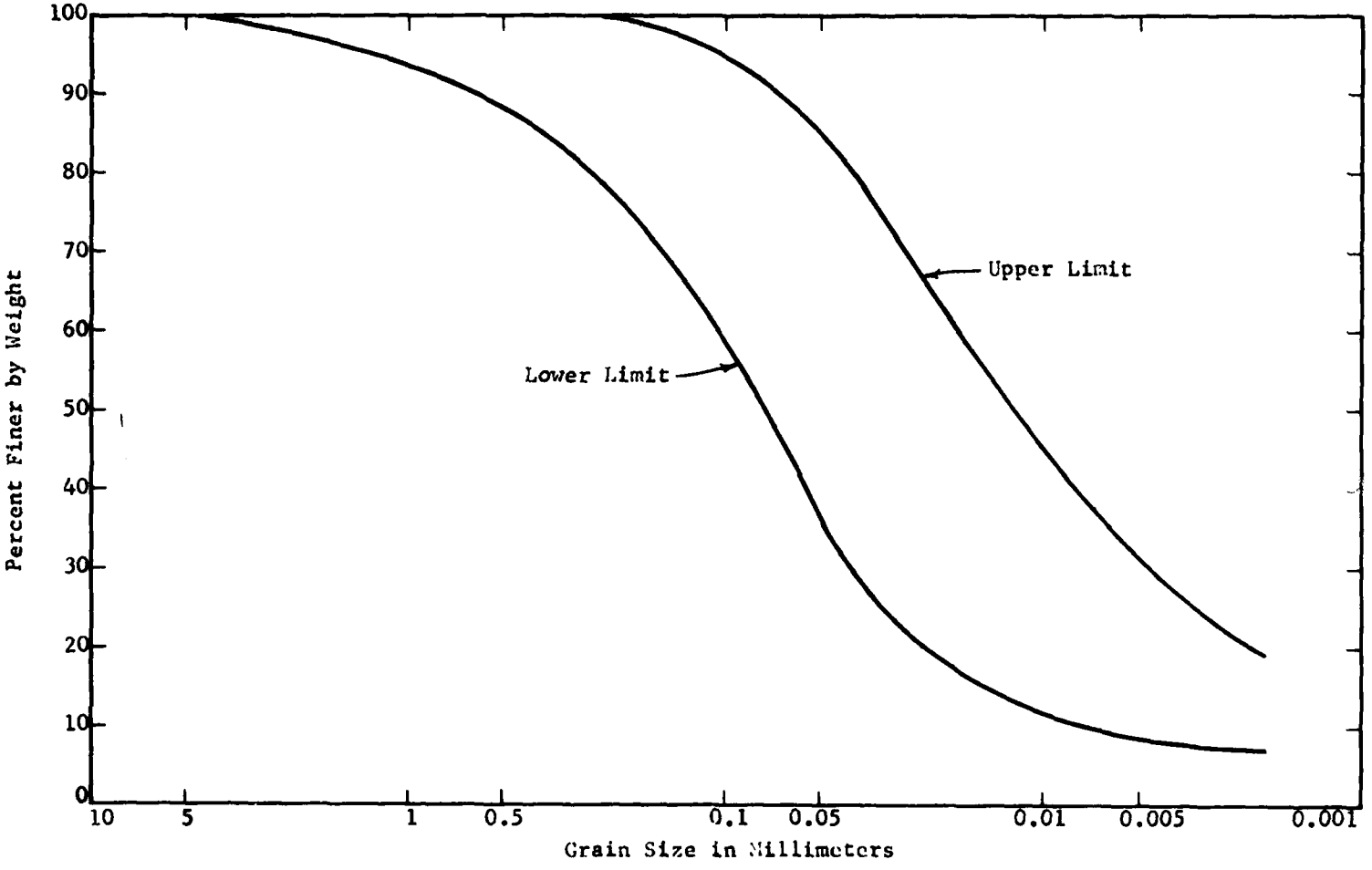

FIG. 2-4 UPPER AND LOWER LIMITS OF SILT OR CLAY IN THE PROPOSED DREDGE AREAS OF THE LOS ANGELES HARBOR

areas. Comparison of this data indicates that the sands and silty sand are very fine grained and poorly graded with uniformity coefficients ranging from 2 to 5 and 6 to 43 respectively. The silts and clays appear to be relatively well graded with a uniformity coefficient ranging from 16 to 20. It should be noted that the surface sludge, in terms of grain sizes, can be associated with the silts and clays in the upper quartile of the gradation range (approximately 80 percent or greater passing the Number 200 sieve). The approximate percentage of each type of material based on the total quantity available in each of the three designated dredge areas is presented in table 2-1.

TABLE 2-1

Approximate Soil Composition of Each Dredge Area

Area	Sand (SP) (%)	Silty Sand (SM) (%)	Clay or Silt (CL-ML) (%)
Main Channel	51	32	17
East Basin	28	47	25
West Basin	42	36	22

It is important to know, however, what the gradation of the channel soils would be after dredging and deposition at the fill site. Thus, in analyzing the future soil conditions it is assumed that dredging will be conducted so that all materials in a given area are removed to the full depth of 10 feet (EL. -45.0 feet) before the dredge is moved. Based on this typical dredging method, the gradations of materials in each test hole were weighted with respect to the total footage of each soil type per testhole and, an overall gradation and classification determined for 10 feet of material. The weighted gradations for all test holes in the channels and basins were then weighted with an areal volume, and the upper and lower limits,

quartiles and median gradations determined. These limits are presented in figures 2-5 through 2-7. This analysis indicates that the dredged materials will consist predominately of fine grained silty sand (SM) with only 10 percent of the material from the main channel and 5 percent of the material from the west basin being classified as a clay (CL) or silt (ML). A summary of the median values of grain size distribution, D_{50} grain size, uniformity coefficient (C_u) and the soil classification for each of the dredge areas is presented in table 2-2.

TABLE 2-2

Dredge Material Characteristics

	Medium Gradation					
	No. 4	No. 40	No. 200	D_{50}		
Location		(% passing)		(MM)	C_u	Classification
Main Channel	100	89	27	0.19	13	Silty Sand (SM)
East Basin	100	90	24	0.14	8	Silty Sand (SM)
West Basin	100	88	24	0.17	13	Silty Sand (SM)

Soil Conditions of Existing Hydraulic Fills

Since the fill being analyzed in this study does not yet exist, in-situ soil parameters would have to be assumed. For this reason, it was decided to analyze several existing hydraulic fills in the harbor area in order to determine how the density and shear strength fluxuate with depth and soil type. The three sites selected for study, as shown on plates 2-1 and 2-2, were analyzed to a depth of 35 feet and found to contain the approximate percentages of different soil types given in table 2-3. These values were determined from weighted soil logs and gradations in which the materials were classified in accordance with the Unified Soil Classification System.

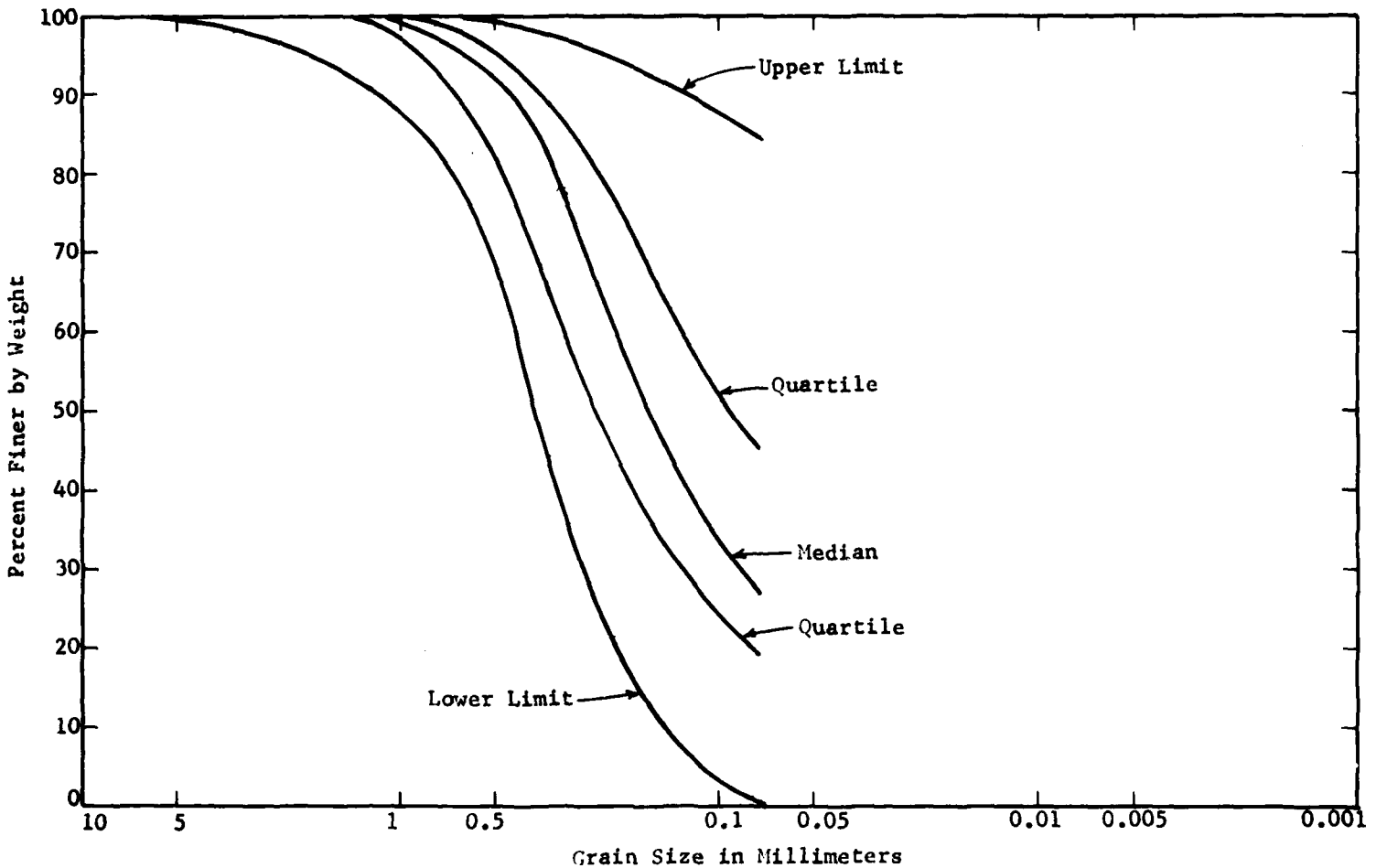

FIG. 2-5 UPPER AND LOWER LIMITS OF THE BLENDED MAIN CHANNEL MATERIALS.

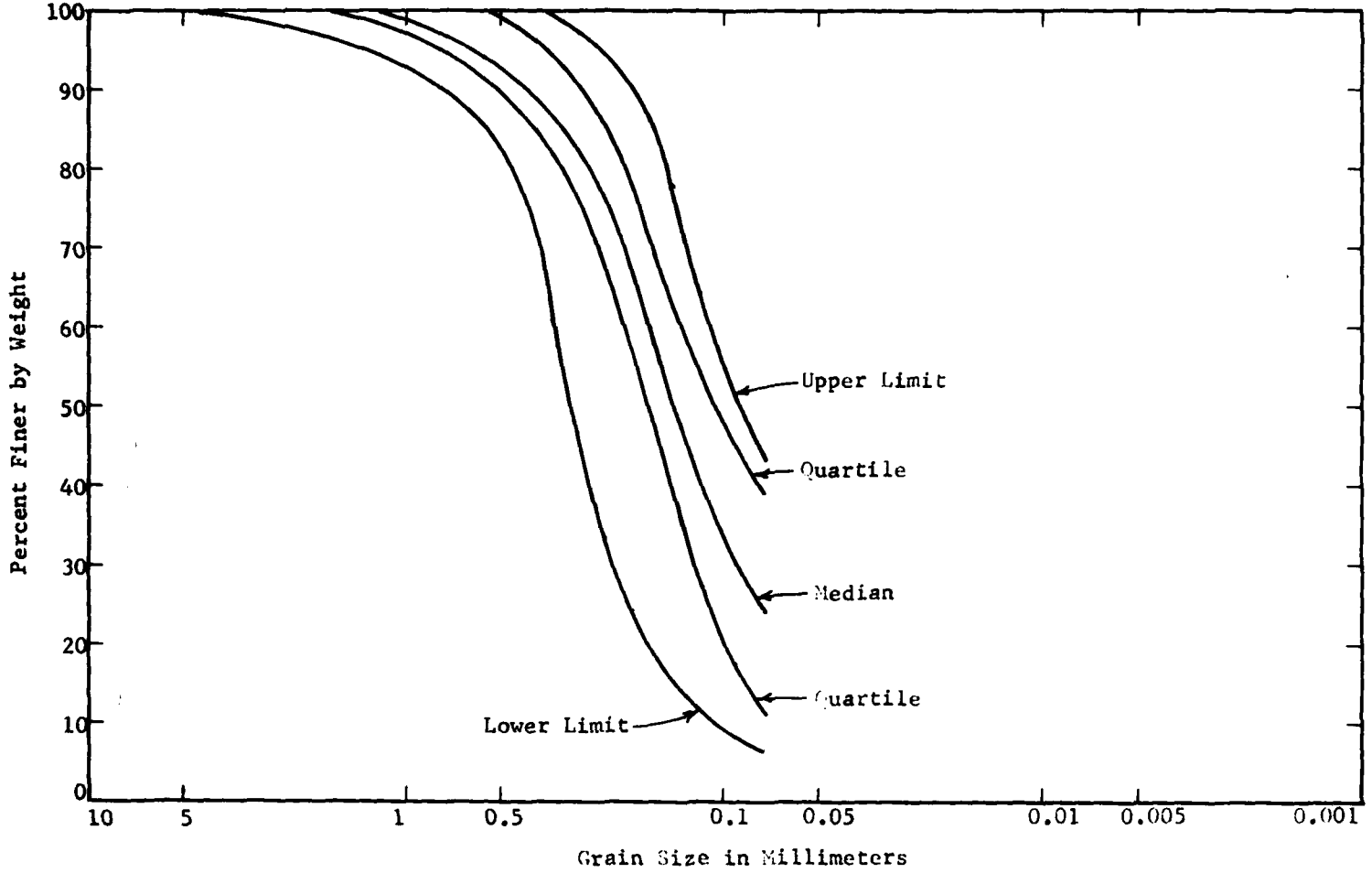

FIG. 2-6 UPPER AND LOWER LIMITS OF THE BLENDED EAST BASIN MATERIAL

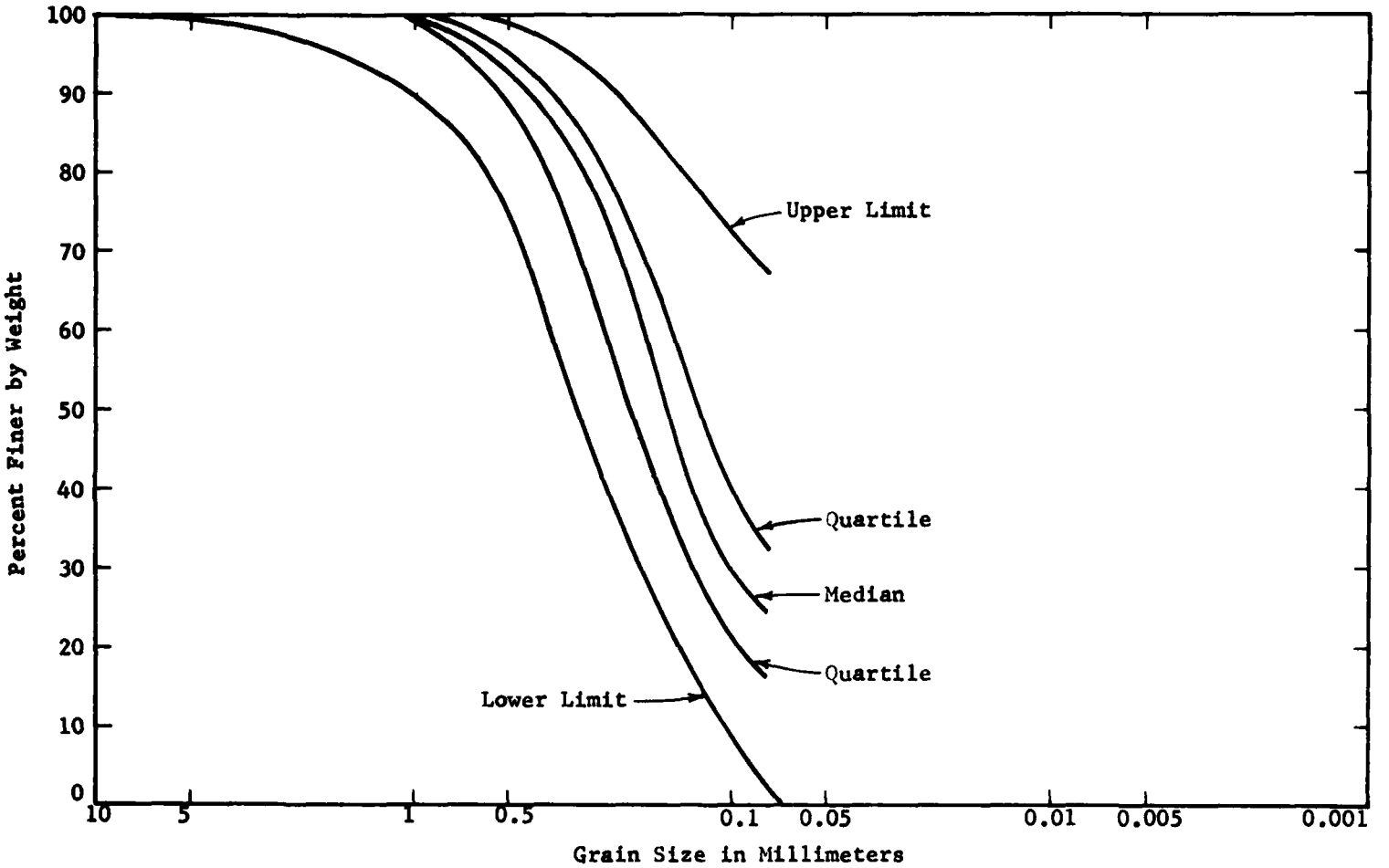

FIG. 2-7 UPPER AND LOWER LIMITS OF THE BLENDED WEST BASIN MATERIAL

TABLE 2-3

Approximate Soil Composition of Each Existing Fill Sites

	Site I (%)	Site II (%)	Site III (%)
Gravel (GP)	--	4	--
Sand (SP)	52	8	3
Silty sand (SM)	37	33	15
Silt or clay (ML-CL)	11	55	81

The silt or clay at site III is fairly uniform for the total depth of the fill with only the near surface materials being a sand or silty sand. Site I is predominately sand and silty sand with intermittent zones and lumps of clay or silt of various dimensions. At Site II, the clay or silt and silty sand appear to be in alternating zones of various thicknesses.

The sands and silty sands at each site are fine grained poorly graded and nonplastic. A small number of available Atterberg Limit test results on the clays and silts, indicate an approximate range in the Liquid Limit (LL) of 56 to 109 and Plasticity Index (PI) of 13 to 33. These values compare fairly well to the Atterberg Limit test results obtained on the potential dredge material which had an LL range of 28 to 83 and a PI range of 3 to 50.

Grain size distribution curves were only available for certain areas of Sites I and II. These curves and the soil logs from each area were the basis for evaluating the upper and lower limits, presented in figure 2-8 as the approximate range in grain size distribution for materials in the existing hydraulic fills. The upper and lower limits of the materials to be dredged are also presented in this figure for comparison. This comparison indicates that

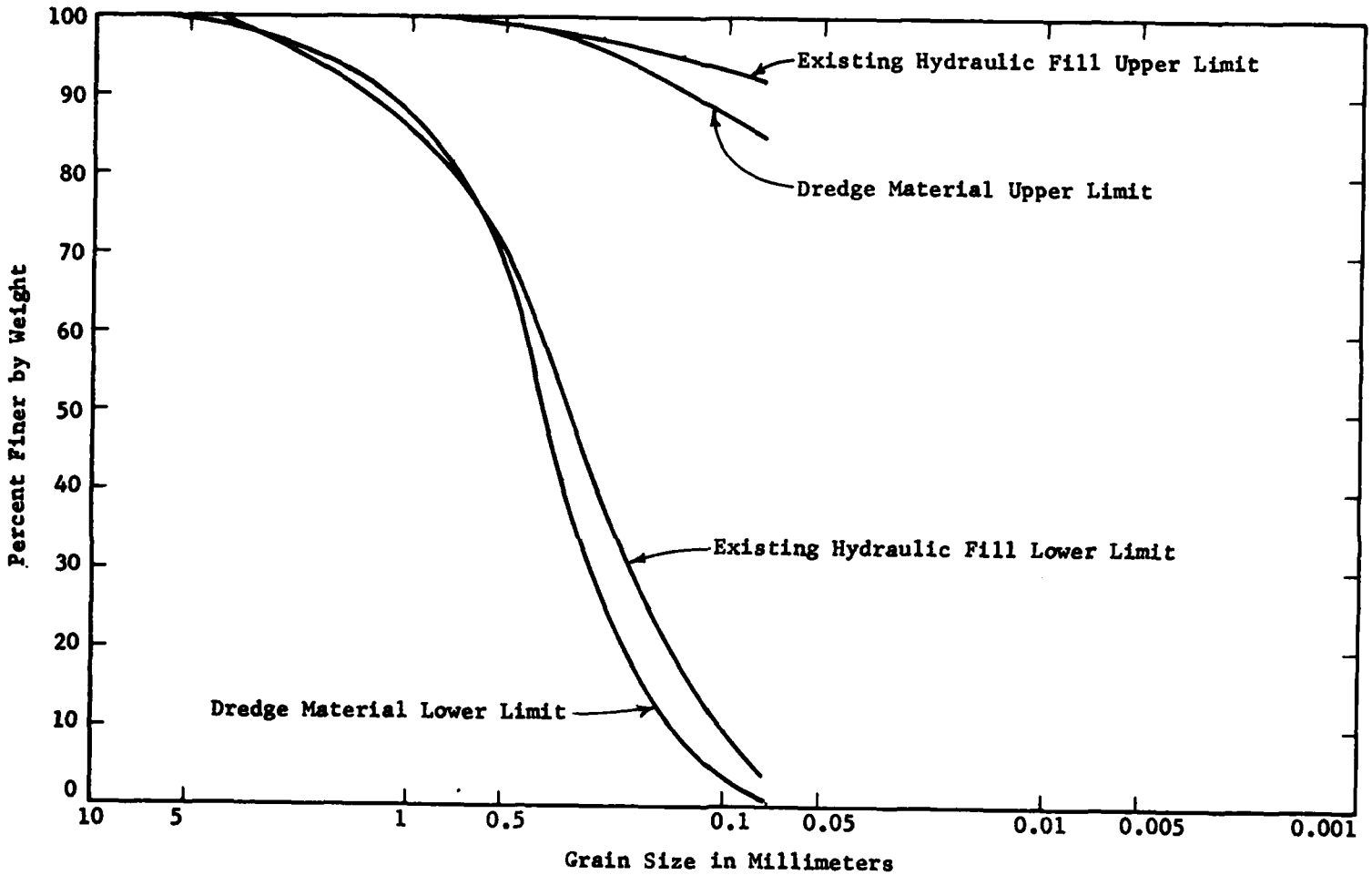

FIG. 2-8 COMPARISON OF UPPER AND LOWER LIMITS OF EXISTING HYDRAULIC FILL MATERIAL TO THE PROPOSED BLENDED DREDGE MATERIAL

there is an excellent agreement between the two gradation ranges. Therefore, the in-situ parameters of each soil type, in the existing fills should be representative of the respective soil type dredged from the main channel and basins and deposited at the proposed fill site.

The soil parameters of each soil type were evaluated based on the previous consideration and assuming that the method of construction of the proposed fill would be similar to that of fills previously built. The dry densities, moisture contents and shear strengths for each soil type, regardless of the site where encountered, were plotted against the respective depth, effective overburden or effective consolidation pressure. The median value, with respect to depth, for each of these parameters was then determined by a best fit line. The following is a detailed discussion on the densities and shear strengths found in the existing hydraulic fills.

Field Density of Existing Hydraulic Fills. The dry density and moisture content data for each soil type, is plotted against depth in figures 2-9 through 2-13. These figures indicate that for sands and silty sands the dry density and moisture content data is well grouped. The dry density values for sand show a tendency to increase with depth, ranging from 91 to 99 pcf, while the density of silty sands remains relatively constant with depth at 95 pcf. The moisture content values for the sands and silty sands are well grouped and remain constant with depth, below the water table, at values of 28 and 26 percent, respectively.

The silts or clays exhibit considerable scatter in both dry density and moisture content with depth, showing no distinct trends and making median or average values meaningless.

A limited number of dutch static cone penetration tests have recently been conducted in the existing hydraulic fill materials at Site I. While the data is not presently available for public review, it was found that the cone resistances within the fill, to a depth of 25 feet, ranged approximately from 3 to 20 kg/cm^2. This corresponds to a very loose or weak material (ref. 6).

Shear Strength of Existing Hydraulic Fills. The available direct shear date on "undisturbed samples" of the three soil types were plotted with respect to effective overburden pressure in figures 2-14 through 2-16. As indicated, the data for the sands and silty sands are well

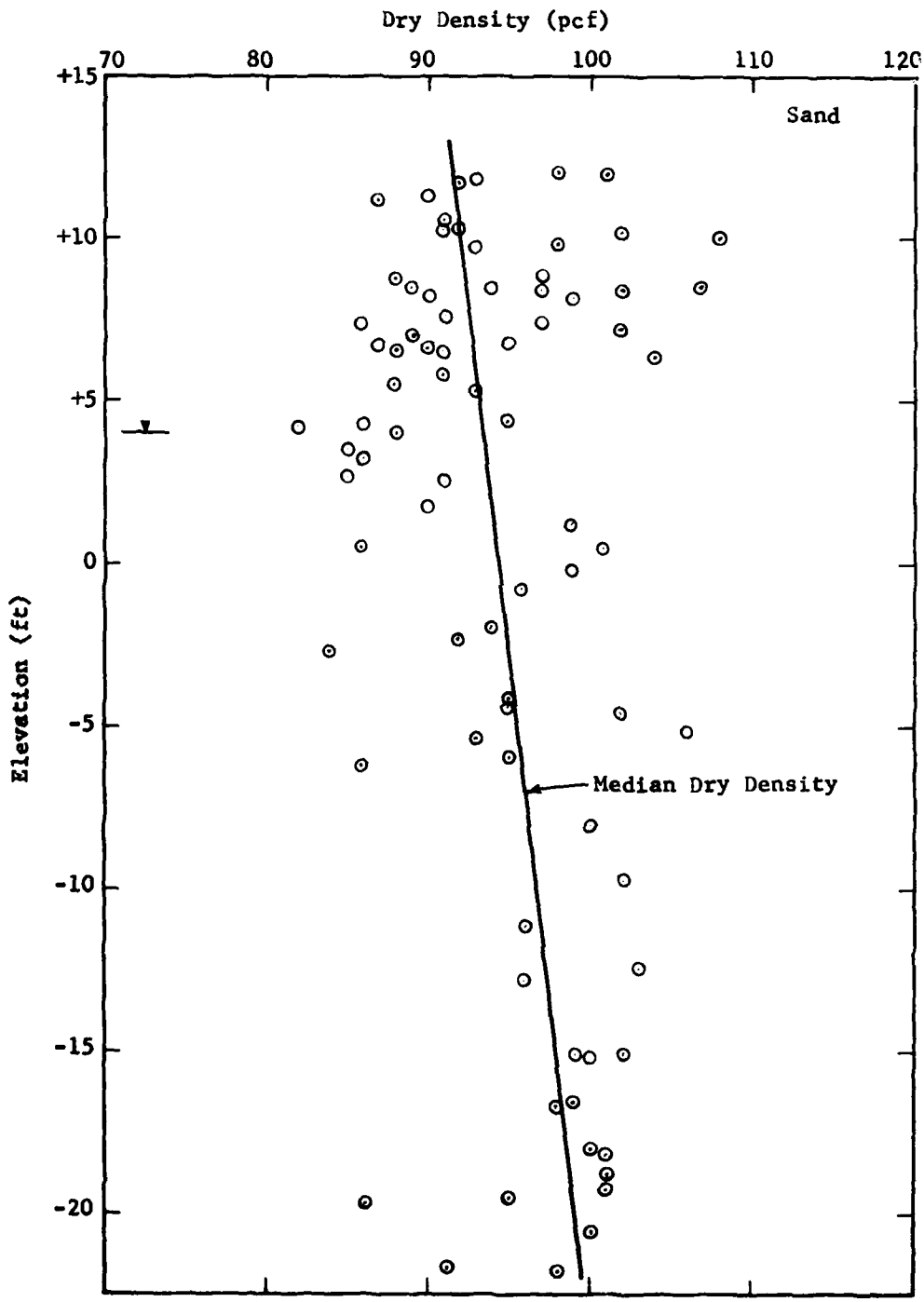

FIG. 2-9 *DRY DENSITY WITH DEPTH OF SAND IN EXISTING HYDRAULIC FILLS*

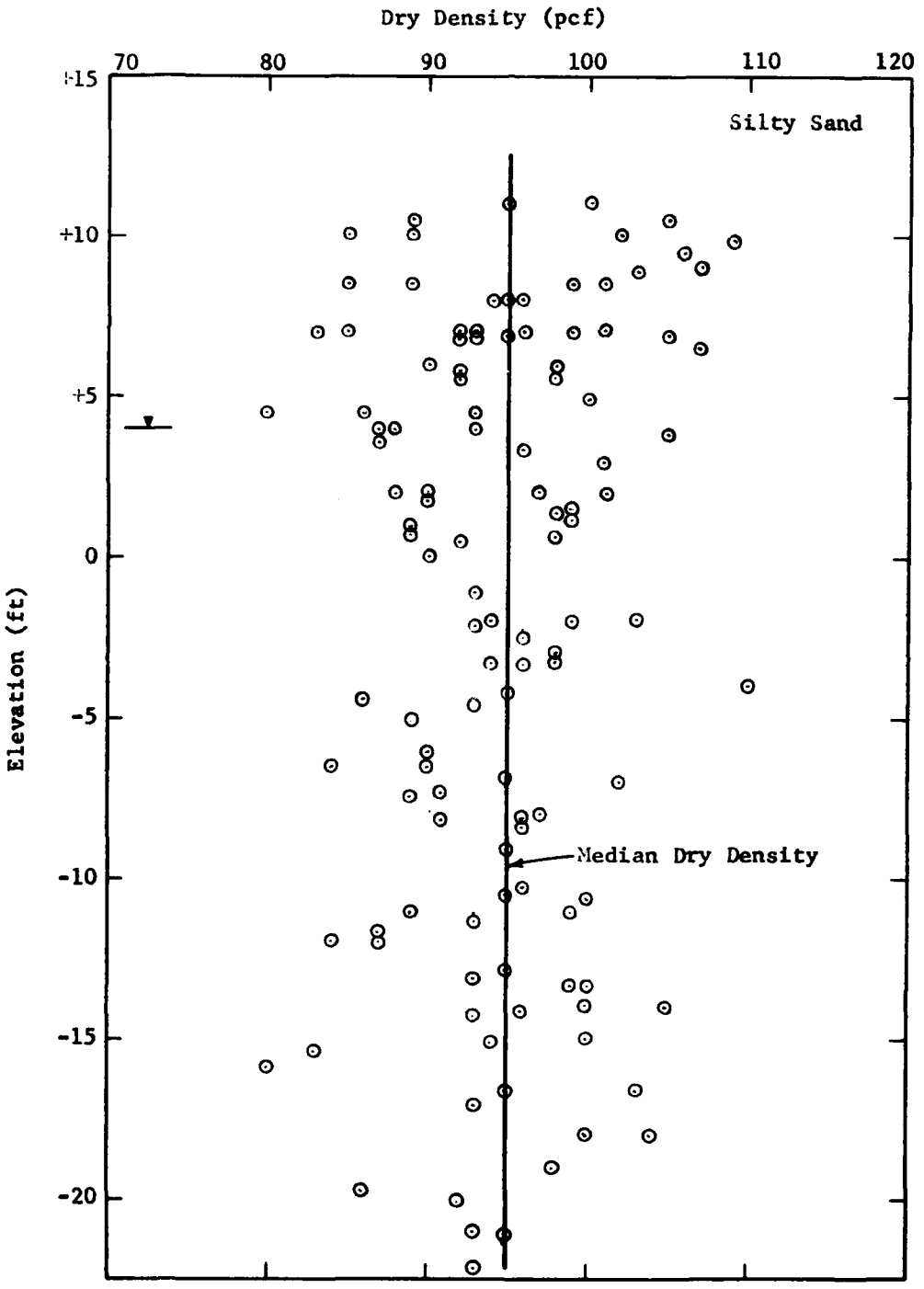

FIG. 2-10 DRY DENSITY WITH DEPTH OF SILTY SAND IN EXISTING HYDRAULIC FILLS

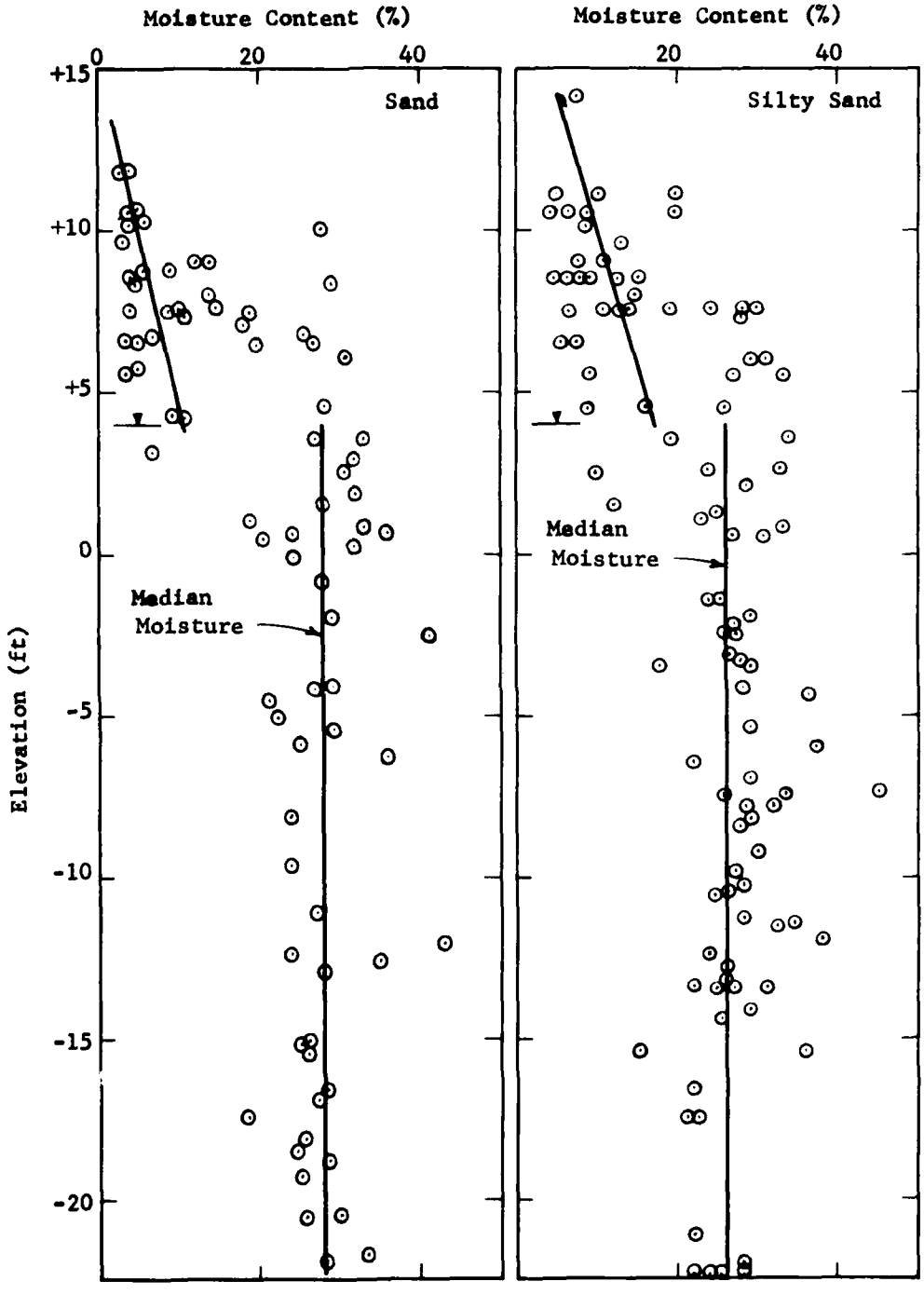

FIG. 2-11 MOISTURE CONTENT WITH DEPTH OF SANDS AND SILTY SANDS IN EXISTING HYDRAULIC FILLS

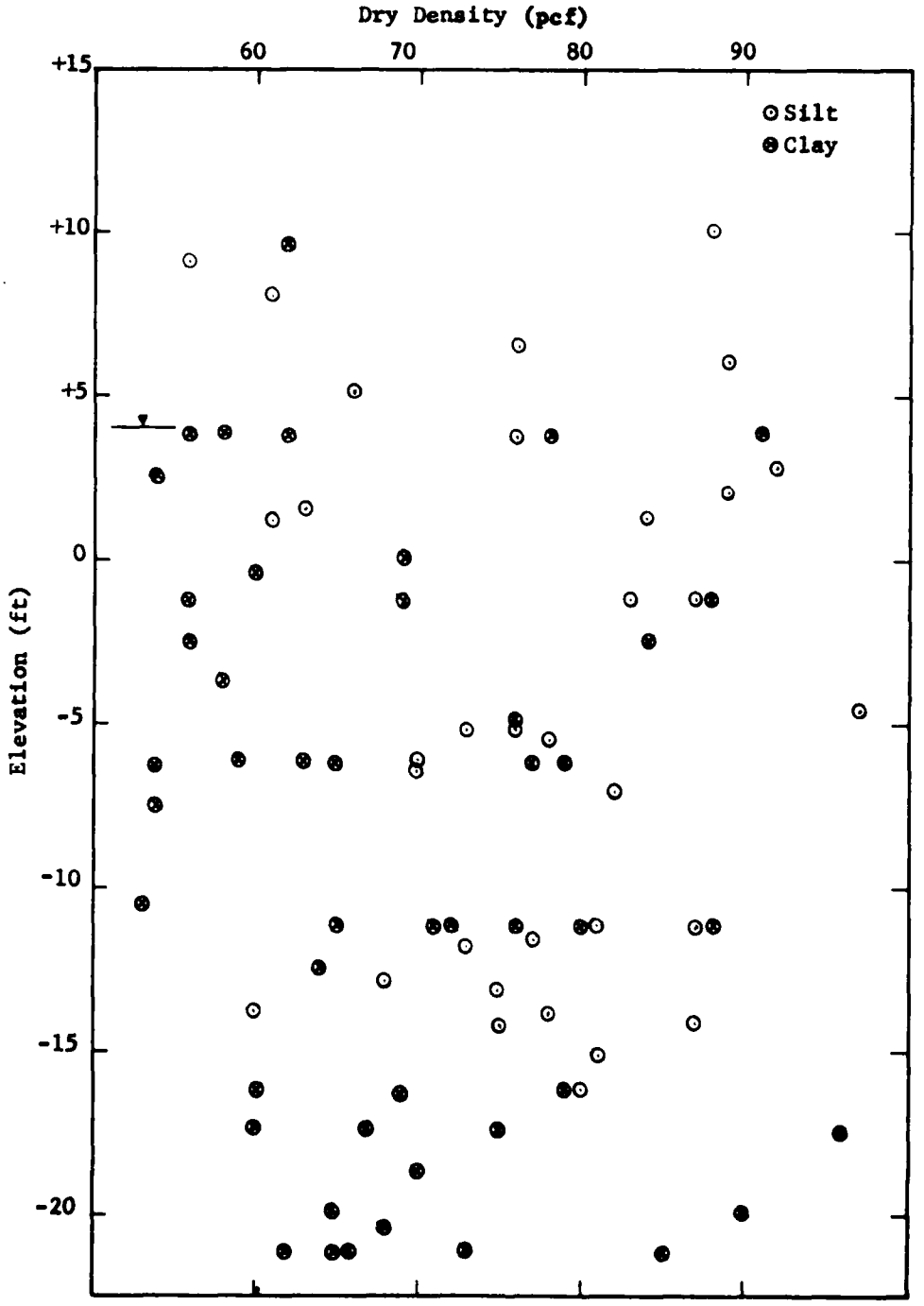

FIG. 2-12 DRY DENSITY WITH DEPTH OF SILTS AND CLAYS IN EXISTING HYDRAULIC FILLS

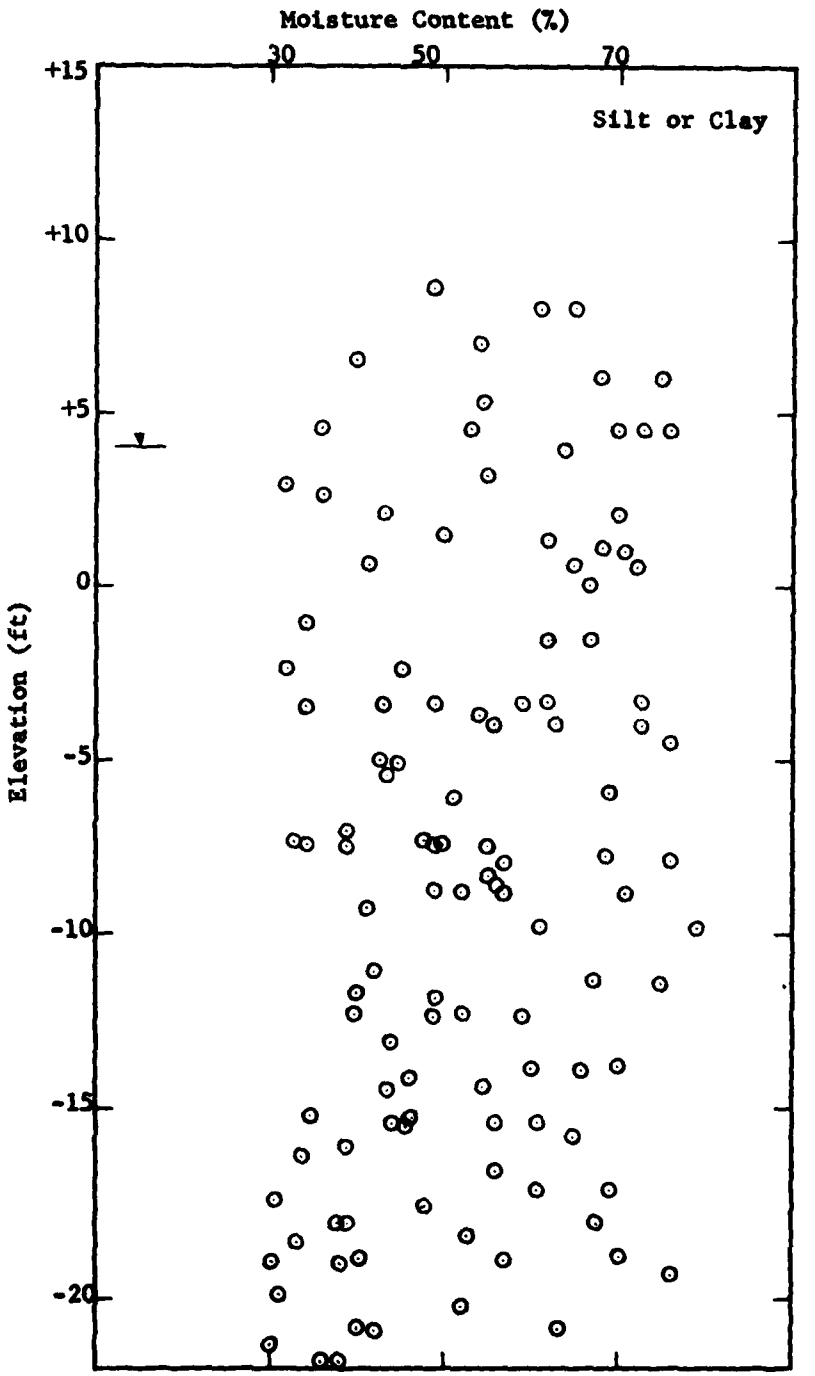

FIG. 2-13 MOISTURE CONTENT WITH DEPTH OF SILTS AND CLAYS IN EXISTING HYDRAULIC FILLS

grouped with minimum values for the friction angle (ϕ) of 27 and 30 degrees respectively, at a dry density of 90 pcf. The direct shear data on the silts and clays shown slightly more scatter but lower limits were still well defined. The minimum value for the friction angle (ϕ) and the corresponding cohesion intercept at a dry density of 65.0 pcf, is 18 degrees and 250 psf, respectively.

There was a small amount of data available on in-situ vane shear tests, unconsolidated undrained and consolidated undrained triaxial tests on the silts or clays at all three fill sites studied. This data, however, was limited to consolidation pressures of less than 3,000 psf and exhibited considerable scatter. The vane shear strengths and the consolidated undrained shear strenghts at failure, are plotted against the consolidation or effective overburden pressure in figure 2-17 for dry densities of 60 and 70 pcf.

Foundation Conditions at the Proposed Fill Site. The subsurface conditions at the proposed fill site were established from the soil logs of test holes 141 through 144 and 146 through 148. Test hole 142 had the deepest penetration of approximately 270 feet. From these logs dry densities, moisture contents, and a small number of standard penetration tests were obtained. Data was also obtained from three static cone soundings.

The soil logs indicate that the materials encountered were primarily medium dense, fine to medium grained sand and silty sand with zones of silt to depths of approximately 80 feet. The median dry density of the material is approximately 95 pcf with a moisture content of approximately 28 percent. At depths greater than 80 feet, the materials are dense to very dense, fine to medium grained sands and silty sands with gravel or coarse sand lenses. The range in median dry density is from 100 to 112 pcf with moisture contents of approximately 22 percent.

The limited amount of standard penetration test data on the foundation materials indicates that at an elevation of -25 feet the blow counts are greater than 50 blows per foot and at an elevation of -30 feet the blow count exceeds 70 blows per foot. Based on the relationship between standard penetration resistance, relative density and effective overburden pressure (ref. 7), these blow counts correspond to relative densities of approximately 90 percent. These values appear to be high compared to the median dry

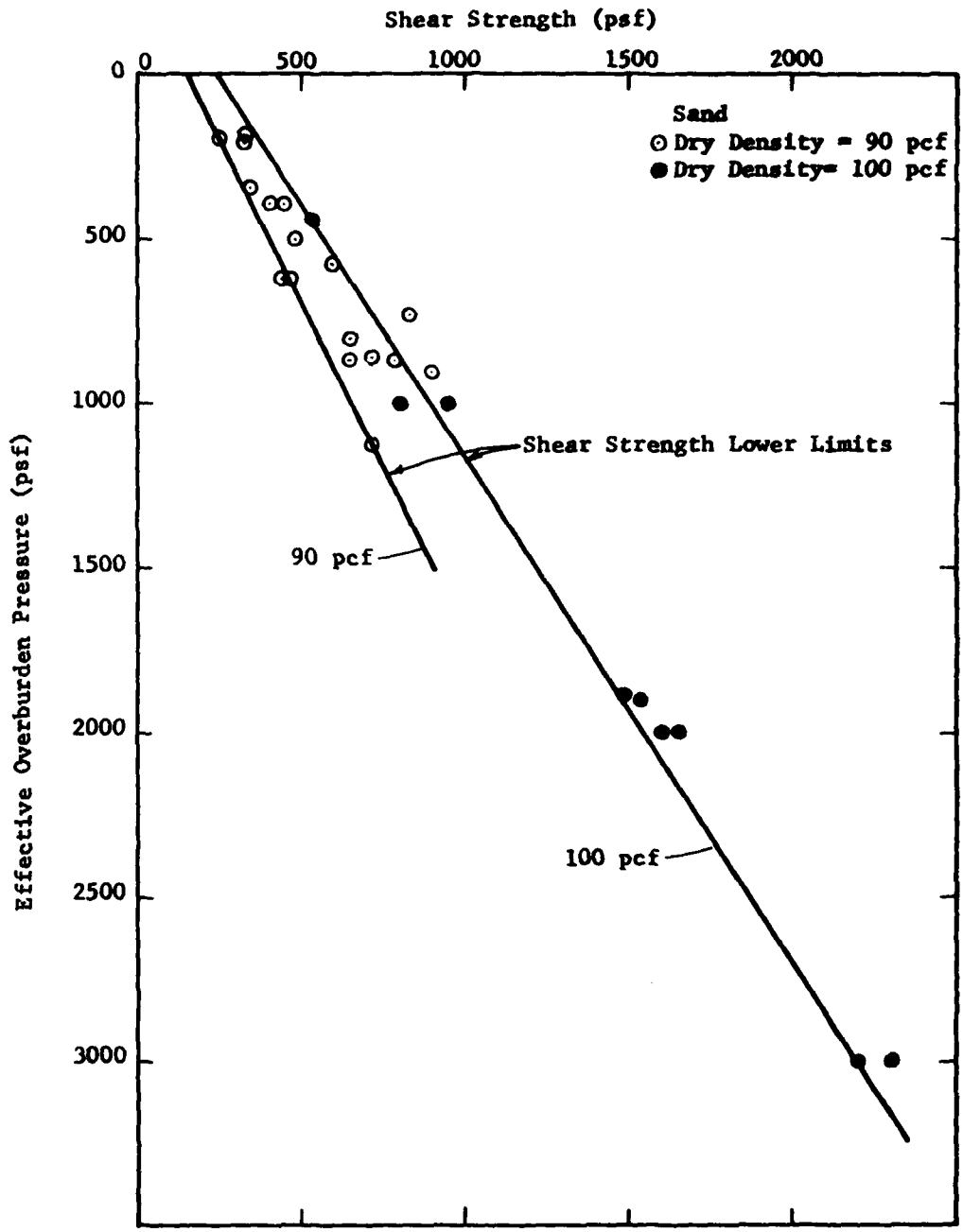

FIG. 2-14 SHEAR STRENGTH OF SAND IN EXISTING HYDRAULIC FILLS WITH RESPECT TO DENSITY

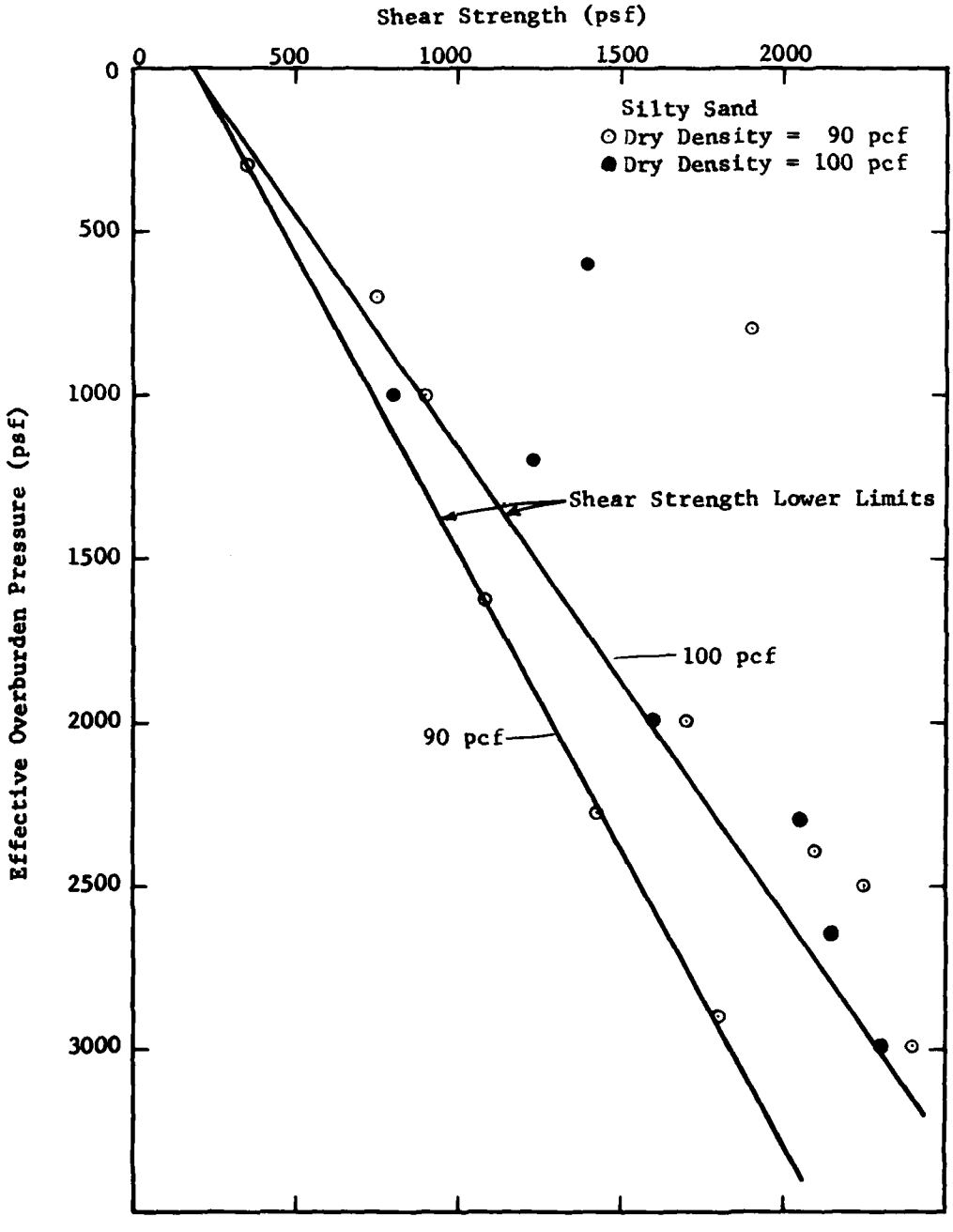

FIG. 2-15 SHEAR STRENGTH OF SILTY SAND IN EXISTING HYDRAULIC FILLS WITH RESPECT TO DENSITY

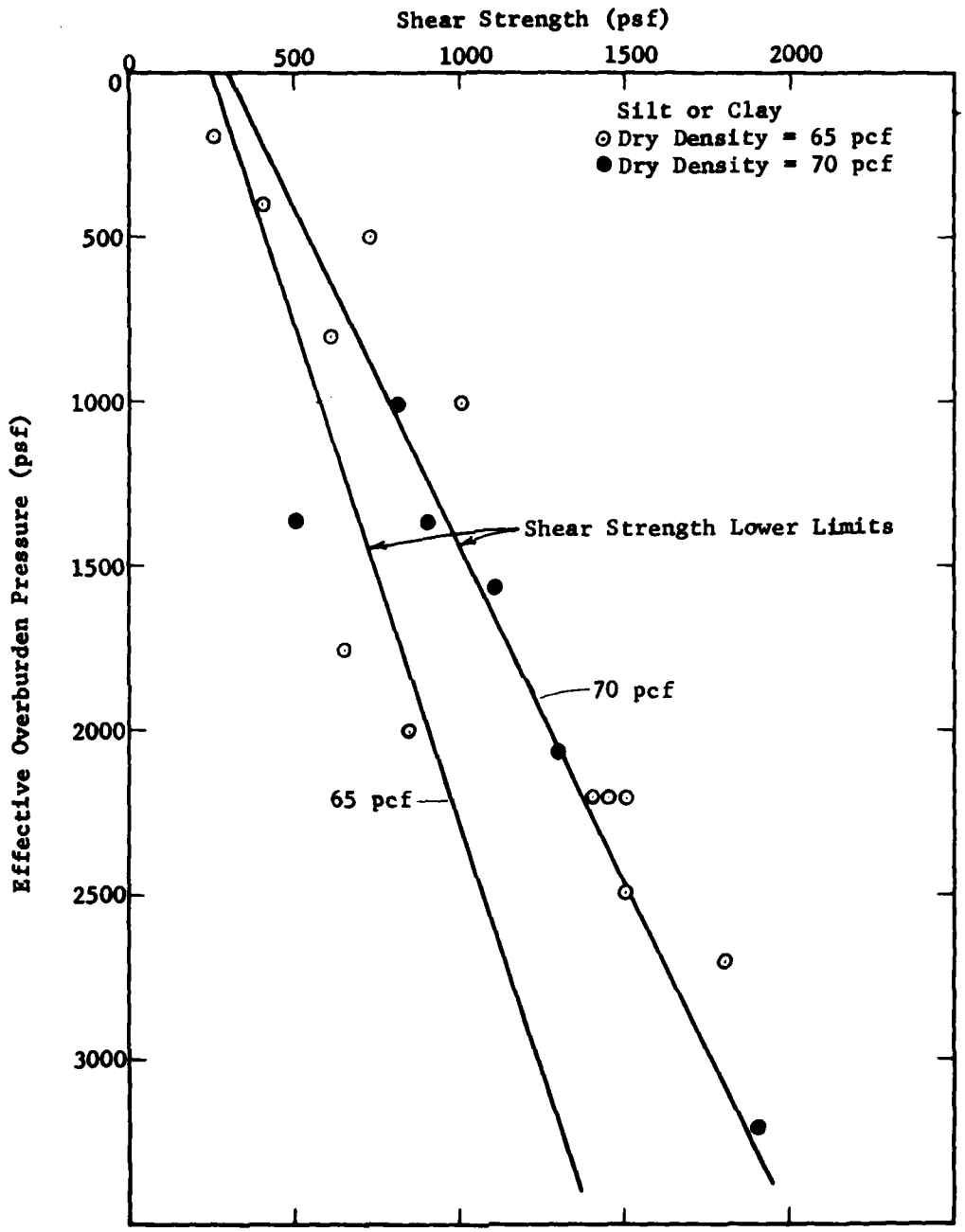

FIG. 2-16 SHEAR STRENGTH OF SILT OR CLAY IN EXISTING HYDRAULIC FILLS WITH RESPECT TO DENSITY

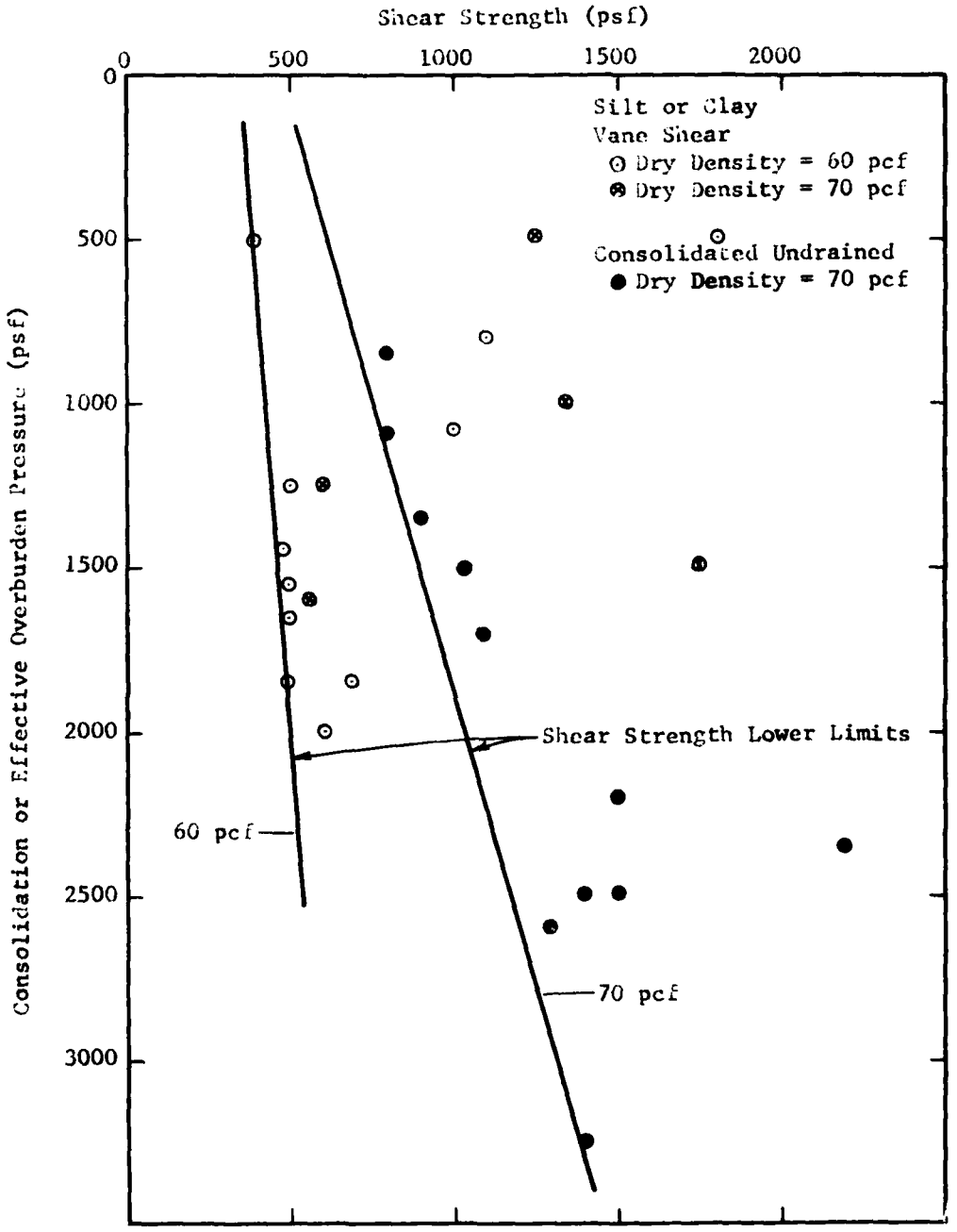

FIG. 2-17 SHEAR STRENGTHS OF SILT OR CLAY DETERMINED BY IN-SITU VANE SHEAR TESTS AND TRIAXIAL TESTS ON EXISTING HYDRAULIC FILLS

density at these depths of approximately 95 pcf. As discussed in Chapter 3, the maximum and minimum dry densities of sand were determened to be approximately 106 and 83 pcf, respectively. This would indicate that a dry density of 95 pcf corresponds to a relative density of approximately 58 percent.

The static cone resistance results are based on tests conducted in the foundation materials at Site I to a depth of approximately 100 feet using a 60 degree dutch static cone with a surface area of 10 sq. cm. The resistance values were converted to relative density based on a relationship between effective overburden pressure, cone resistance and relative density (Schmertmann, unpublished, 1971), figure 2-18. This conversion resulted in a high median relative density ranging from 80 to 95 percent with the 95 percent value occuring from elevation −20 to −40 feet and the 80 percent value occuring from −80 to −100 feet. Due to the poor correlation with the absolute density values, which show an increase in magnitude with depth, the static cone results were not utilized to a large extent in this report.

The results of all available soil testing at various depths within the foundation materials near the vicinity of the proposed fill have been summarized and presented in figure 2-19.

There were no shear strength data available on the silts or clays of the foundation materials under the existing in-situ conditions of approximately 5,000 psf of effective overburden pressure. In order to expand on the shear strength data presented in figure 2-17, consolidated undrained test results of silts from the lower portion or mouth of the Los Angeles River were obtained from the Corps of Engineers. This data included consolidation pressures as great as 8,000 psf and dry densities of 70 and 90 pcf, figure 2-20.

A direct comparison of the Los Angeles River material to the silts existing in the foundation materials at the fill site was not possible because gradation and Atterberg Limit data were unavailable. The upper and lower gradation limits of the materials in the Los Angeles River are presented in figure 2-21 along with the limits of the silts which would be dredged from the channels and basins. This comparison can be made because the stratigraphic position of the silts is similar between the fill site and dredge area and the material should therefore be similar assuming a common origin. The Atterberg Limit tests on the Los Angeles River materials indicate Liquid Limits ranging from 27 to 61 and a Plasticity Index range from 0 to 36 which is in good agreement with the dredge material values.

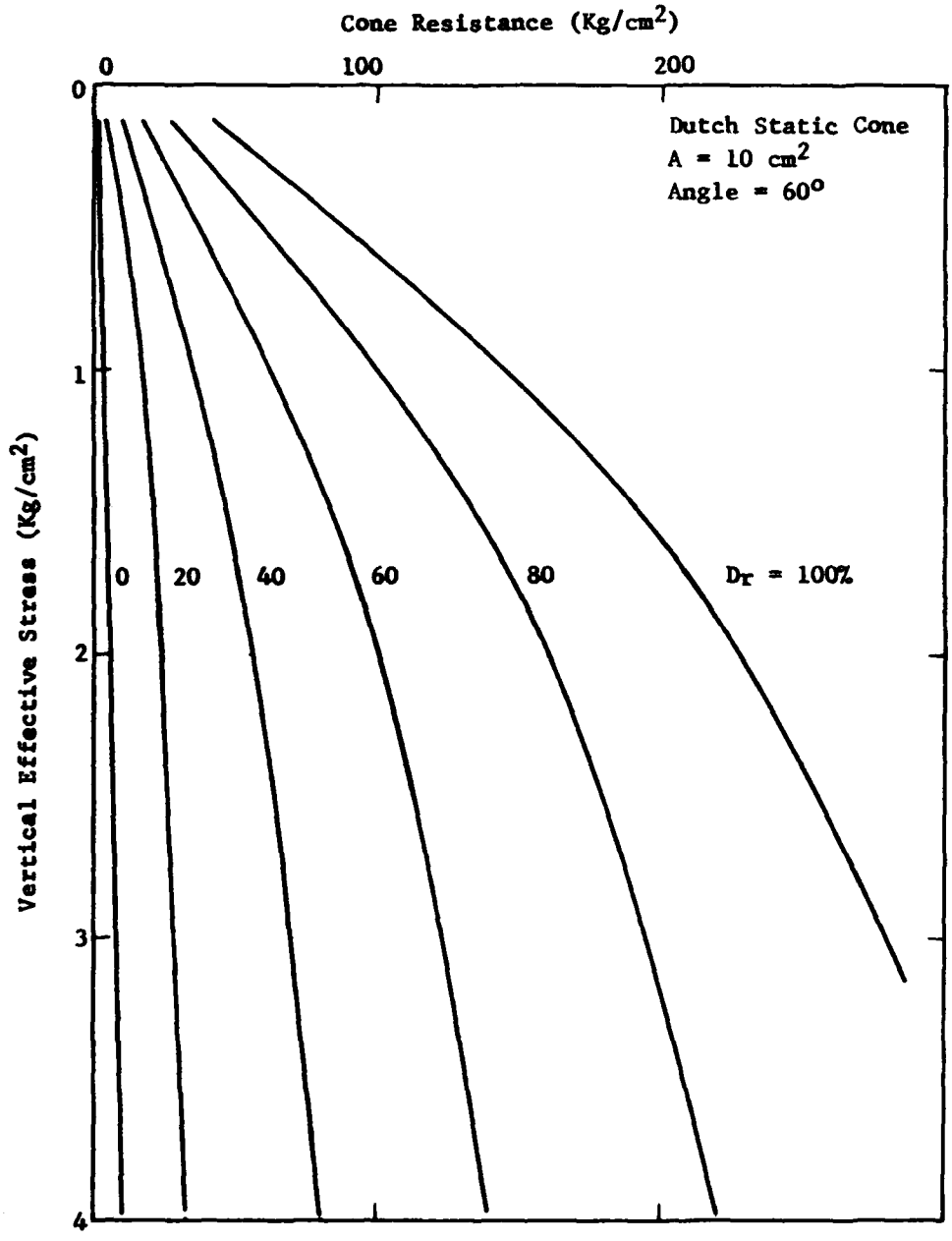

FIG. 2-18 CORRELATION BETWEEN CONE RESISTANCE AND RELATIVE DENSITY FOR SILTY SANDS. (Schmertmann, Unpublished 1971)

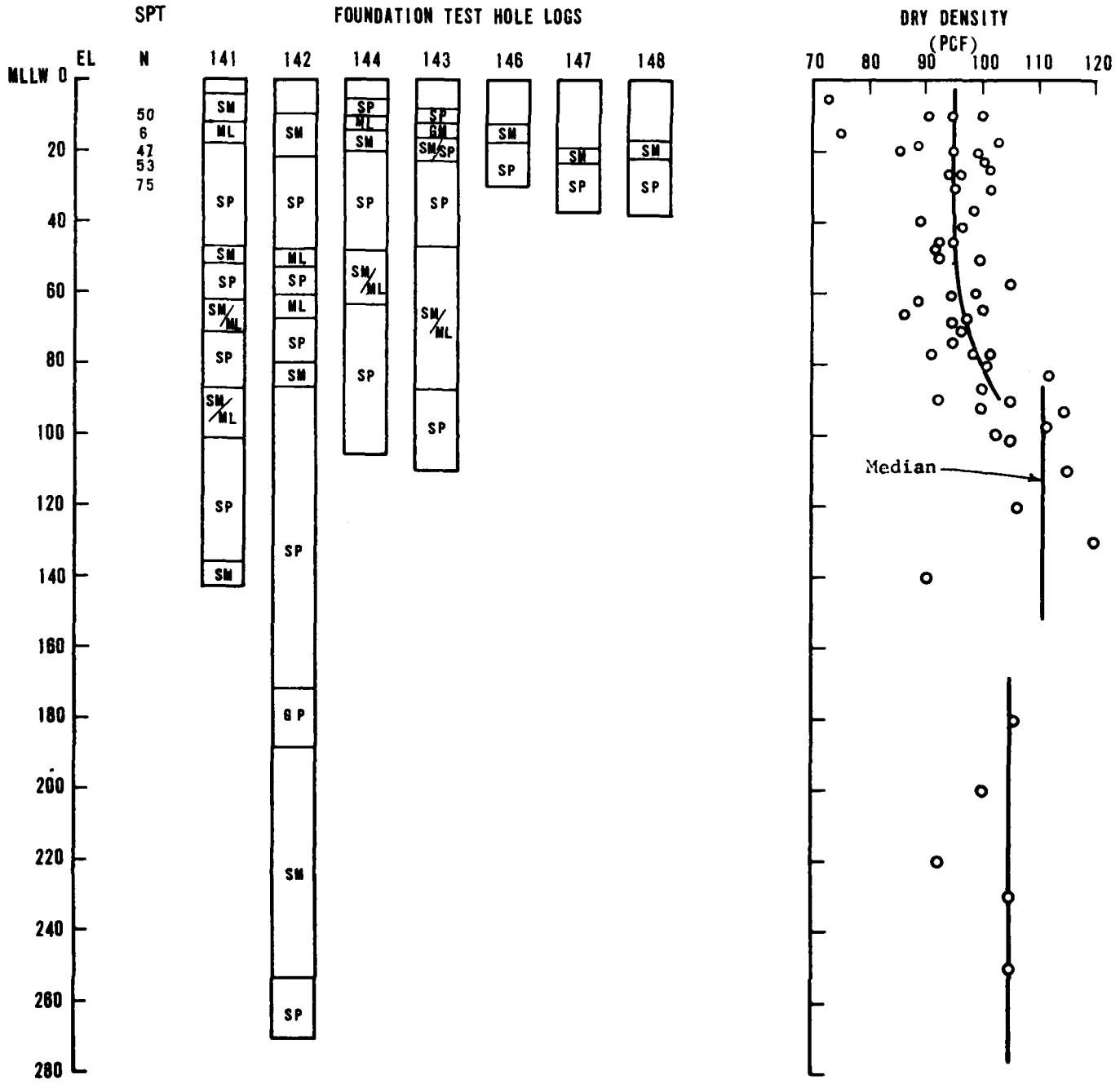

FIG. 2-19 SUMMARY OF AVAILABLE SOIL DATA ON THE FOUNDATION MATERIALS C

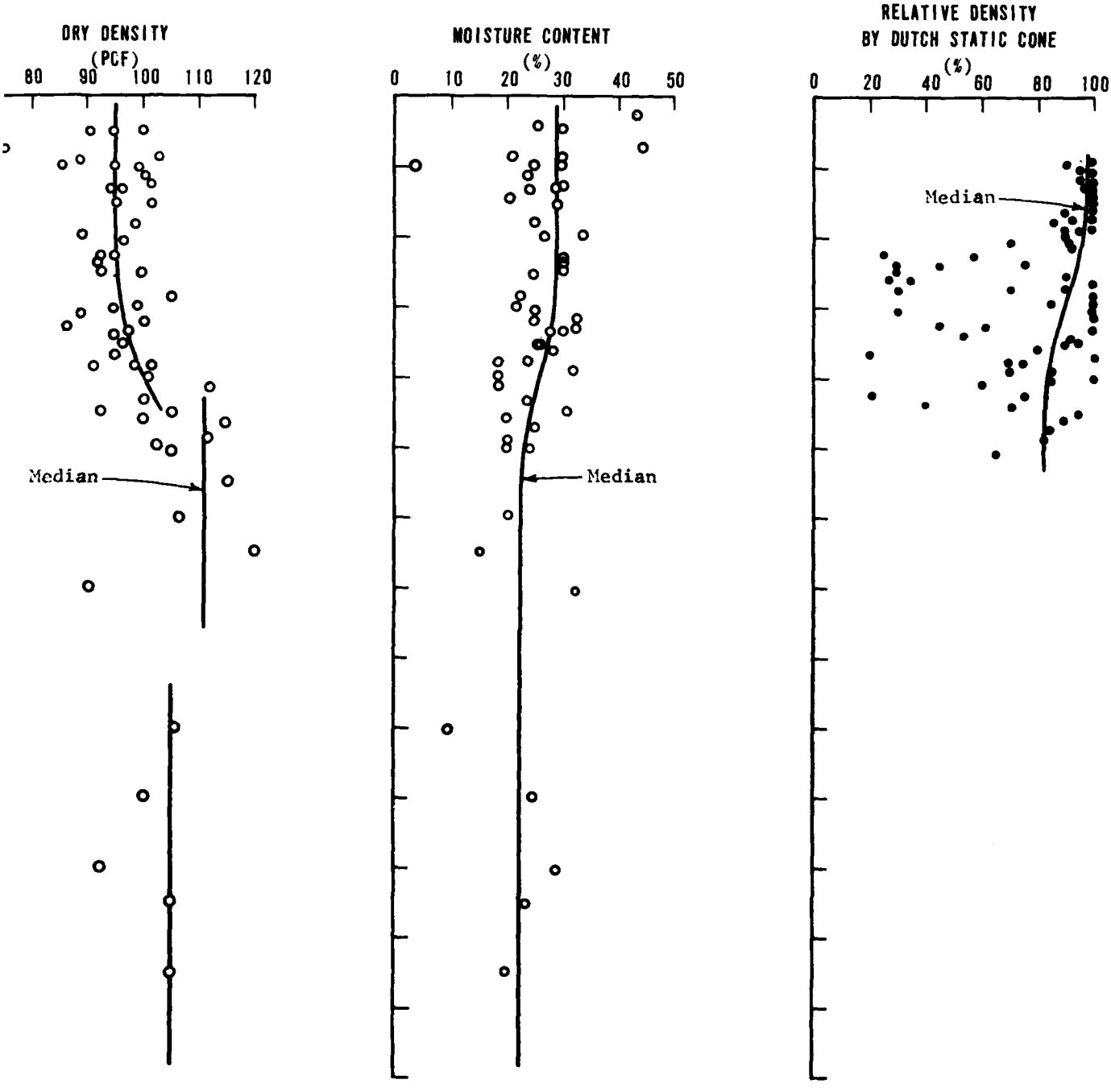

ATA ON THE FOUNDATION MATERIALS OF THE POTENTIAL FILL SITE

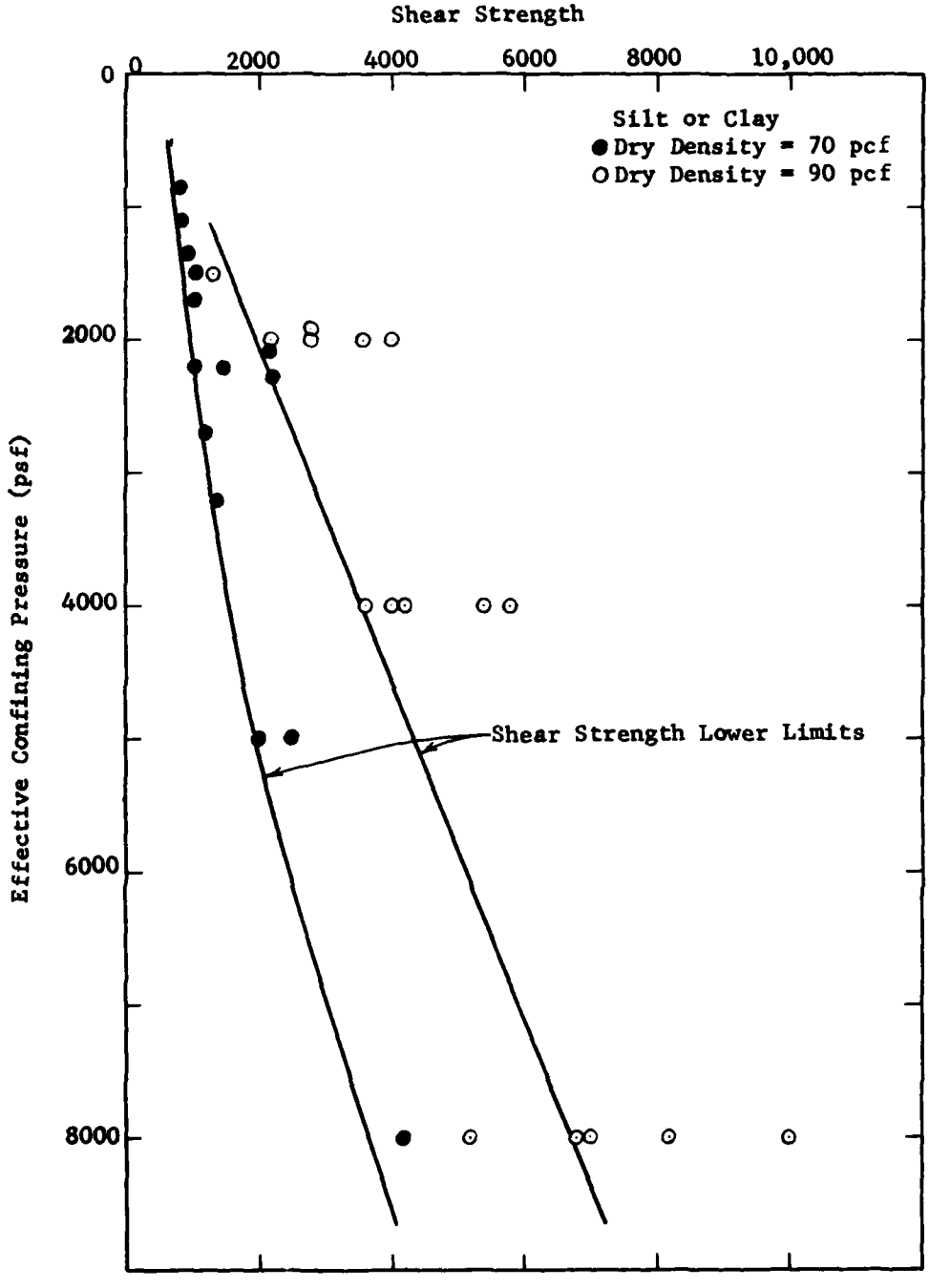

FIG. 2-20 COMBINED SHEAR STRENGTHS OF SILT OR CLAY FROM THE LOS ANGELES RIVER AND THE POTENTIAL DREDGE AREA

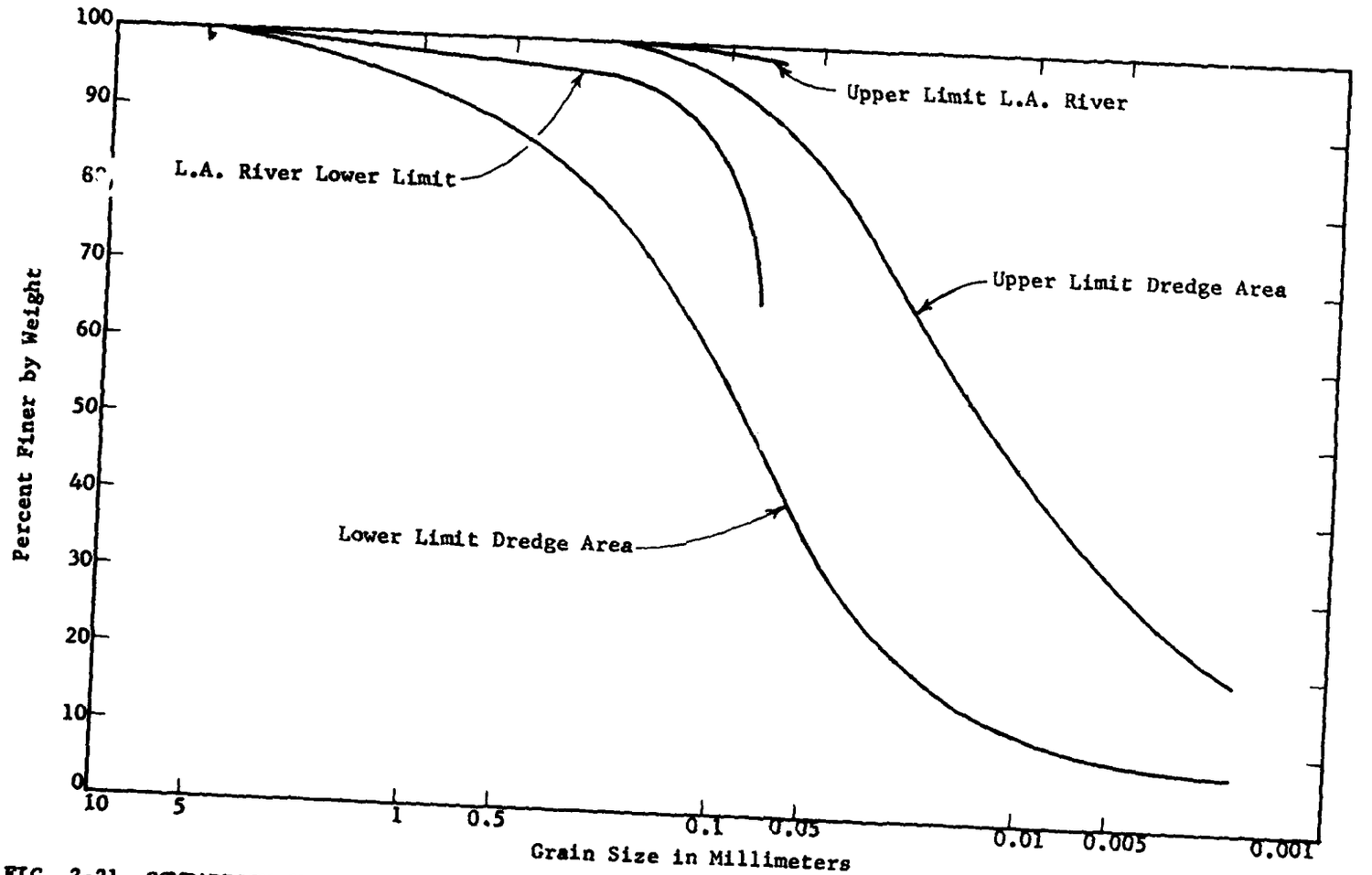

FIG. 2-21 COMPARISON OF UPPER AND LOWER LIMITS OF SILT OR CLAY FROM THE PROPOSED DREDGE AREAS TO THE LIMITS OF SIMILAR MATERIAL FROM THE MOUTH OF THE LOS ANGELES RIVER

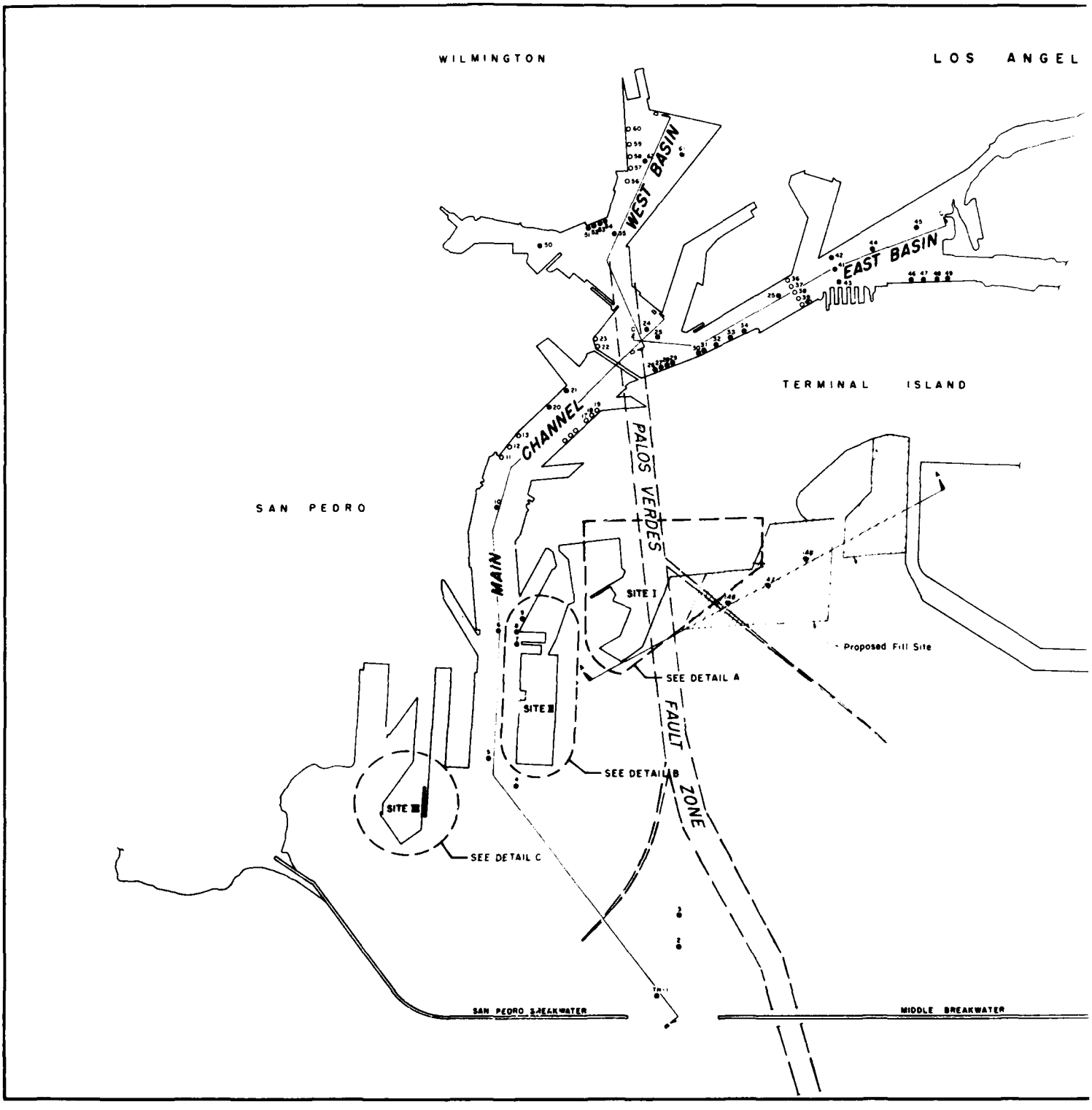
WILMINGTON
LOS ANGEL
WEST BASIN
EAST BASIN
TERMINAL ISLAND
CHANNEL
PALOS VERDES
SAN PEDRO
MAIN
SITE I
SITE II
SITE III
Proposed Fill Site
SEE DETAIL A
SEE DETAIL B
SEE DETAIL C
FAULT ZONE
SAN PEDRO BREAKWATER
MIDDLE BREAKWATER

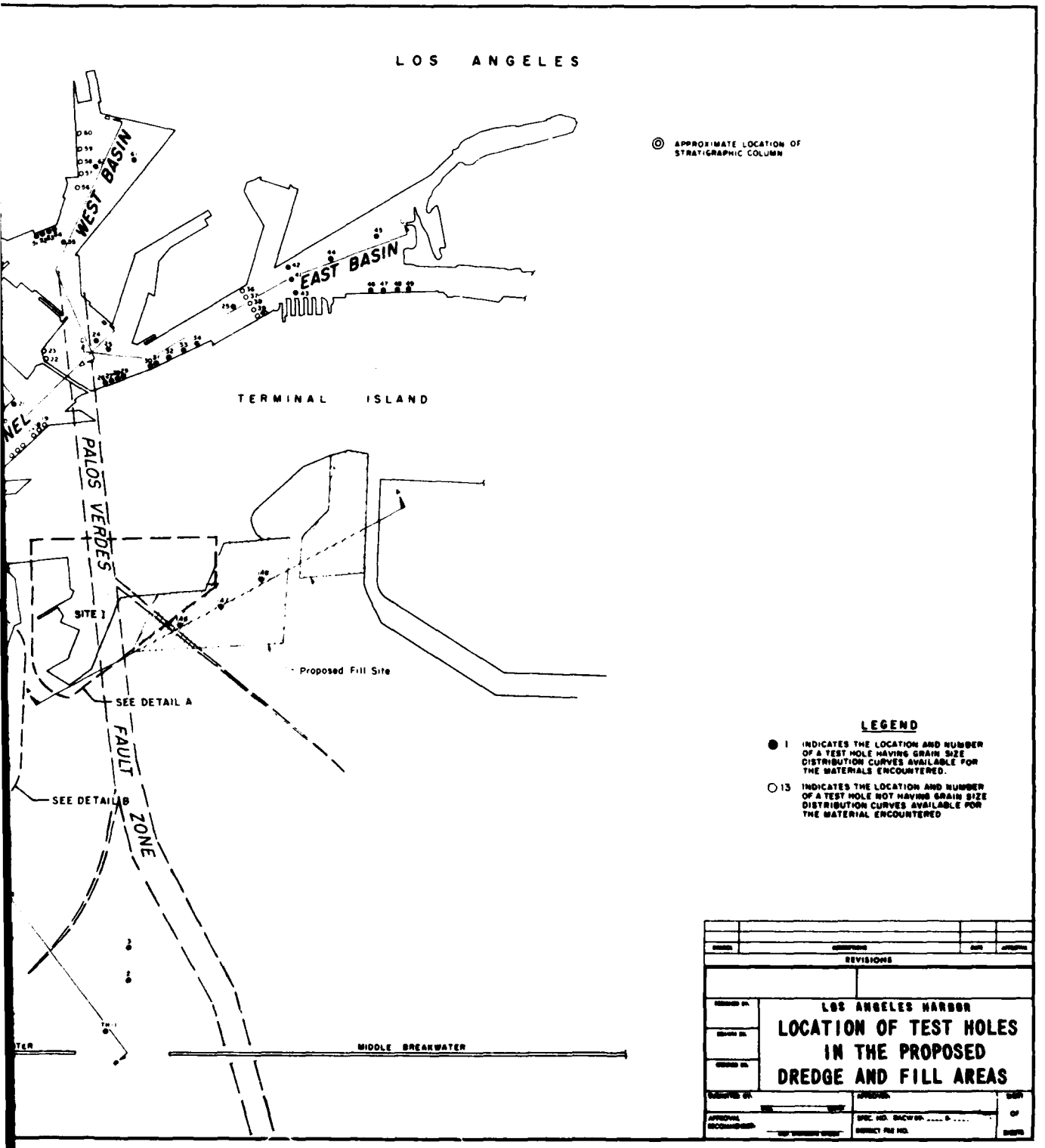
LOS ANGELES
APPROXIMATE LOCATION OF STRATIGRAPHIC COLUMN
WEST BASIN
EAST BASIN
TERMINAL ISLAND
PALOS VERDES
SITE 1
Proposed Fill Site
SEE DETAIL A
FAULT ZONE
SEE DETAIL B
MIDDLE BREAKWATER
LEGEND
1 INDICATES THE LOCATION AND NUMBER OF A TEST HOLE HAVING GRAIN SIZE DISTRIBUTION CURVES AVAILABLE FOR THE MATERIALS ENCOUNTERED.
13 INDICATES THE LOCATION AND NUMBER OF A TEST HOLE NOT HAVING GRAIN SIZE DISTRIBUTION CURVES AVAILABLE FOR THE MATERIAL ENCOUNTERED
REVISIONS
LOS ANGELES HARBOR
LOCATION OF TEST HOLES IN THE PROPOSED DREDGE AND FILL AREAS

PLATE 2-1

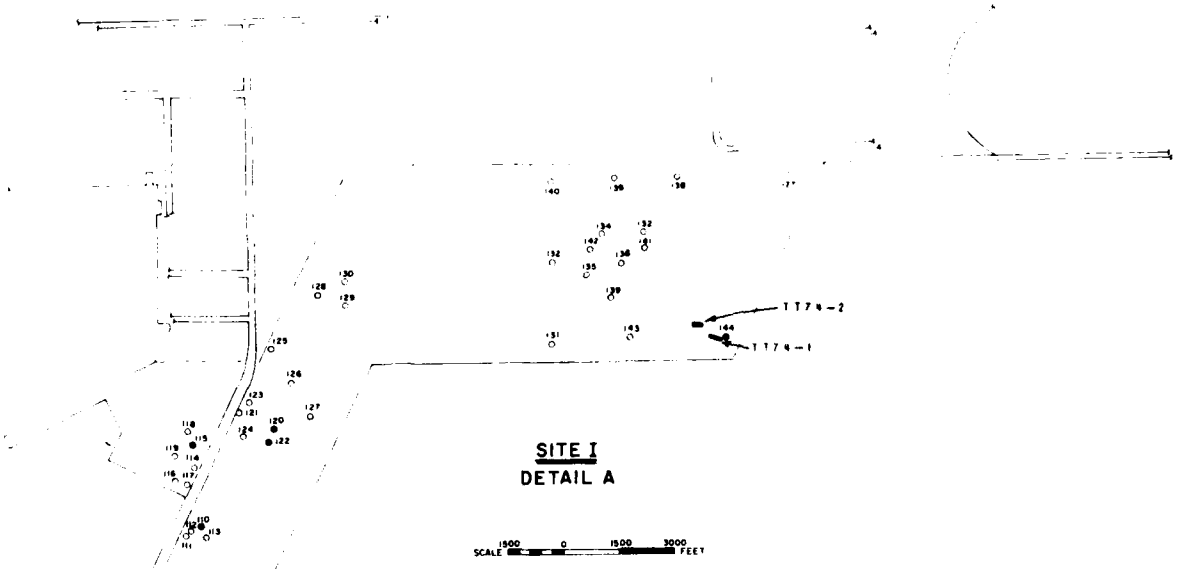

SITE I
DETAIL A

SCALE 1500 0 1500 3000 FEET

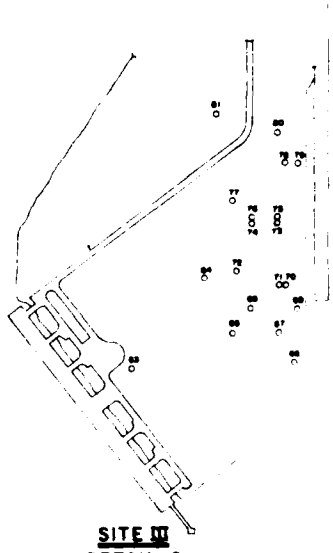

SITE III
DETAIL C

SCALE FEET

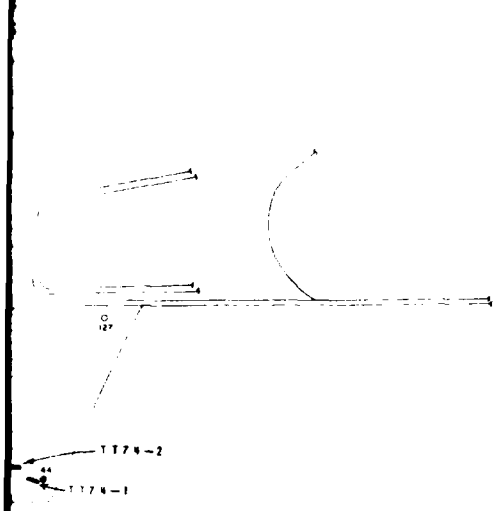

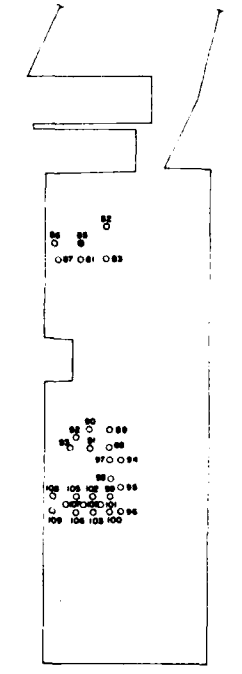

SITE II
DETAIL B

SCALE 1500 0 1500 3000 FEET

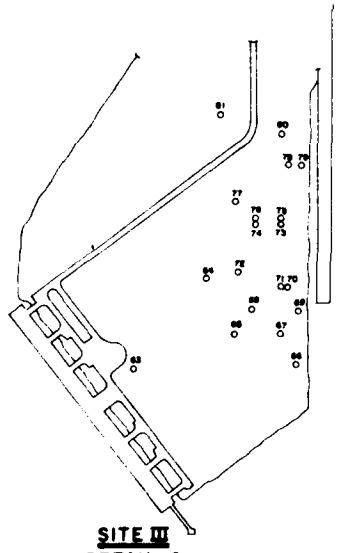

SITE III
DETAIL C

SCALE 750 0 1500 3000 FEET

NOTE:

1. SEE LEGEND ON PLATE 1 FOR TEST HOLE SYMBOL IDENTIFICATION

SYMBOL	DESCRIPTION	DATE	APPROVAL
REVISIONS			

LOS ANGELES HARBOR

LOCATION OF TEST HOLES IN EXISTING HYDRAULIC FILL SITES

SUBMITTED BY	APPROVED	SHEET
APPROVAL RECOMMENDED	SPEC. NO. DACW ...	OF
	DISTRICT FILE NO.	SHEETS

PLATE 2-2

2

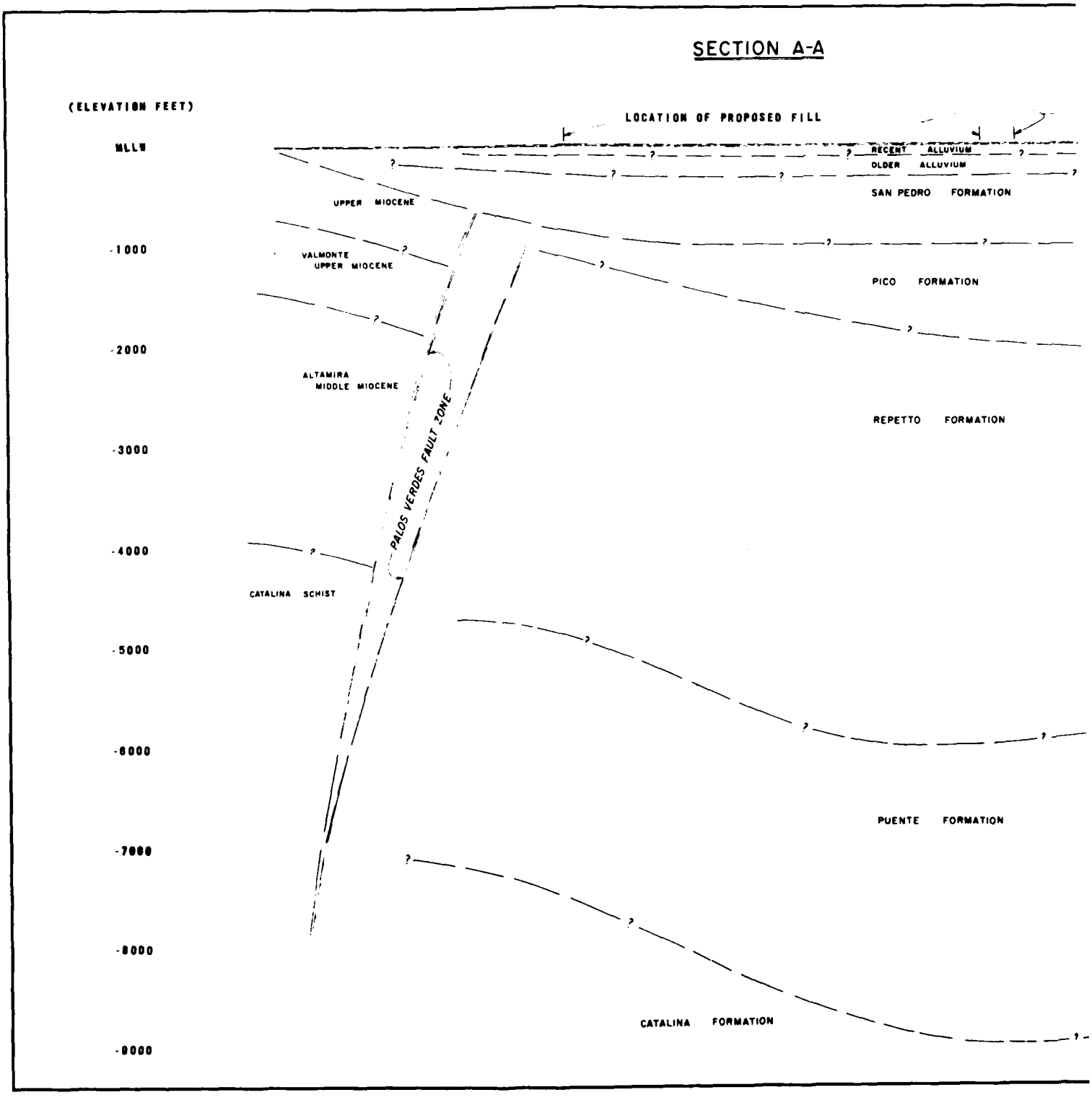
SECTION A-A
(ELEVATION FEET)
MLLW
-1000
-2000
-3000
-4000
-5000
-6000
-7000
-8000
-9000
LOCATION OF PROPOSED FILL
RECENT ALLUVIUM
OLDER ALLUVIUM
SAN PEDRO FORMATION
UPPER MIOCENE
VALMONTE
UPPER MIOCENE
PICO FORMATION
ALTAMIRA
MIDDLE MIOCENE
REPETTO FORMATION
PALOS VERDES FAULT ZONE
CATALINA SCHIST
PUENTE FORMATION
CATALINA FORMATION

SECTION A-A

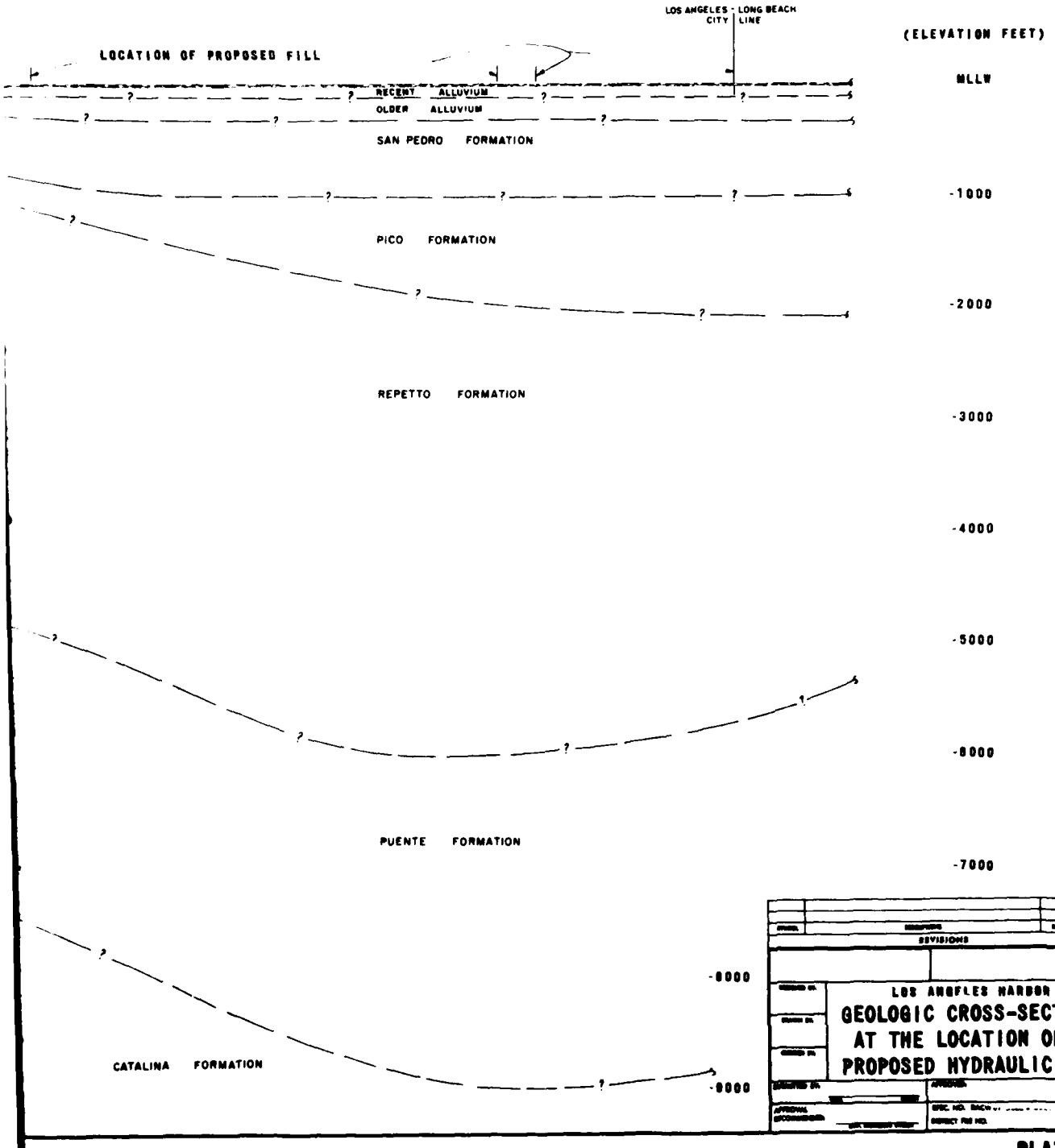

SYMBOL	DESCRIPTION	DATE	APPROVAL
	REVISIONS		

LOS ANGELES HARBOR

GEOLOGIC CROSS-SECTION AT THE LOCATION OF PROPOSED HYDRAULIC FILL

DESIGNED BY | APPROVED | SHEET OF SHEETS

APPROVAL RECOMMENDED | CHIEF, ENGINEERING DIVISION | SPEC. NO. | DRAWING NO. | PROJECT FILE NO.

PLATE 2-3

2

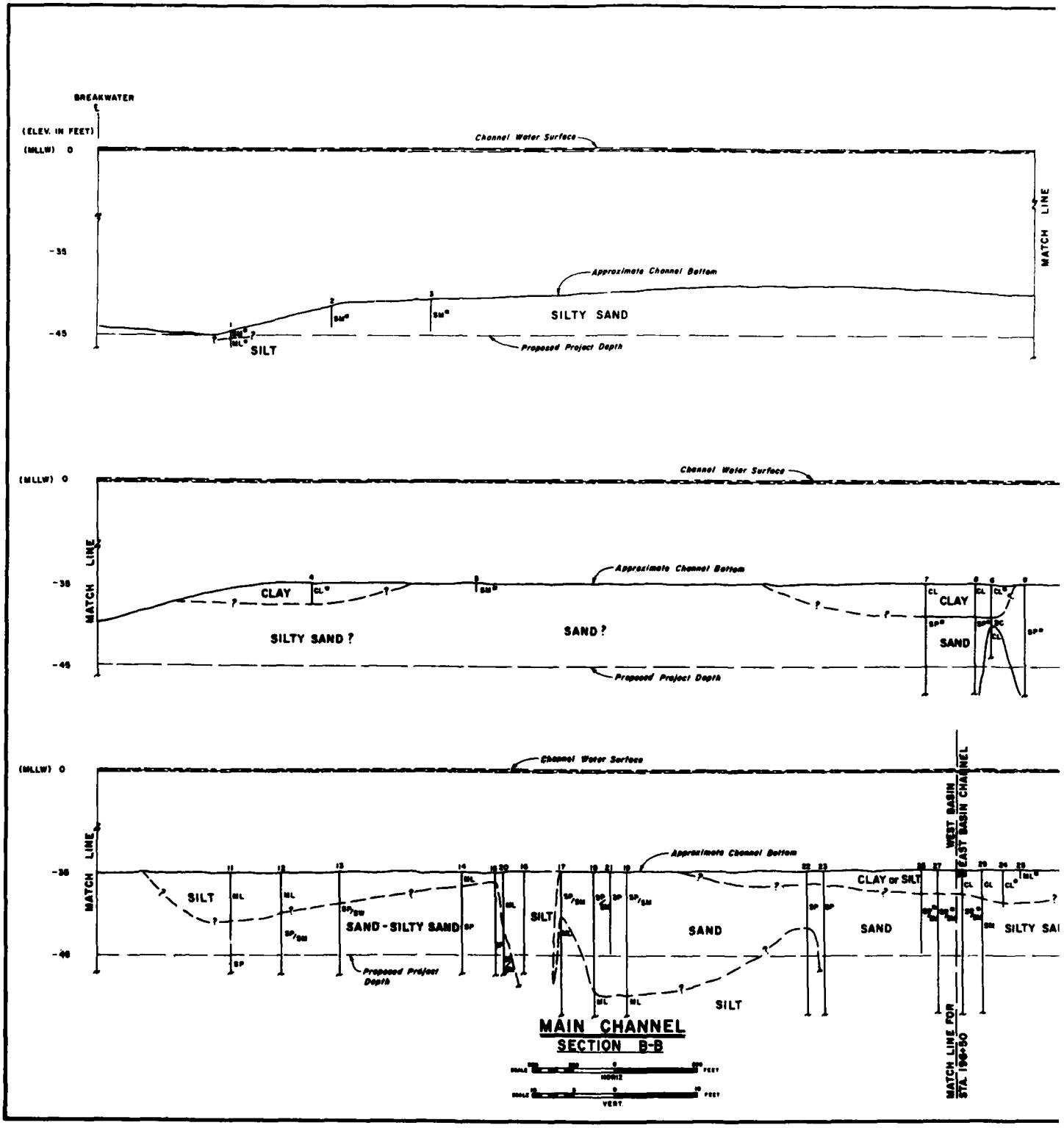
BREAKWATER
(ELEV. IN FEET)
(MLLW) 0
Channel Water Surface
-35
-45
Approximate Channel Bottom
SILTY SAND
SILT
Proposed Project Depth
MATCH LINE
(MLLW) 0
Channel Water Surface
MATCH LINE
-38
-46
Approximate Channel Bottom
CLAY
SILTY SAND ?
SAND ?
CLAY
SAND
Proposed Project Depth
(MLLW) 0
Channel Water Surface
MATCH LINE
-38
-46
Approximate Channel Bottom
SILT
SAND - SILTY SAND
Proposed Project Depth
SILT
SAND
SAND
CLAY or SILT
SILTY SAI
SILT
WEST BASIN
EAST BASIN CHANNEL
MAIN CHANNEL
SECTION B-B
MATCH LINE FOR
STA. 196+50
HORIZ
VERT.

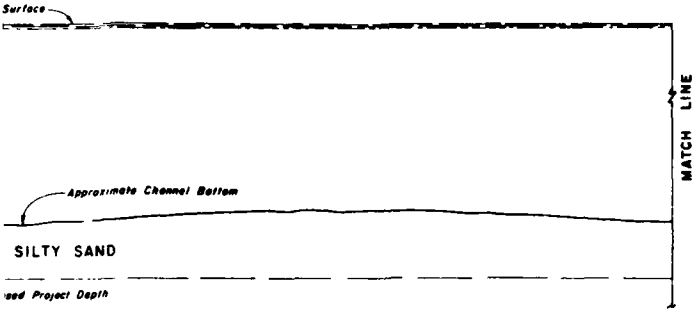

UNIFIED SOIL CLASSIFICATION SYSTEM

MAJOR DIVISIONS			GROUP SYMBOLS	TYPICAL NAMES
COARSE GRAINED SOILS More than half of material is larger than no. 200 sieve size.	GRAVELS More than half of coarse fraction is larger than no. 4 sieve size.	Clean gravels	GW	Well-graded gravels, gravel-sand mixtures, little or no fines.
			GP	Poorly-graded gravels, gravel-sand mixtures, little or no fines.
		Gravels with fines	GM	Silty gravels, gravel-sand-silt mixtures.
			GC	Clayey gravels, gravel-sand-clay mixtures.
	SANDS More than half of coarse fraction is smaller than no. 4 sieve size.	Clean sands	SW	Well-graded sands, gravelly sands, little or no fines.
			SP	Poorly-graded sands, gravelly sands, little or no fines.
		Sands with fines	SM	Silty sands, sand-silt mixtures.
			SC	Clayey sands, sand-clay mixtures.
FINE GRAINED SOILS More than half of material is smaller than no. 200 sieve size.	SILTS AND CLAYS	Low liquid limit	ML	Inorganic silts and very fine sands, rock flour, silty or clayey fine sands, or clayey silts with slight plasticity.
			CL	Inorganic clays of low to medium plasticity, gravelly clays, sandy clays, silty clays, lean clays.
			OL	Organic silts and organic silty clays of low plasticity.
		High liquid limit	MH	Inorganic silts, micaceous or diatomaceous fine sandy or silty soils, elastic silts.
			CH	Inorganic clays of high plasticity, fat clays.
			OH	Organic clays of medium to high plasticity, organic silts.
Highly organic soils			PT	Peat and other highly organic soils.

NOTES:

1. Boundary Classification: Soils possessing characteristics of two groups are designated by combinations of group symbols. For example, GW-GC, well-graded gravel-sand mixture with clay binder.
2. All sieve sizes on this chart are U. S. Standard.
3. The terms "silt" and "clay" are used respectively to distinguish materials exhibiting lower plasticity from those with higher plasticity. The minus no. 200 sieve materials is silt if the liquid limit and plasticity index plot below the "A" line on the plasticity chart (Table VI, Military Standard 619A), and is clay if the liquid limit and plasticity index plot above the "A" line on the chart.
4. For a complete description of the Unified Soil Classification System, see "Military Standard 619A" dated 20 March 1958.

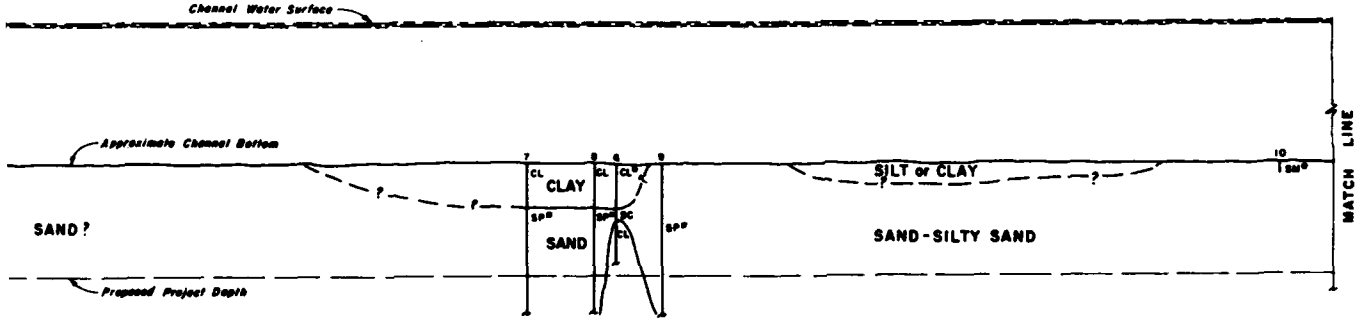

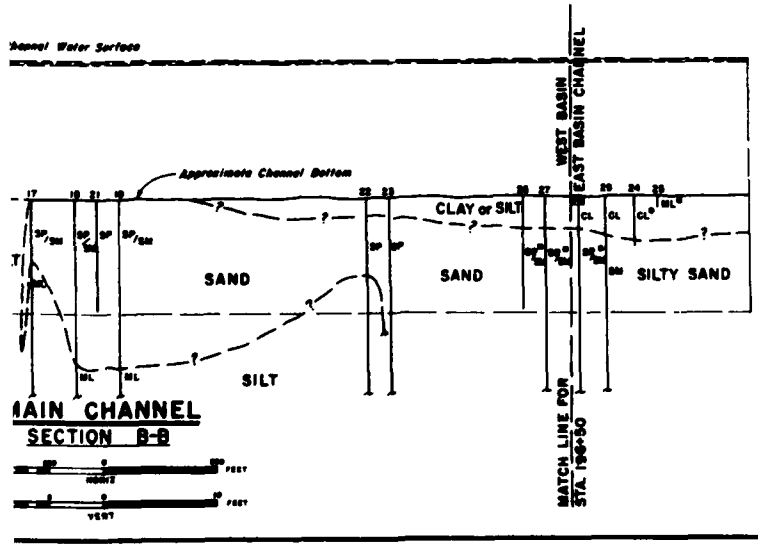

NOTE:

● GRAIN SIZE DISTRIBUTION CURVE AVAILABLE FOR THESE MATERIALS.

DESIGNED	RECOMMENDED	DATE	APPROVED
REVISIONS			
DESIGNED BY	LOS ANGELES HARBOR		
DRAWN BY	MAIN CHANNEL SOIL PROFILE		
CHECKED BY			
QUANTITIES BY	APPROVED		SHEET
APPROVAL RECOMMENDED	ENG. HQ. DWG'S. — PROJECT FILE NO.		OF SHEETS

PLATE 2-4

2

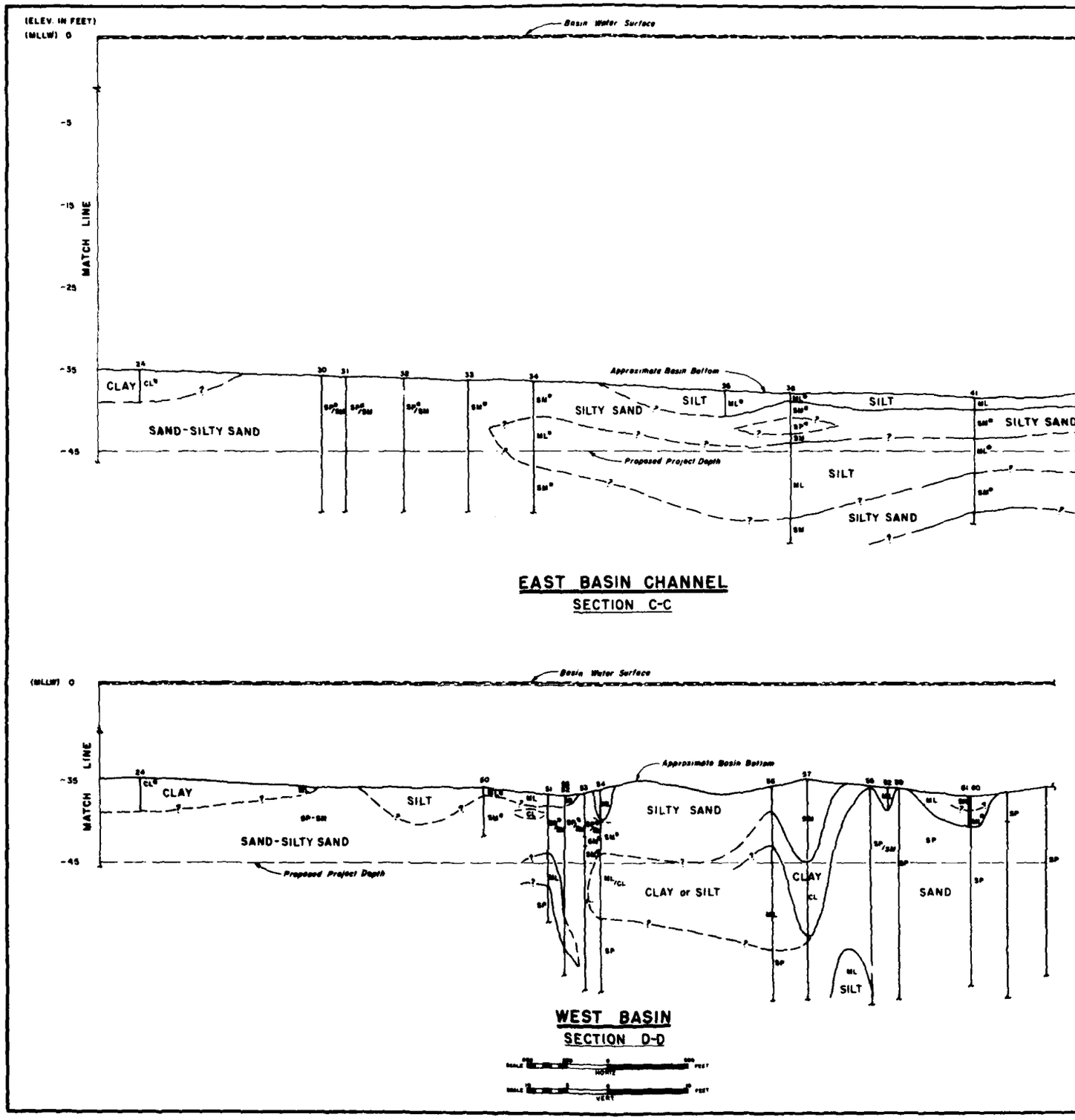
(ELEV. IN FEET)
(MLLW) 0
Basin Water Surface
-5
-15
MATCH LINE
-25
-35
-45
CLAY
SAND-SILTY SAND
Approximate Basin Bottom
SILTY SAND
SILT
Proposed Project Depth
SILT
SILTY SAND
EAST BASIN CHANNEL
SECTION C-C
(MLLW) 0
Basin Water Surface
MATCH LINE
-35
-45
CLAY
SILT
SAND-SILTY SAND
Approximate Basin Bottom
SILTY SAND
Proposed Project Depth
CLAY or SILT
CLAY
SAND
SILT
WEST BASIN
SECTION D-D

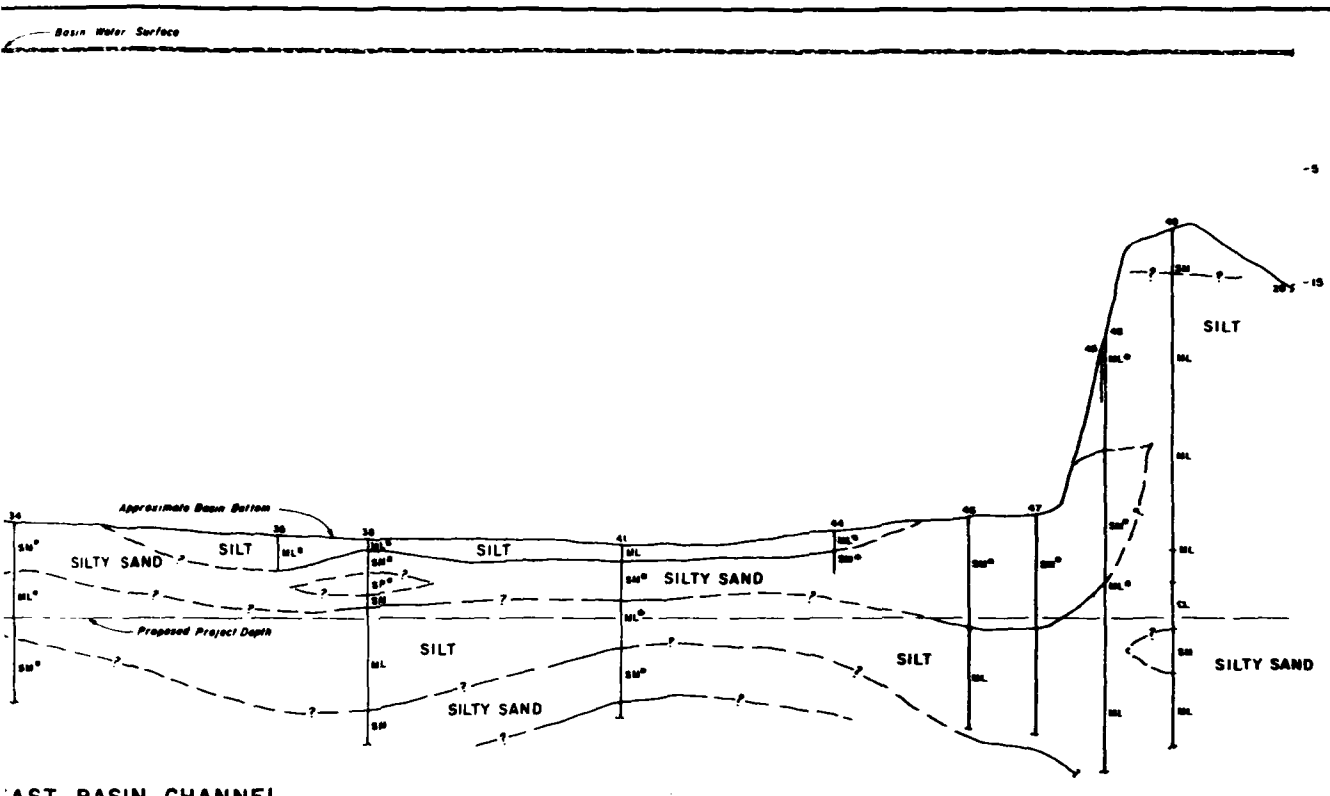

EAST BASIN CHANNEL
SECTION C-C

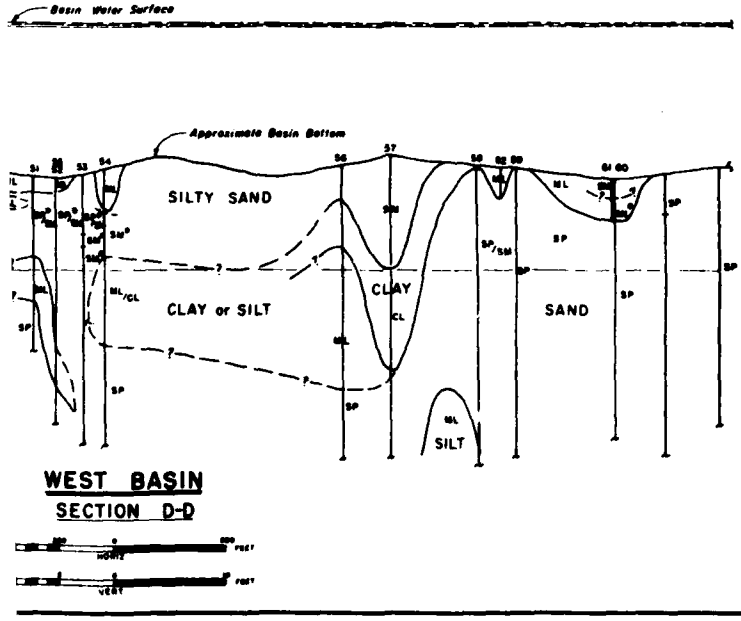

WEST BASIN
SECTION D-D

NOTE:
● GRAIN SIZE DISTRIBUTION CURVE AVAILABLE FOR THESE MATERIALS.

LOS ANGELES

EAST & WEST BASIN
SOIL PROFILES

PLATE 2-5

CHAPTER 3

FIELD AND LABORATORY INVESTIGATIONS

Field Investigation.

The field investigation consisted of excavating two test trenches, TT 74-1 and 2, in the existing hydraulic fill materials immediately north of the proposed fill site. The main purpose of the exploration was to obtain samples similar to the materials in the area to be dredged for laboratory testing under cyclic loading conditions. The approximate locations of the two test trenches are shown on plate 2-2. Both trenches were excavated to a depth of approximately 6 feet, at which point ground water was encountered and further excavation was impractical. Caving was a major problem even with very shallow excavations due to the looseness of the materials.

The test trenches were logged and disturbed samples of representative material obtained for laboratory classification tests. In addition, approximately 100 pounds of each of the three major soil types, sand, silty sand and clay or silt were obtained for detailed laboratory testing. A summary of the soil conditions encountered in each test trench is presented in table 3-1.

The materials in test trench 1 were primarily clean fine grained non-plastic sands to a depth of 4 feet. At a depth ranging from 4 to 6 feet the sands changed color from buff to gray and occasional silt or clay lenses were present. The materials in test trench 2 were predominately fine grained non-plastic borderline sands-silty sands to a depth of 4 feet. At a depth ranging from 4 to 5 feet the materials were gray fine grained non plastic silty sands.

TABLE 3-1

Summary of Soil Conditions in Recent Investigations

Test Trench No.	Depth (ft)	Classification	Mechanical Analysis (% passing) No. 4	No. 40	No. 200	Atterberg Limits LL	PI
1	0-2	Sand (SP)	100	88	3	--	NP
	2-4	Sand (SP)	100	92	3	--	NP
	4-4.5	Sandy Clay (CH)	100	92	77	57	35
	4.5-6	Sand (SP)	100	90	3	--	NP
2	0-2	Sand-Silty Sand (SP/SM)	100	93	7	--	NP
	2-4	Sand-Silty Sand (SP/SM)	100	96	8	--	NP
	4-5	Silty Sand (SM)	100	100	43	--	NP

Laboratory Investigation

The laboratory testing of the samples was divided between the Soil Mechanics Laboratory at the University of California, Los Angeles (UCLA) and the Los Angeles District, Army Corps of Engineers laboratory. The grain size tests and compaction studies were performed at the Corps laboratory, and all cyclic load tests were performed at UCLA.

Previous studies have shown that clay soils are not as susceptible to liquefaction under cyclic loading as sands and since the clays makeup a small percentage of the total dredge material, samples of clay were not tested. The cyclic triaxial testing program was conducted on the fine grained sand and silty sands. Since the materials in the proposed fill will be primarily silty sands, the testing program on the sand was less extensive than that for the silty sand.

Grain Size Distribution

The range in grain size distribution curves for the disturbed samples tested are shown in figure 3-1. Also shown in this figure is the range of the blended materials from the proposed dredge area, which indicates that the materials sampled and tested are representative of the material to be dredged from the channels and basins.

Maximum Density Tests

Maximum density values were determined using three precedures: impact compaction by the modified AASHO test procedure, vibratory compaction of saturated soil, and vibratory compaction of oven dry soil. The compaction studies were performed on the composite samples of sand, silty sand, and sandy clay taken from the test trenches.

The dry vibratory compaction method consisted of placing approximately 400 grams of oven dry soil into a 1,000 cc graduate cylinder and vibrating until a minimum volume was obtained. The wet vibratory compaction was developed to simulate the saturated field condition. In this method, approximately 400 grams of oven dry soil were slowly deposited in a 1,000 cc graduate cylinder fill with clear water. When the soil had fully settled, the graduate was vibrated until a minimum volume was obtained. Using the minimum volumes determined by both methods, the maximum densities were calculated.

The results of these three types of maximum density tests on seven different samples of fill material, along with the D_{50} grain size, and the percent of material passing the U.S. Standard No. 200 sieve are presented in table 3-2. Comparison of this maximum density data indicates that for the sands, the highest density was obtained by vibration of a dry sample, and for the silty sands and clay the highest density was obtained by the modified AASHO test procedure.

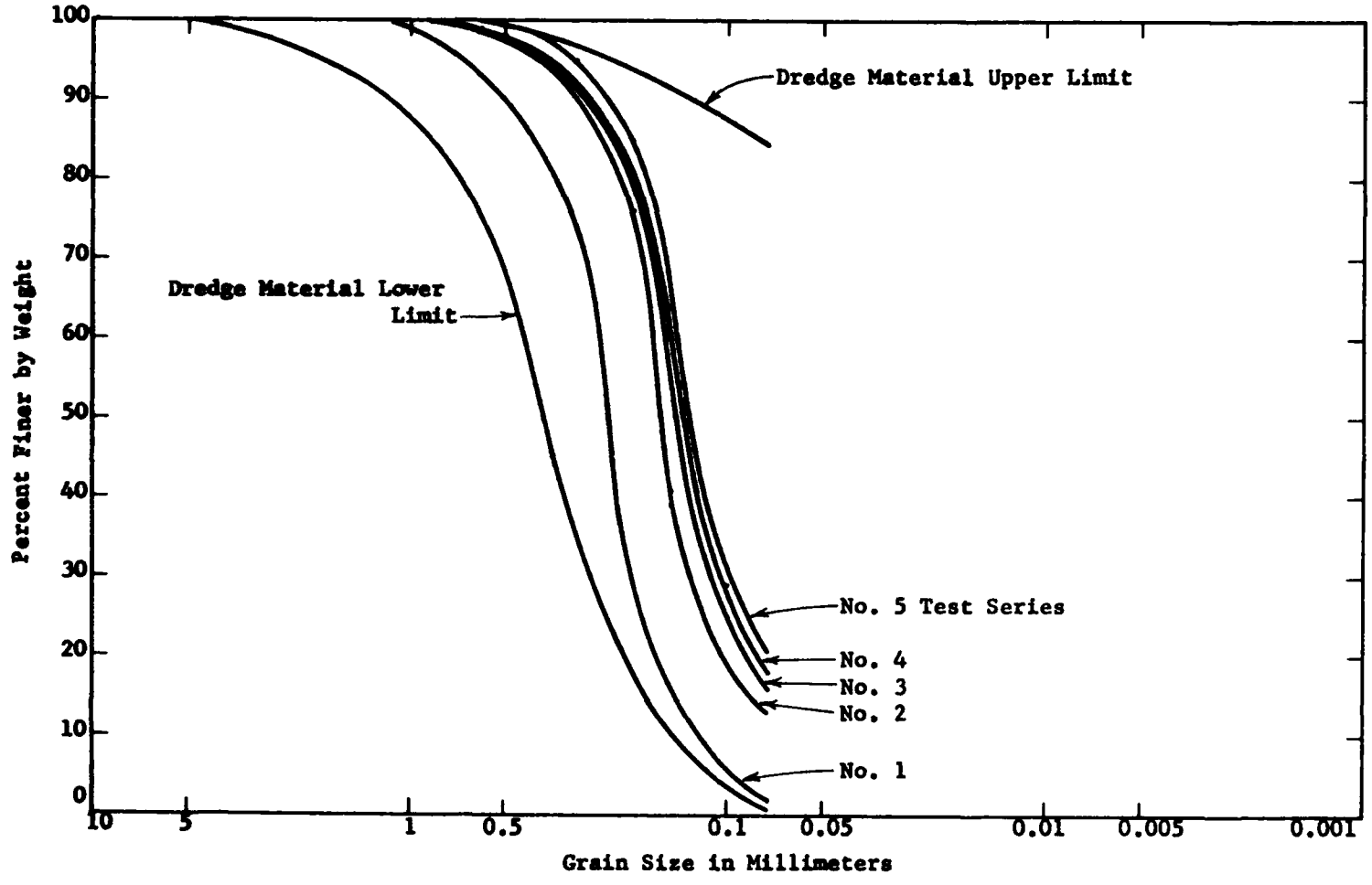

FIG. 3-1 COMPARISON OF THE SAMPLES USED FOR TESTING TO THE UPPER AND LOWER LIMITS OF THE BLENDED DREDGE MATERIAL

TABLE 3-2

Results of Maximum Density Tests

Maximum Density Method	Classification	No. 200 (% passing)	D_{50} (MM)	Maximum Dry Density (pcf)	Optimum Moisture Content (%)
Modified AASHO	Sand (SP)	3	0.2	102.4	15.5
Modified AASHO	Silty sand (SM)	25	0.12	111.9	11.8
Modified AASHO	Sandy clay (CL)	64	0.045	122.8	11.5
Vibrated wet	Sand (SP)	4	0.2	104.2	—
Vibrated wet	Sand (SP)	5	0.18	102.0	—
Vibrated dry	Sand (SP)	2	0.2	106.0	—
Vibrated dry	Silty sand (SM)	13	0.15	106.0	—

Minimum Density Tests

Two different types of minimum density tests were performed on the sands and silty sands. The first method used was to place approximately 400 grams of oven dried soil into a 1,000 cc graduate cylinder. The cylinder was then very slowly rocked end for end and then slowly rotated to thoroughly stir the soil into a loose state. The second method was developed to try and simulate the saturated field condition where the soils are deposited in water. In this method, approximately 400 grams of oven dry soil were slowly deposited into a 1,000 cc graduate cylinder filled with clear water. The final volume of soil which settled to the bottom of the graduate was read and the minimum density calculated. This procedure may introduce some error since it caused particle size segregation, with the coarse soil settling out faster than the finer portion. Densities by this method were slightly higher than the minimum densities obtained by rotating the dry soil.

The results of these two types of minimum density tests on composite samples of fill material, along with the D_{50} grain size, and the percent of material passing the U.S. Standard No. 200 sieve are presented in table 3-3.

TABLE 3-3

Results of Minimum Density Tests

Minimum Density Method	Classification	No. 200 (% passing)	D_{50} (MM)	Minimum Dry Density (pcf)
Rotated dry	Sand	2	0.2	85.5
Rotated dry	Silty sand	16	0.14	76.0
Sedimentation	Sand	4	0.2	86.0
Sedimentation	Sand	5	0.18	82.8

Relative Density

The best fit curves for the maximum and minimum density test data discussed previously are presented together in figure 3-2 for comparison purposes. It may be seen that they form a consistent pattern of increasing maximum density and decreasing minimum density with decreasing mean grain size.

From this data, the relative density for absolute field density data at a given D_{50} grain size may be computed. This is done using the relationship given in equation (3-1).

$$D_r = \frac{\gamma_{d\ max}}{\gamma_d} \left(\frac{\gamma_d - \gamma_{d\ min}}{\gamma_{d\ max} - \gamma_{d\ min}} \right) \times 100\% \qquad (3\text{-}1)$$

Where $\gamma_{d\ max}$ = Maximum laboratory density

$\gamma_{d\ min}$ = Minimum laboratory density

γ_d = Absolute field density

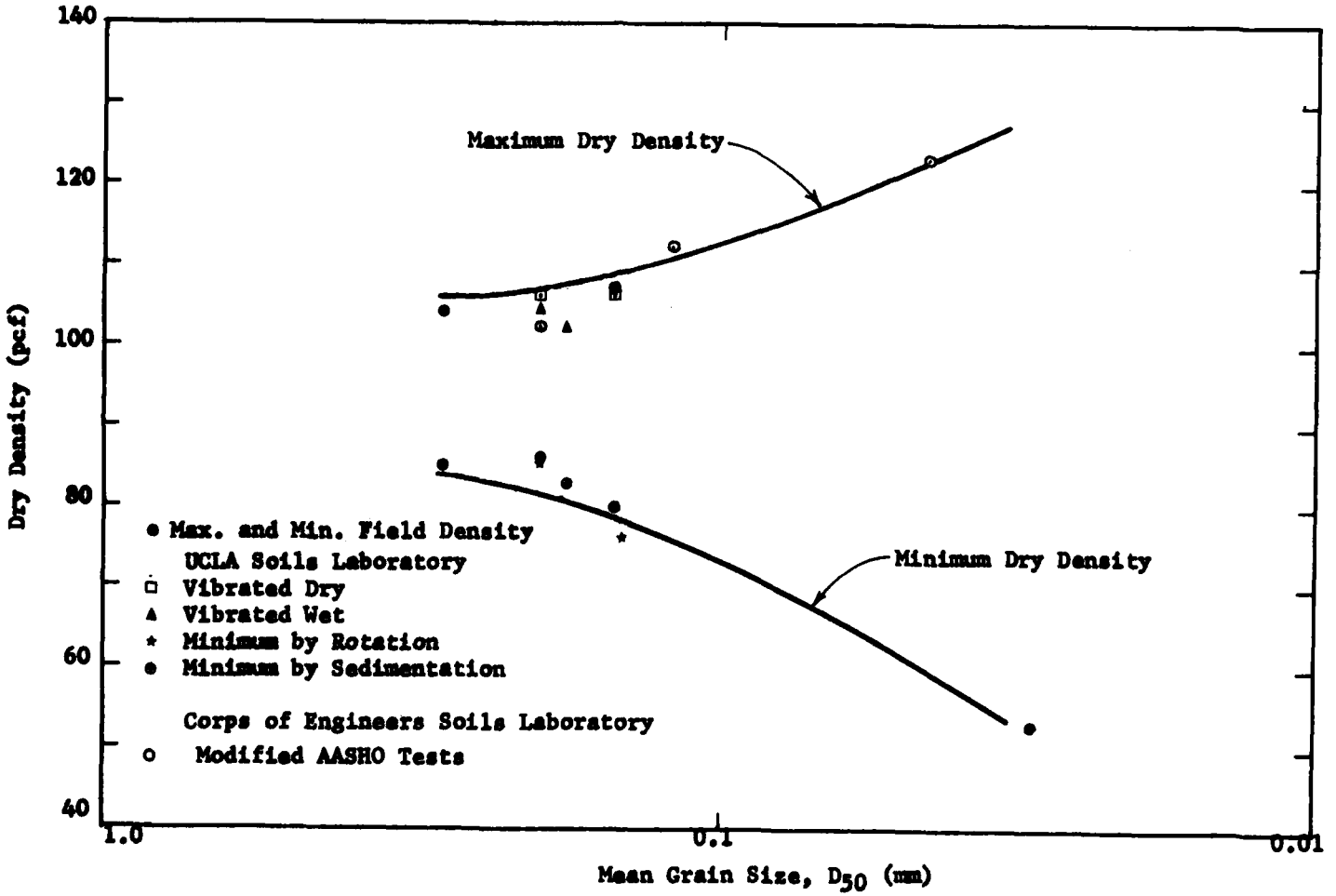

FIG. 3-2 COMPARISON OF THE RESULTS OF MAXIMUM AND MINIMUM DENSITY TESTS ON SAMPLES OF HYDRAULIC FILL MATERIAL

The estimated relative density of the proposed hydraulic fill would range from 23 to 80 percent, with a median value of 59 percent. This estimate was based on the average of the median blended grain size distribution curves shown in figures 2-5 through 2-7 and the median dry density shown in figure 2-10. The estimated relative densities of the sands and silty sands were determined for the upper and lower field density values using the mean grain size curves determined from figures 2-2 and 2-3. The range in field densities are presented in figure 3-3 along with the maximum and minimum density test results.

Cyclic Loading Tests

A total of 13 cyclic loading triaxial tests were performed on soil samples taken from the existing hydraulic fill. Since undisturbed sampling was impossible, the specimens were remolded to dry densities representative of the existing median dry density values. Dry densities of 92 and 95 pcf, corresponding to relative densities of 42 and 60 percent, were used for the sand and silty sand, respectively. In addition, several tests were conducted on silty sand samples remolded to dry densities ranging up to approximately 100 pcf which corresponds to relative density of approximately 74 percent. These higher density samples were tested to evaluate the effects on strength of slightly higher densities.

The test specimens were each approximately 2.8 inches in diameter and 6 inches in height and consisted of sands and silty sands which were passed through a U.S. Standard No. 4 sieve to remove any large shells. These materials were first oven dried then sufficient material carefully weighed out to produce the correct density specimen in a predetermined volume. This weighed soil was then de-aired by placing the materials into flasks partially filled with de-aired water and boiled under a vacuum for approximately 15 minutes to remove all air. This water-soil mixture was allowed to cool while under the vacuum and then topped-off with de-aired water and plugged. It took four flasks to construct one sample. Each flask, in turn, was then inverted into the mouth of a de-aired water filled mold, the plug removed, and the soil allowed to flow down from the flask to the mold, entirely under water.

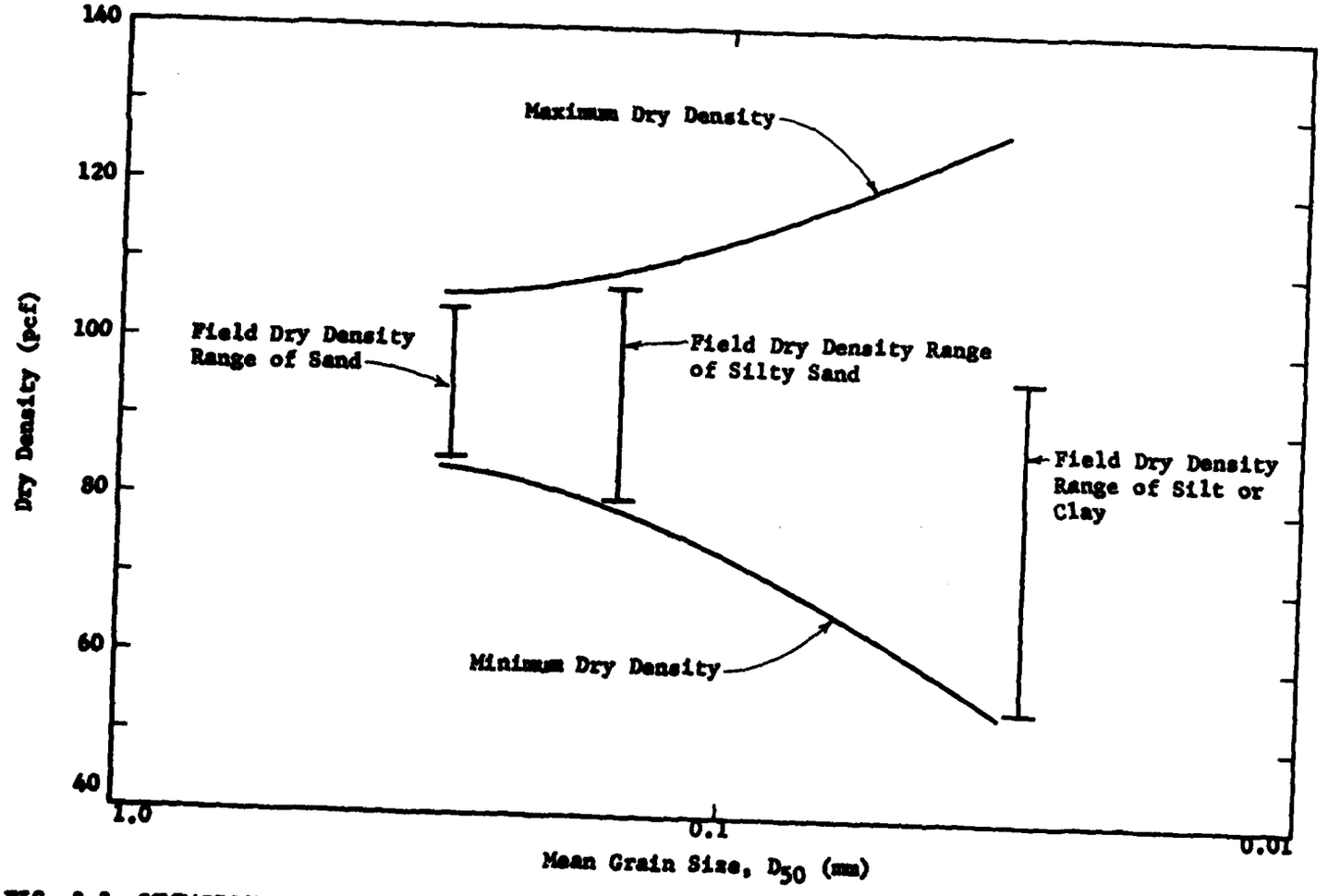

FIG. 3-3 COMPARISON OF THE RANGE IN FIELD DRY DENSITIES TO THE MAXIMUM AND MINIMUM DENSITY TEST RESULTS.

This method of sample preparation was slightly modified for the silty sands in order to prevent the loss of fines and minimize segregation of various sizes. This involved using the fines, which had remained in solution from the preceeding specimen preparation, and placing them into the mold in the form of a de-aired muddy water instead of the clean de-aired water previously used. The layering and grain size segregation was kept to a minimum during sample preparation by placing the neck of the flask deep in the mold and keeping it close to the sample surface.

These specimens were than measured, placed in a standard triaxial cell with top and bottom drainage, and consolidated under isotropic stress conditions using two consolidation pressures; 6.5 and 13.5 psi. Tests conducted on isotropically consolidated samples are intended to simulate a field condition in which there is no initial static shear stress acting on a horizontal plane prior to the earthquake. This stress condition is typical of hydraulic fills with level surfaces (ref. 8).

A summary of the density values attempted and those actually obtained along with the initial test conditions for each test specimen and the number of stress cycles to cause liquefaction are presented in table 3-4. Also given in this table is a test series number which indicates the corresponding gradation curve for the sample presented in figure 3-1.

TABLE 3-4

Summary of Cyclic Test Data

Test Series	Test No.	Soil Type	Dry Density Attempted (pcf)	Dry Density Obtained (pcf)	Effective Confining Pressure (psi)	Deviator Stress (psi)	Cycles to Failure
	1	Sand	92	91.9	6.5	1.93	39
1	2	Sand	92	90.5	6.5	2.5	21
	3	Sand	92	91.2	6.5	3.75	7
	4	Silty Sand	95	93.2	6.5	2.0	46
2	5	Silty Sand	95	94.2	6.5	2.5	19
	6	Silty Sand	95	93.1	6.5	3.75	3
	7	Silty Sand	95	93.9	13.0	4.0	3
3	8	Silty Sand	95	94.6	13.5	2.5	122
	9	Silty Sand	95	94.7	13.5	3.75	11
	10	Silty Sand	100	98.7	6.5	2.5	15
4	11	Silty Sand	100	97.3	6.5	2.0	21
	12	Silty Sand	100	100.8	14.0	3.75	53
5	13	Silty Sand	100	98.1	13.0	4.25	9

The behavior of saturated cohesionless materials subject to cyclic loading triaxial tests has been described in other publications (refs. 8, 9, 10) and will not be discussed in this report. However, to illustrate the methods used to reduce the data, the following discussion is presented.

A typical plot of measurements made during cyclic load testing is presented in figure 3-4 for illustrative purposes. Using this information, it has been found convenient to plot the maximum pore pressure and respective peak to peak strain developed in different numbers of stress cycles. The typical test results, on six of the samples tested, are shown in figures 3-5 and 3-6 as well as the number of stress cycles required to cause liquefaction, N_l for different values of the cyclic deviator stress, σ_{dp} . The pore pressure values are presented as the ratio of the change in pore pressure, Δu , to the initial consolidation stress, σ_{3c} , a maximum pore pressure ratio, $\frac{\Delta u}{\sigma_{3c}}$, of 1 represents initial liquefaction. These figures also indicate that the strength data for an axial strain of plus or minus 2-1/2 percent is quite close to that for initial liquefaction.

A comparison of the strengths of the sand and the silty sand under cyclic loading conditions is presented in figure 3-7. It may be seen that at the same confining pressure the sand is stronger than the silty sand under cyclic loading even though the sand was at the lower relative density of 42 percent compared to 59 percent for the silty sand. As a result of this finding, no further cyclic loading tests were performed on the sand.

The results of all the cyclic loading tests on silty sand samples are plotted in figure 3-8 in terms of the cyclic stress ratio, $\frac{\sigma_{dp}}{2\sigma_{3c}}$, to eliminate the effect of small changes in the confining pressure. This figure presents two curves for the material at dry densities of approximately 94.5 pcf and confining pressures of 6.5 and 13.5 psi. All of the data at the low confining pressure define a relatively smooth curve typical of cyclic loading test results obtained in other investigations. The data obtained at the higher confining pressure showed slightly more scatter and produced a curve with a relatively flatter slope.

The cyclic loading tests on similar materials at higher densities indicated no change in strength at low confining pressures and an increase in strength of approximately 25 percent at the higher confining pressure.

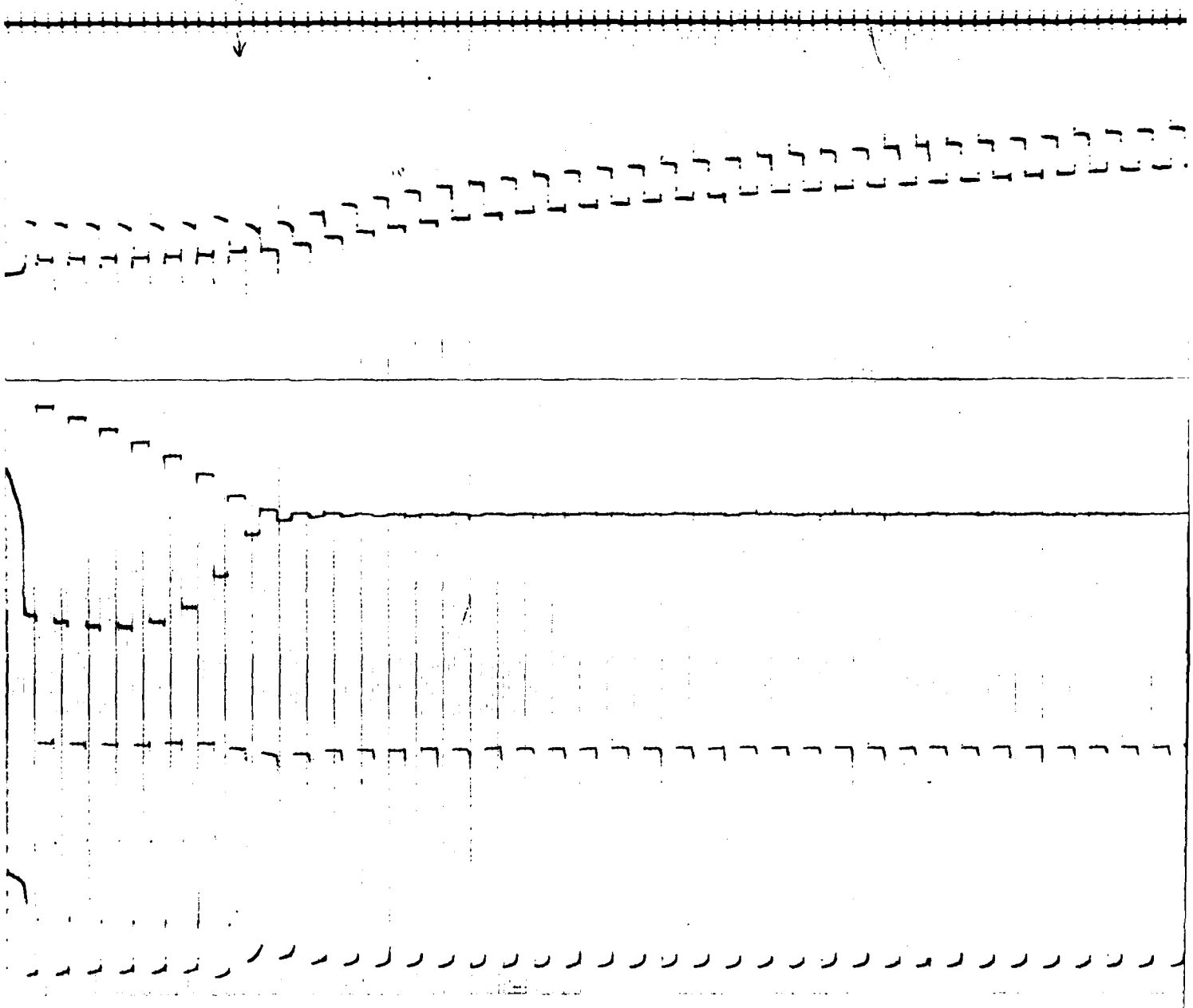

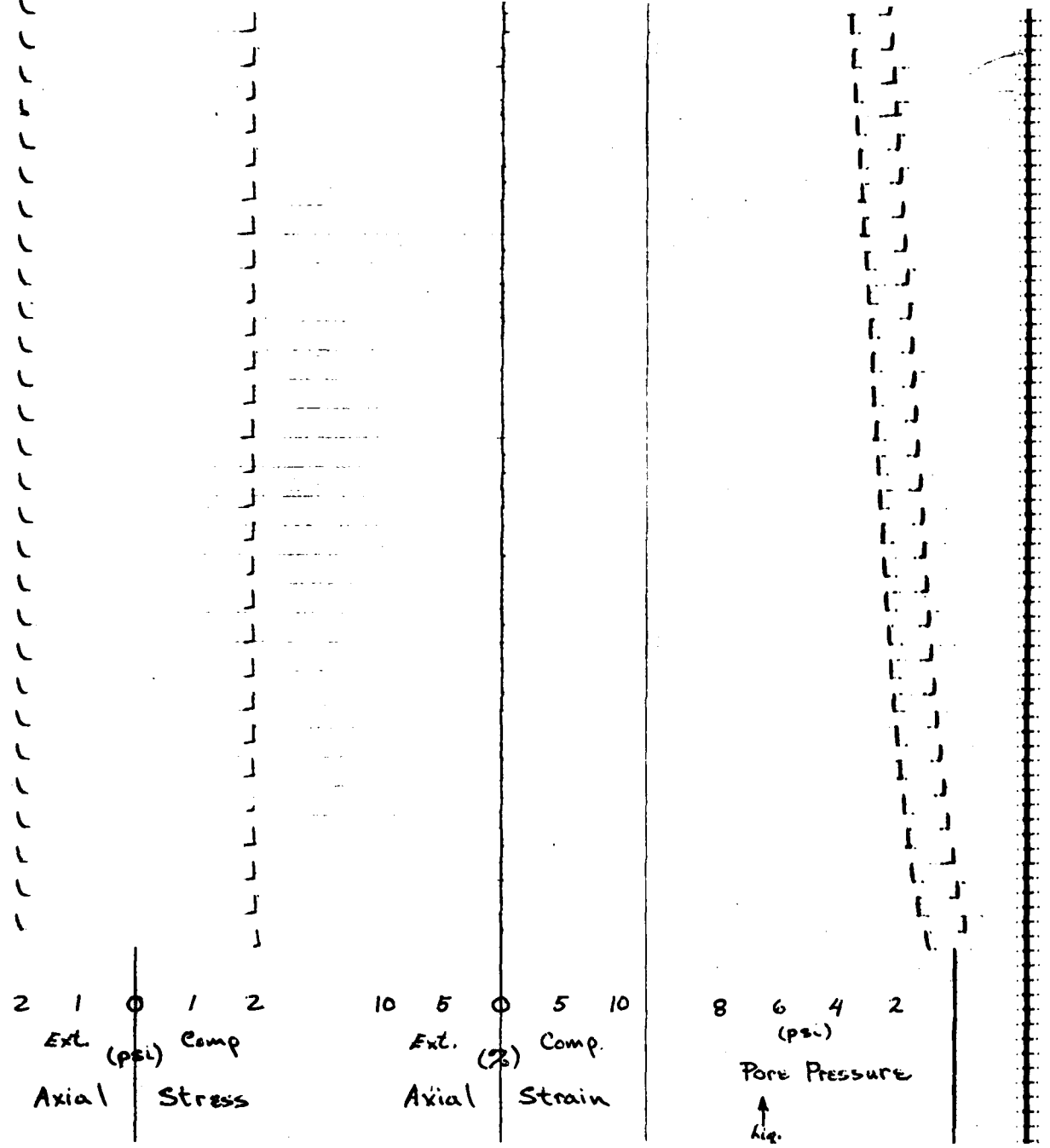

FIG. 3-4 TYPICAL PLOT OF MEASUREMENTS MADE DURING CYCLIC LOAD TRIAXIAL TESTING - TEST 74-4

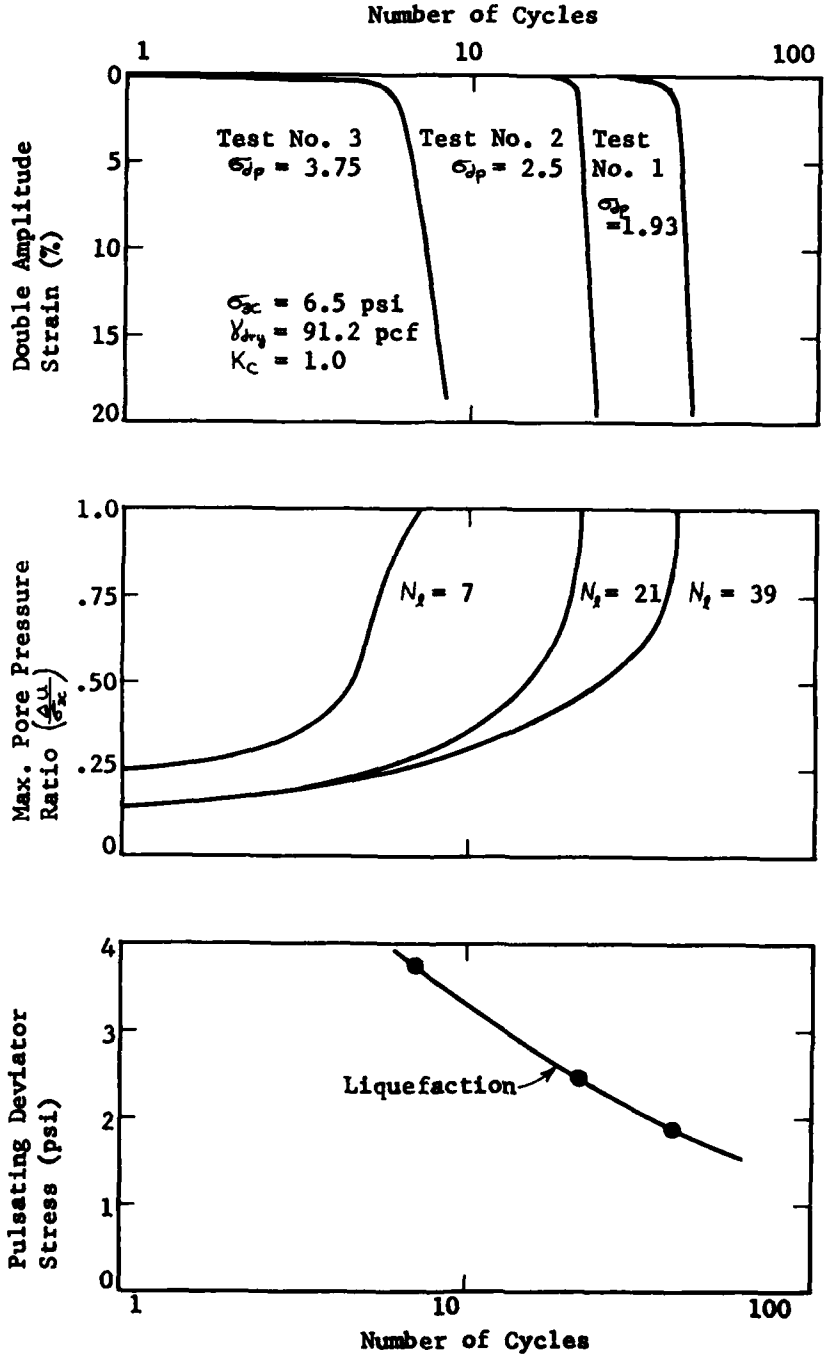

FIG. 3-5 RESULTS OF CYCLIC LOAD TESTS ON ISOTROPICALLY CONSOLIDATED SAMPLES OF SAND - TEST SERIES NO. 1

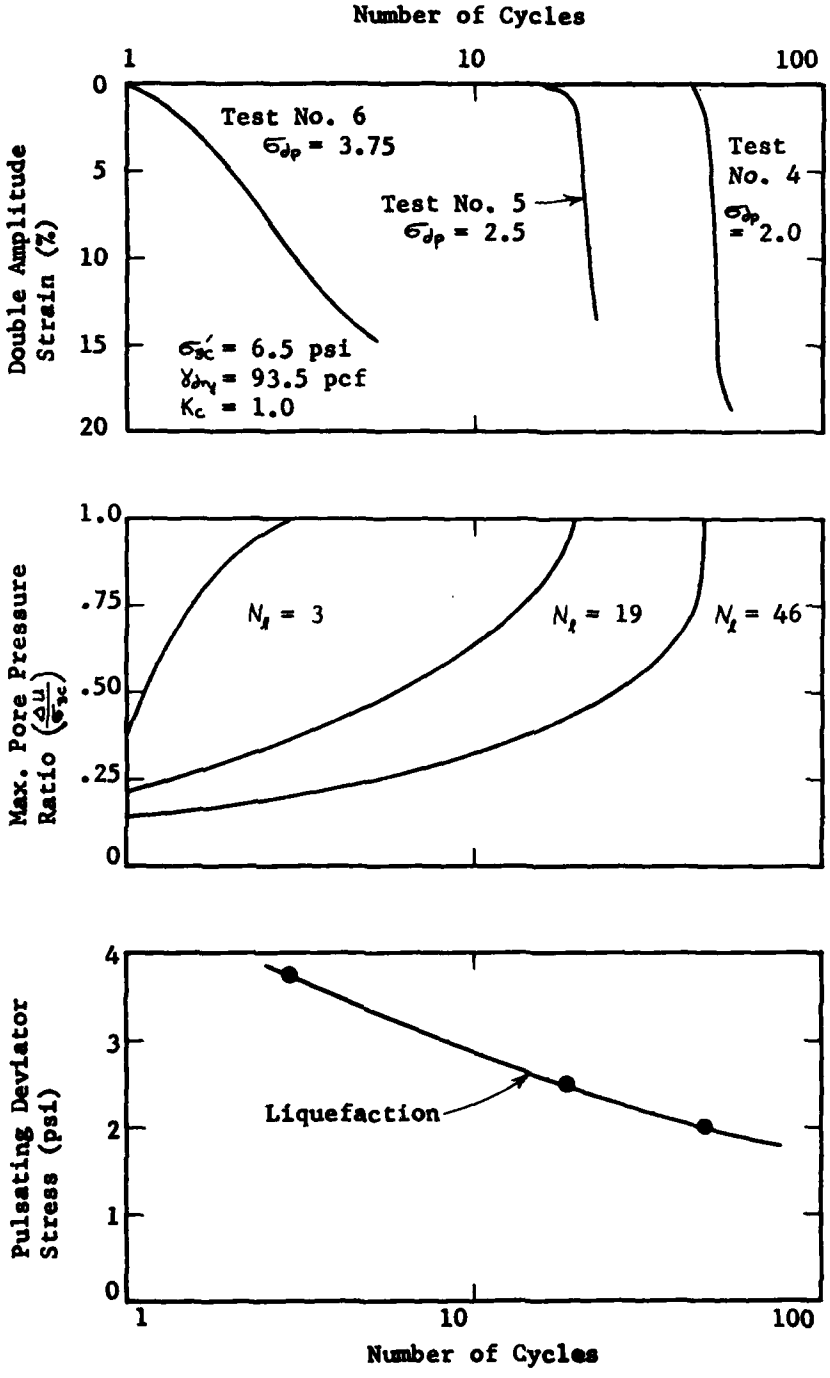

FIG. 3-6 RESULTS OF CYCLIC LOAD TESTS ON ISOTROPICALLY CONSOLIDATED SAMPLES OF SILTY SAND - TEST SERIES NO. 2

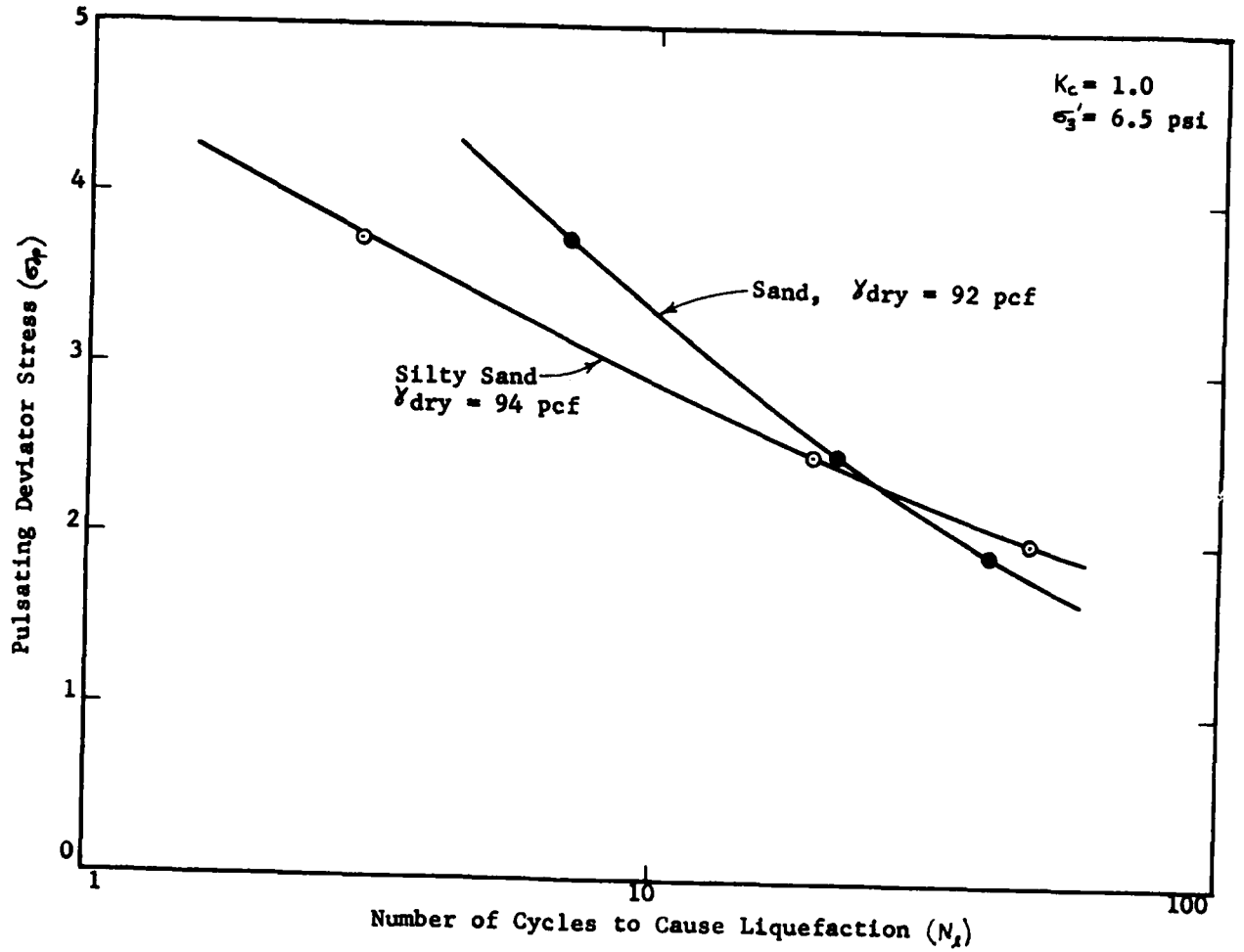

FIG. 3-7 COMPARISON OF THE STRENGTHS OF SAND AND SILTY SAND UNDER CYCLIC LOADING

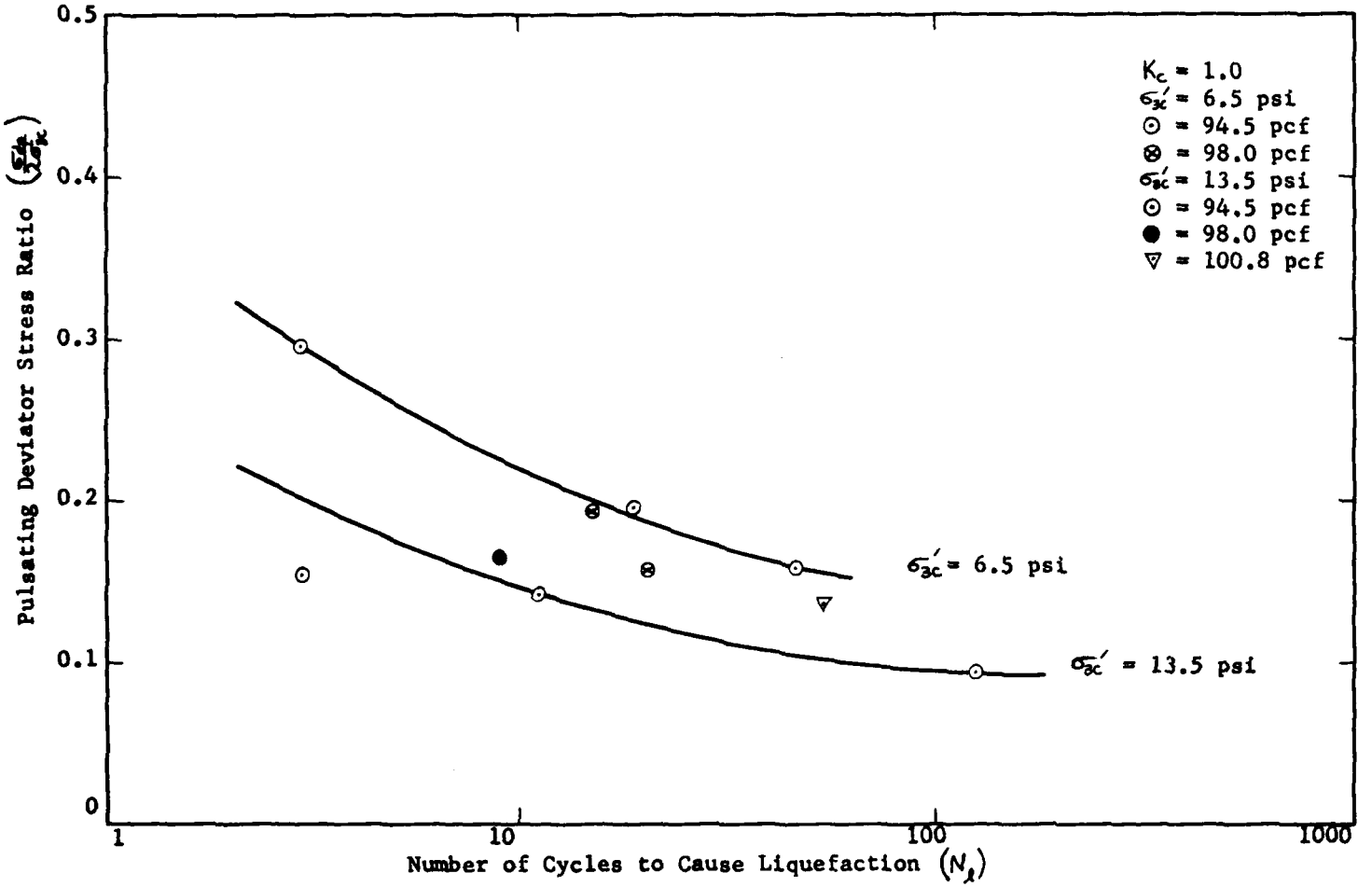

FIG. 3-8 SUMMARY OF THE TEST RESULTS FOR ALL SILTY SAND SAMPLES TESTED UNDER CYCLIC LOADING

The stress ratios causing liquefaction at 10 and 30 cycles for the silty sand, are compared to similar data for sand determined by Seed et. al. in figure 3-9 (ref. 8). In order to make this comparison, it was necessary to adjust the stress ratios given in figure 3-8 to represent the strengths at a relative density of 50 percent. This adjustment was made through the direct relationship which exists between strength and relative density (ref. 8). The comparison indicates that there is a good strength agreement at a confining pressure of 6.5 psi, but the strength determined at the higher confining pressure of 13.5 psi is somewhat lower. However, it should be noted that slight deviation from this established data can be expected due to the difference in strength characteristics exhibited by different soil types, as indicated in figure 3-5.

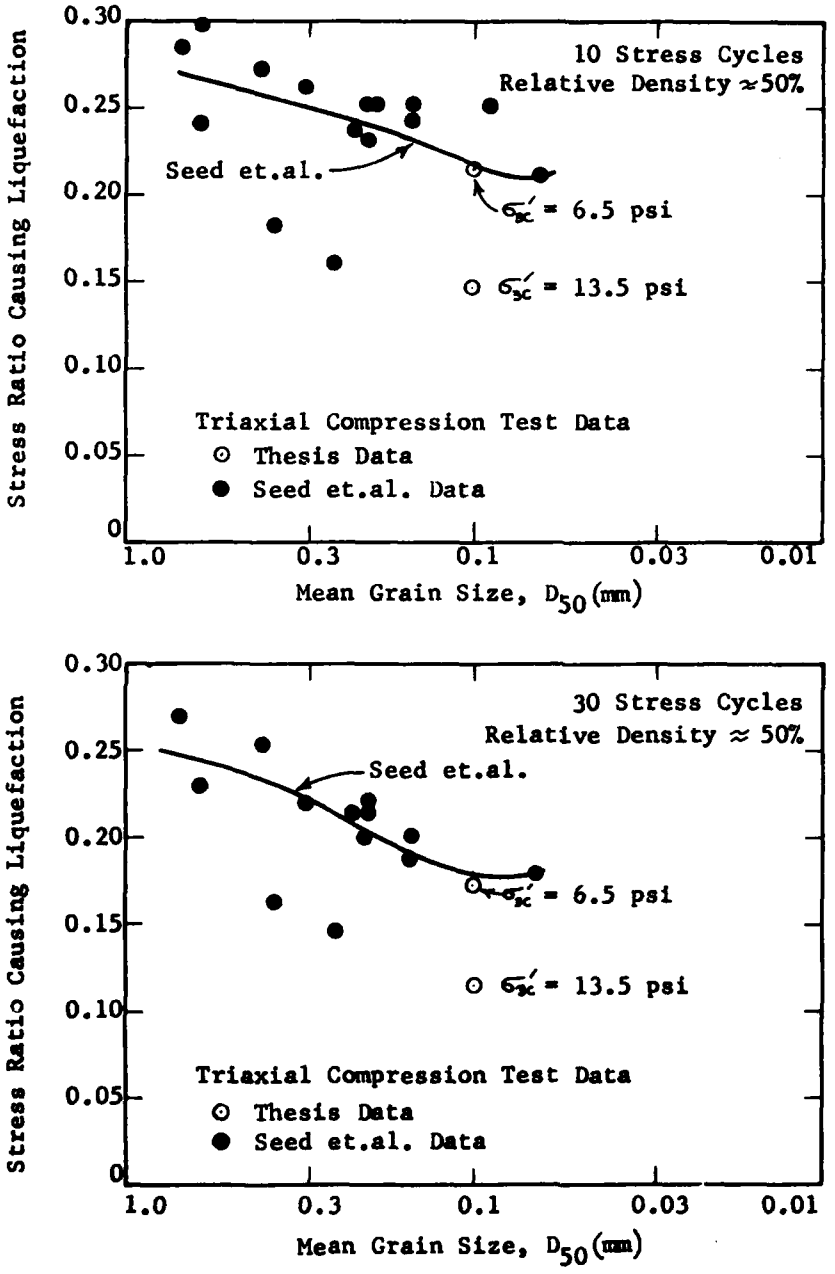

FIG. 3-9 COMPARISON OF LOS ANGELES HARBOR SILTY SAND TEST DATA TO THE STRESS CONDITIONS CAUSING LIQUEFACTION OF SANDS IN 10 AND 30 CYCLES (SEED AND IDRISS)

CHAPTER 4

EARTHQUAKE SELECTION

Magnitudes and Locations

The principal active and potentially active faults in the Los Angeles Basin, their maximum earthquake generating capability and the maximum anticipated bedrock accelerations at the study site are presented in table 4-1. The three faults which are of greatest significance to the Los Angeles Harbor are listed below.

a. The Palos Verdes Fault because it transverses the study area.

b. The Newport-Inglewood Fault because of the very high ground motions which may develope and because of the faults close proximity to the site.

c. The San Andreas Fault because it has a high probability of occurrence and is expected to generate one of California's "great earthquakes".

This report deals with these three faults because they are the most critical based on probability of occurrance and potential damage to the Los Angeles Harbor area. Significant earthquakes may also occur on other faults, however, the data presented in table 4-1 indicates that their effect on the harbor area will probably be of less significance than those selected for analysis. Figure 4-1, shows the locations of the major faults in the Los Angeles Basin.

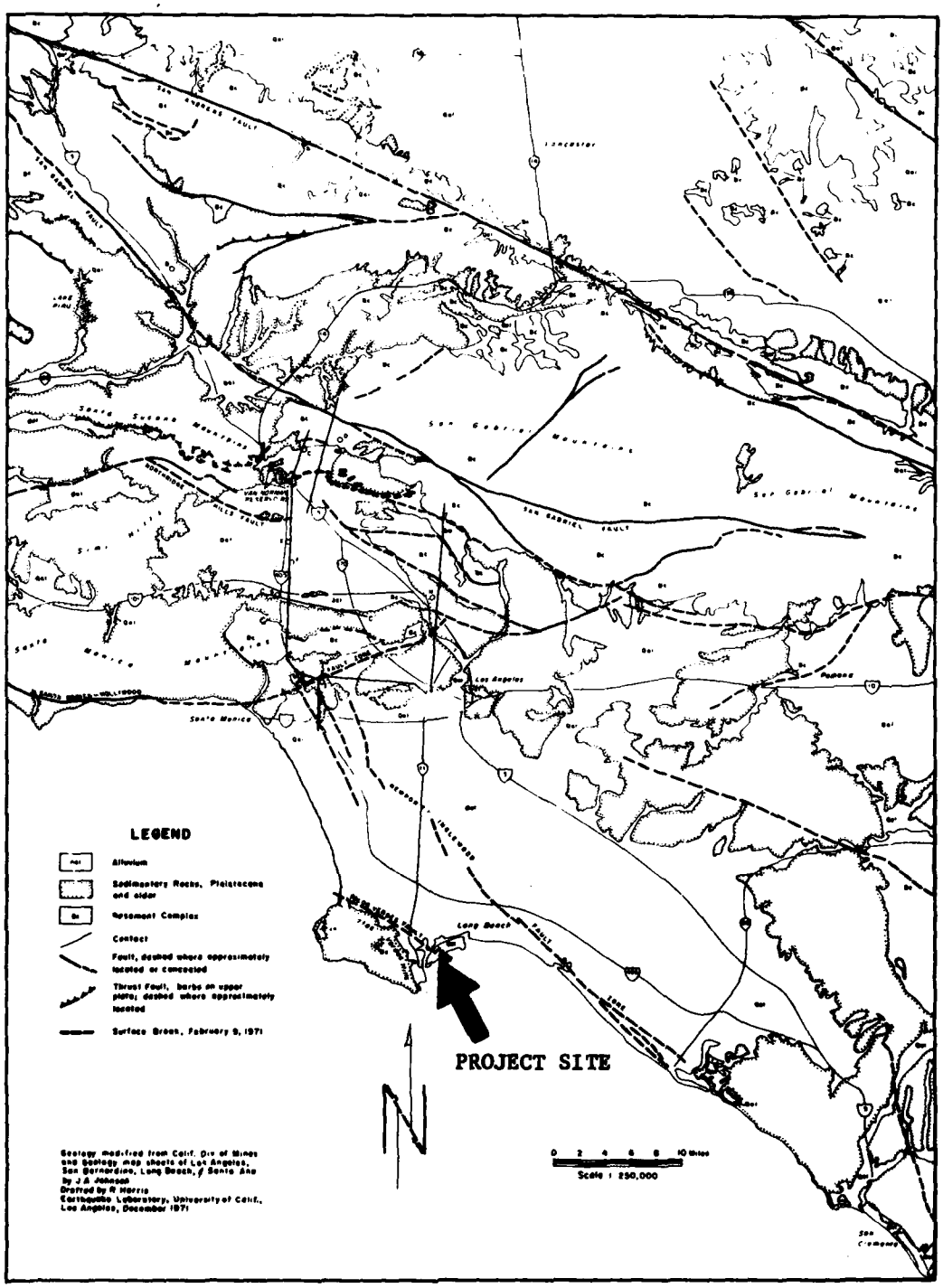

FIG. 4-1 FAULT AND GENERALIZED GEOLOGIC MAP OF THE LOS ANGELES AREA

TABLE 4-1

Summary of Major Faults in the Los Angeles Area

Fault	Closest Distance from site (miles)	Maximum Credible Richter Magnitude*	Maximum Rock Acceleration (g)**
Newport-Inglewood	6.5	7.0	0.47
Whittier	23.0	6.5	0.16
San Fernando-Sierra Madre	32.5	7.0	0.05
San Andreas	52.0	8.5	0.15
San Jacinto	59.0	7.0	0.05
Palos Verdes	0.0	6.0	0.6

*Maximum credible Richter Magnitude was determined from the Bonilla relationship (ref. 14).

**Maximum rock acceleration was determined from the Schnabel and Seed relationship (ref 15) shown in figure 4-3.

Long Beach Earthquake. The Long Beach earthquake of March 10, 1933 is the largest earthquake to effect the harbor complex within historic time. The Richter Magnitude was 6.3, and the epicenter was located off Newport Beach approximately 3 to 4 miles southwest of the surface trace of the Newport-Inglewood Fault. Rupture did not extend to the surface, however, subsurface movement of the fault is estimated to have extended from Newport Beach to Signal Hill (refs, 16, 17).

The maximum Modified Mercalli Intensity for this earthquake was IX at locations exhibiting poor soil conditions such as Long Beach and Compton (ref 18). The Los Angeles Harbor probably exhibited similar intensities ranging from VII to IX depending on the soil conditions.

Horizontal and vertical accelerations were measured at several locations, at various distances from the epicenter, on rock and deep alluvium. A summary of the peak surface accelerations is presented in table 4-2.

The horizontal accelerations for the Long Beach area were not accurately established but the peak values have been estimated, from the Long Beach Public Utilities Building record, to be 0.23g on deep alluvium (ref. 19). Evidence which indicates that higher horizontal accelerations may have occured is the well documented peak vertical acceleration, at the above site, of 0.25g (ref. 19). It should be noted that horizontal accelerations are often of the order of about 50 percent greater than vertical accelerations.

TABLE 4-2

Recorded Surface Accelerations for the
Long Beach Earthquake

Location	Site Geology	Distance to nearest point of fault movement (miles)	Distance to the epicenter (miles)	Peak Horizontal acceleration (ref. 19) (g)	Peak Vertical acceleration (ref. 19) (g)
Long Beach	Deep alluvium	3	17	0.23	0.25
Vernon	Deep alluvium	16	33	0.15	0.05
Los Angeles	Rock	20	37	0.06	0.02

The harbor area is approximately 6.5 miles from the causative fault and approximately 22 miles from the epicenter. This proximity may have resulted in maximum rock accelerations at the site of approximately 0.35g based on the Schnabel and Seed relationship shown in figure 4-2 (ref. 15). Also presented in this figure, for comparison are the accelerations given in table 4-2 plotted with respect to both epicentral distance and the distance to the nearest point of the fault.

The greatest recorded damage was in the coastal cities, particularly Long Beach, where many [unsuitable] buildings had been constructed on fill or saturated alluvium and sand (refs. 19, 20). Written accounts of the earthquake indicate that liquefaction occured at various locations in the Los Angeles Basin, particularly west of Santa Ana and north and northwest of Newport Beach and Huntington Beach. The Compton area also exhibited this effect (ref. 19). Documented data on the earthquake's effect on the Los Angeles-Long Beach Harbor does not appear to exist, although the San Pedro area was reported to have suffered damage.

Thus, the 1933 Long Beach earthquake should be considered as the minimum probable design earthquake for construction within the Los Angeles Harbor.

Recurrence and Risks

The following is a brief discussion on the magnitude of earthquakes expected to occur on the three previously selected faults. As explained subsequently, the Palos Verdes and San Andreas Faults did not require an in depth study of their past earthquake history to arrive at their design earthquakes. Due to the close proximity and high degree of activity of the Newport-Inglewood Fault, it required a probability analysis. The probability procedure used is a limited version of the method presently being used by many earthquake engineering firms in the Los Angeles area.

Palos Verdes Fault Zone. The Palos Verdes Fault was a zone of faulting and intense folding in the miocene age. However, evidence indicates the fault zone is not active and has not been active since the late lower pleistocene age (refs. 5, 18). For this reason, any possible seismic activity is reguarded as extremely unlikely and not considered further in this report.

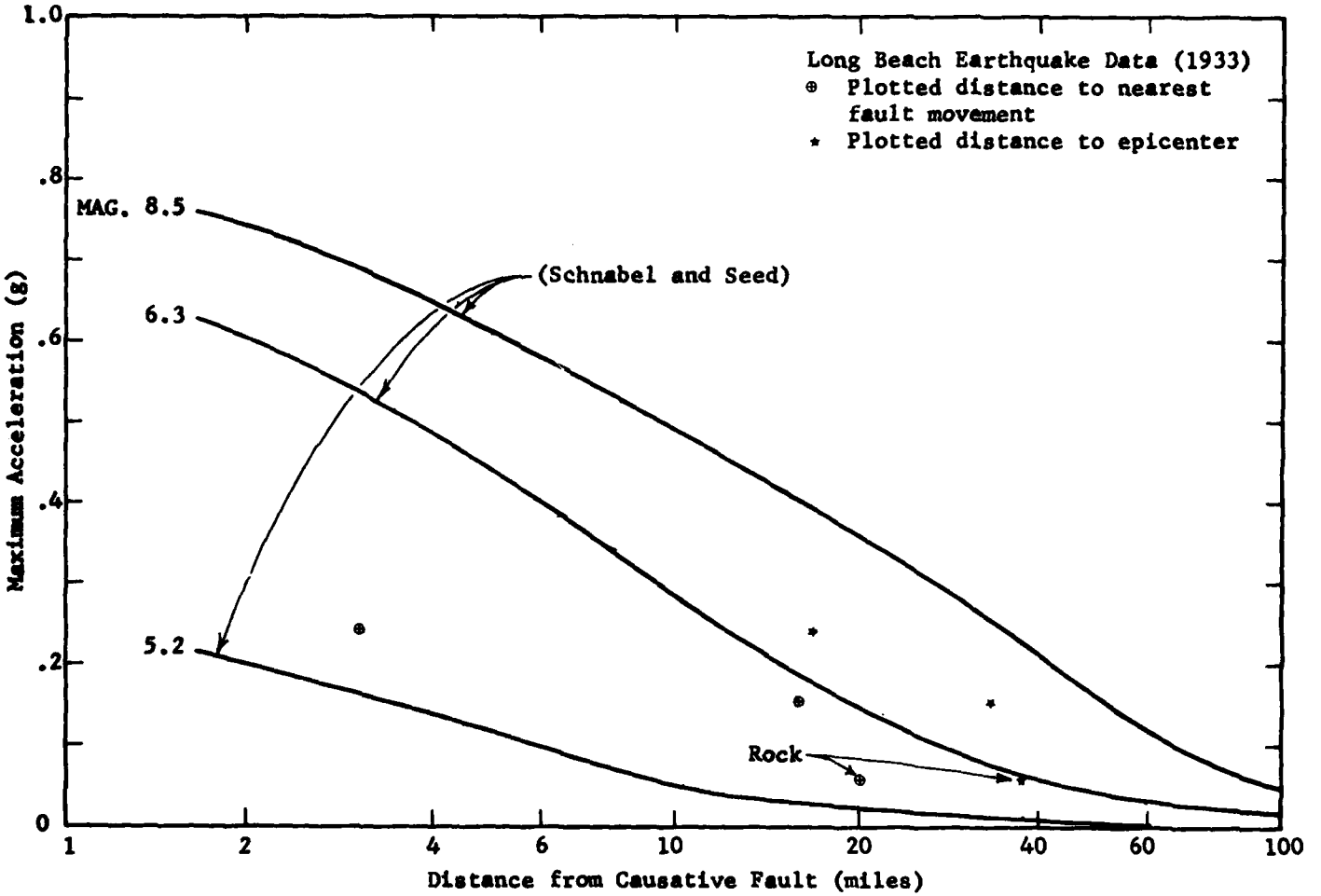

FIG. 4-2 COMPARISON OF MEASURED HORIZONTAL ACCELERATIONS OF THE 1933 LONG BEACH EARTHQUAKE TO AVERAGE VALUES OF MAXIMUM ACCELERATION IN ROCK

San Andreas Fault Zone. The portion of the San Andreas Fault of particular interest in this study is that segment between San Bernardino and Parkfield. This is the closest position of the fault to the Los Angeles Harbor, approximately 52 miles, and it is generally considered a segment capable of generating a large earthquake. The important consideration is that 116 years have past since this segment last moved (Fort Tejon Earthquake 1857) and that considerable amounts of displacement are occurring in the active areas on both ends of this segment. Therefore, there is probably enough energy stored in this segment of the San Andreas Fault to generate a magnitude 8+ earthquake at anytime.

For purposes of further studies a magnitude 8.25 earthquake is assumed possible on the San Andreas Fault occurring at a distance of 52 miles from the study site.

Newport-Inglewood Fault Zone. Earthquakes that have had a significant effect on the Los Angeles Harbor area have originated principally as the result of movements along the Newport-Inglewood Fault zone. Excellent records of earthquakes in this area have been kept since the Long Beach Earthquake. A breakdown of earthquakes assumed to have occured on the Newport-Inglewood fault, giving the date of occurrence, general location, maximum intensity, magnitude and location of the epicenter may be found in reference 18. For use in this study, a summary of these earthquakes with magnitudes of 4.0 or greater are presented in table 4-3. This data was further evaluated in terms of the rate of recurrence of magnitudes greater than or equal to 4.0 and is shown on figure 4-3 for a normalized 100 year period, also shown in this fugure is the recurrence curve for the Los Angeles Basin based on Allen et. al, 1965, for comparison purposes (ref. 21).

TABLE 4-3

Recurrence of Magnitude on the Newport-Inglewood Fault
1933-1974

Richter Magnitude	Number of Occurrences	Occurrence Rate/year of M ≥ M	
4.0	10	0.585	
4.2	3	0.342	
4.3	1	0.268	
4.4	1	0.244	
4.5	4	0.219	
4.6	1	0.122	
5.0	1	0.098	
5.4	1	0.073	
5.5	1	0.049	
6.3	1	0.024	(Long Beach, March 10, 1933)

It is desirable and economical to select an earthquake magnitude for design purposes, which has a specific probability of occurring within the design lifetime of the structure being analyzed. This probability of occurrence of a specific event was based on the Poisson Time Distribution (Benjamin 1968) and determined using the relationship given in equation (4-1).

$$P(N \geq 1/t) = 1-e^{-\mu t} \qquad (4\text{-}1)$$

Where $P(N \geq 1/t)$ = Probability that the event will occur at least once.

t = design life of the structure

μ = Mean rate of recurrence of specific magnitude event per year

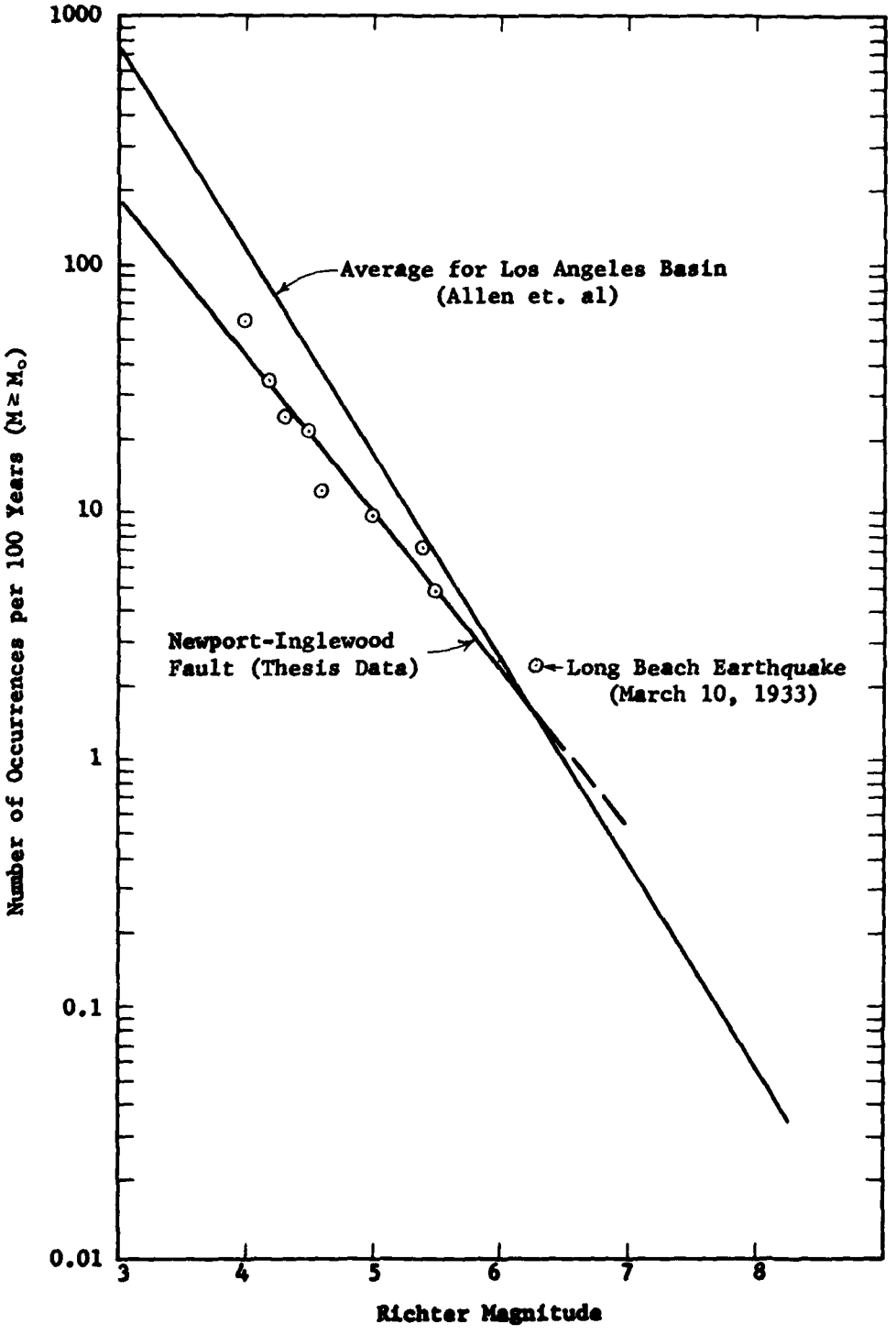

FIG. 4-3 RECURRENCE CURVES FOR THE NEWPORT-INGLEWOOD FAULT AND AND THE LOS ANGELES BASIN

The results of these calculations are presented in figure 4-4 where the probability of occurrence was determined for design lifes of 50 and 100 years, representing the lifes of a major building and the hydraulic fill respectively. For most engineering design purposes the specific probability of earthquake occurrence may be taken in the 30 to 50 percent range, but may vary considerably based on the type of structure or specific deisgn requirements. The 50 percent probability of occurrence corresponds to a minimum earthquake magnitude of 6.8 occurring at some point on the Newport-Inglewood Fault zone during the 100 year design life of the hydraulic fill. Therefore, for design purposes the fill should be engineered to be stable under the stresses induced by a magnitude 6.8 to 7.0 earthquake occuring on the Newport-Inglewood fault.

In this report a lesser earthquake of magnitude 5.25 orginating at the nearest point of the Newport-Inglewood fault zone to the study area, approximately 6.5 miles, has been selected for analysis to dramatize the instability of existing and proposed fills. This magnitude and as selected for the following reasons:

a. It is a low magnitude earthquake with minimal damage producing capability and has approximately a 100 percent probability of occurring within the design life of the fill.

b. The motions generated by this magnitude earthquake are low enough that most modern man-made structures would suffer little damage.

c. The location is the most critical to the Los Angeles Harbor area with respect to the Newport-Inglewood Fault.

Earthquake Accelerogram Selection

Based on the previously selected magnitudes and distances to causative faults, the maximum bedrock accelerations and predominate periods at the site may be determined for each of the earthquake motions using published relationships. The average values of maximum accelerations in rock were determined from the Schnabel and Seed relationship, (ref. 15) figure 4-5, and the predominate period from the relationship between earthquake magnitude and distance from the causative fault after Figueroa, (ref. 14), figure 4-6.

These relationships yield the values shown in table 4-4 for the two earthquakes selected for analysis.

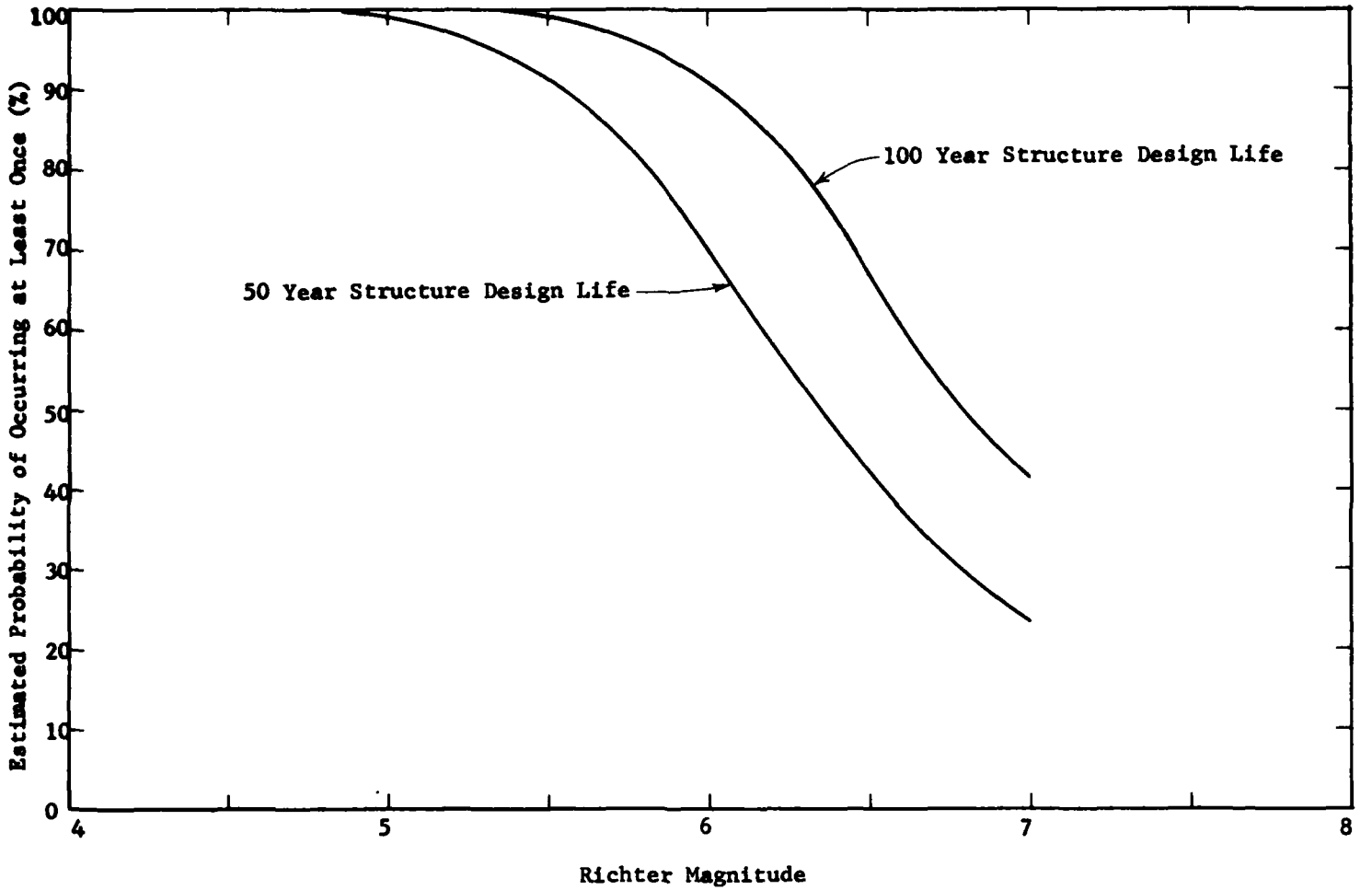

FIG. 4-4 ESTIMATED PROBABILITY THAT THE GIVEN MAGNITUDE EARTHQUAKE WILL OCCUR AT LEAST ONCE AT SOME POINT ON THE NEWPORT-INGLEWOOD FAULT

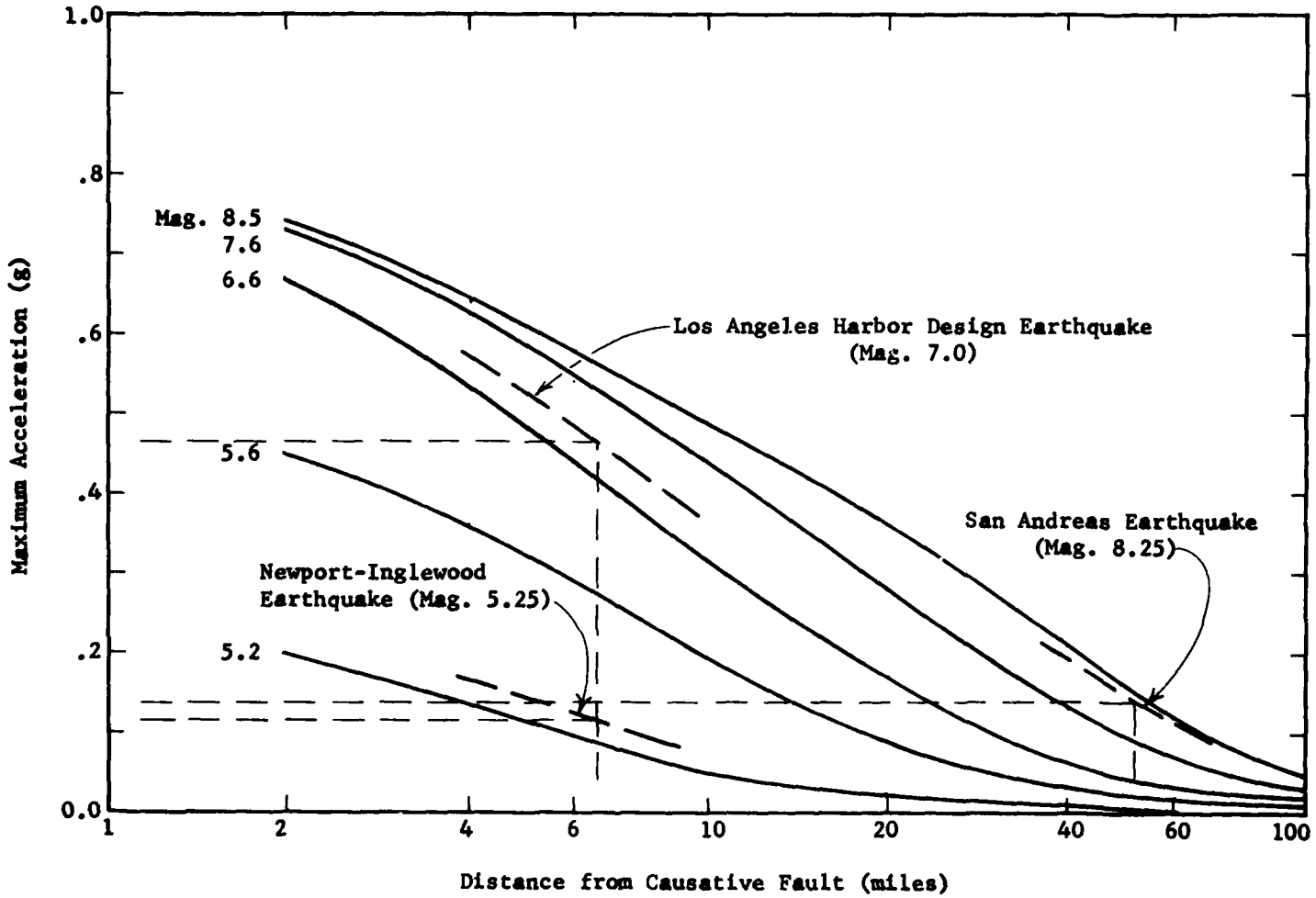

FIG. 4-5 AVERAGE VALUES OF MAXIMUM ACCELERATIONS IN ROCK (Schnabel and Seed)

AD A136 667 LIQUEFACTION POTENTIAL OF PROPOSED FILLS LOS ANGELES HARBOR APPENDIX D LOS ANGELES-LONG BEACH HARBORS(U) ARMY ENGINEER DISTRICT LOS ANGELES CA L A KNUPPEL 1974 2/2

UNCLASSIFIED F/G 8/13 NL

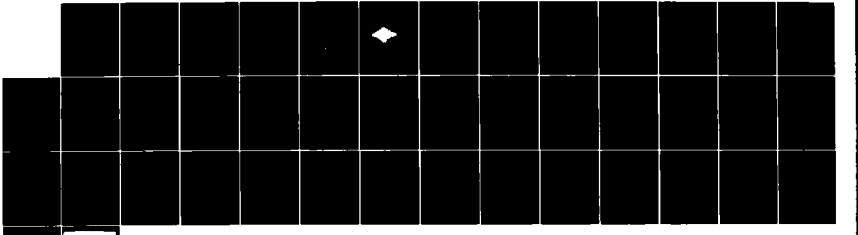

END

DATE FILMED

2 84

DTIC

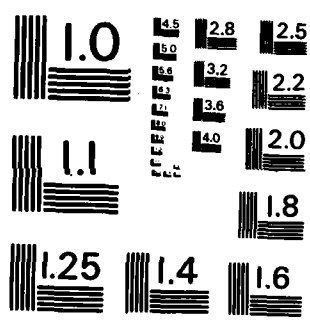

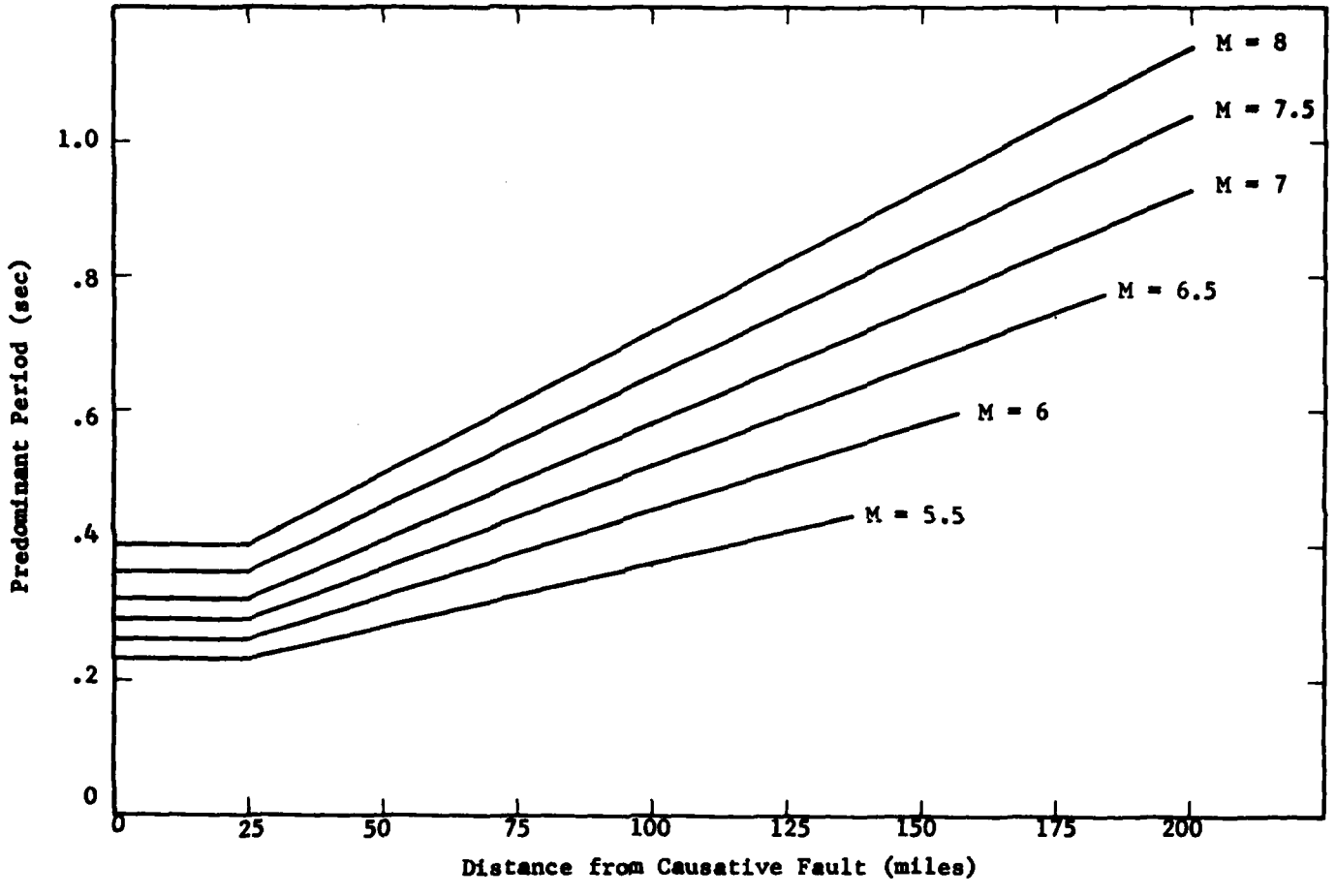

FIG. 4-6 PREDOMINANT PERIODS FOR MAXIMUM ACCELERATIONS IN ROCK. (Figueroa)

TABLE 4-4

Estimated Earthquake Characteristics

Fault	Richter Magnitude	Approximate Duration (sec.)	Distance to site, miles	Maximum Bedrock Acceleration(g)	Predominate Period (sec.)
Newport-Inglewood	5.25	15	6.5	0.11	0.21
San Andreas	8.25	60	52.0	0.13	0.54

Based on the data in this table, the Golden Gate Park and Artificial Seed-Idriss records were selected to represent the predicted rock motions at the site induced by movement of the Newport-Inglewood and San Andreas Faults respectively. The Golden Gate Park record, with a magnitude of 5.25, had predominate frequency characteristics close to the desired values so that adjustment was limited to the amplitudes of motions. The Artificial Seed-Idriss record, with a magnitude greater than 8.0, required adjustment of both the predominate frequency and the amplitudes of motion. The characteristics of the two existing accelerogram records are presented in table 4-5.

TABLE 4-5

Characteristics of Existing Earthquake Accelerogram Records

Selected for Use in the Dynamic Analysis

Existing Accelerogram	Geology of recording site	Richter Magnitude	Distance to recording site (miles)	Maximum acceleration (g)	Predominate period (sec.)
Golden Gate Park, 1957	Rock	5.25	7	0.13	0.15
Artificial Seed-Idriss	Stiff Soil or Rock	8+	—	1.00	0.40

In order to modify the motions of these two existing records, it was necessary to apply scale factors to the ordinates or abscissas. The scale factors used are presented in table 4-6 and the adjusted acceleration time histories of the predicted bedrock motions at the site are shown in figures 4-7 and 4-8.

TABLE 4-6

Accelerogram Scaling Factors

Accelerogram	Predominate Period	Acceleration
Golden Gate Park	No adjustment	0.85
Artificial Seed-Idriss	1.35	0.13

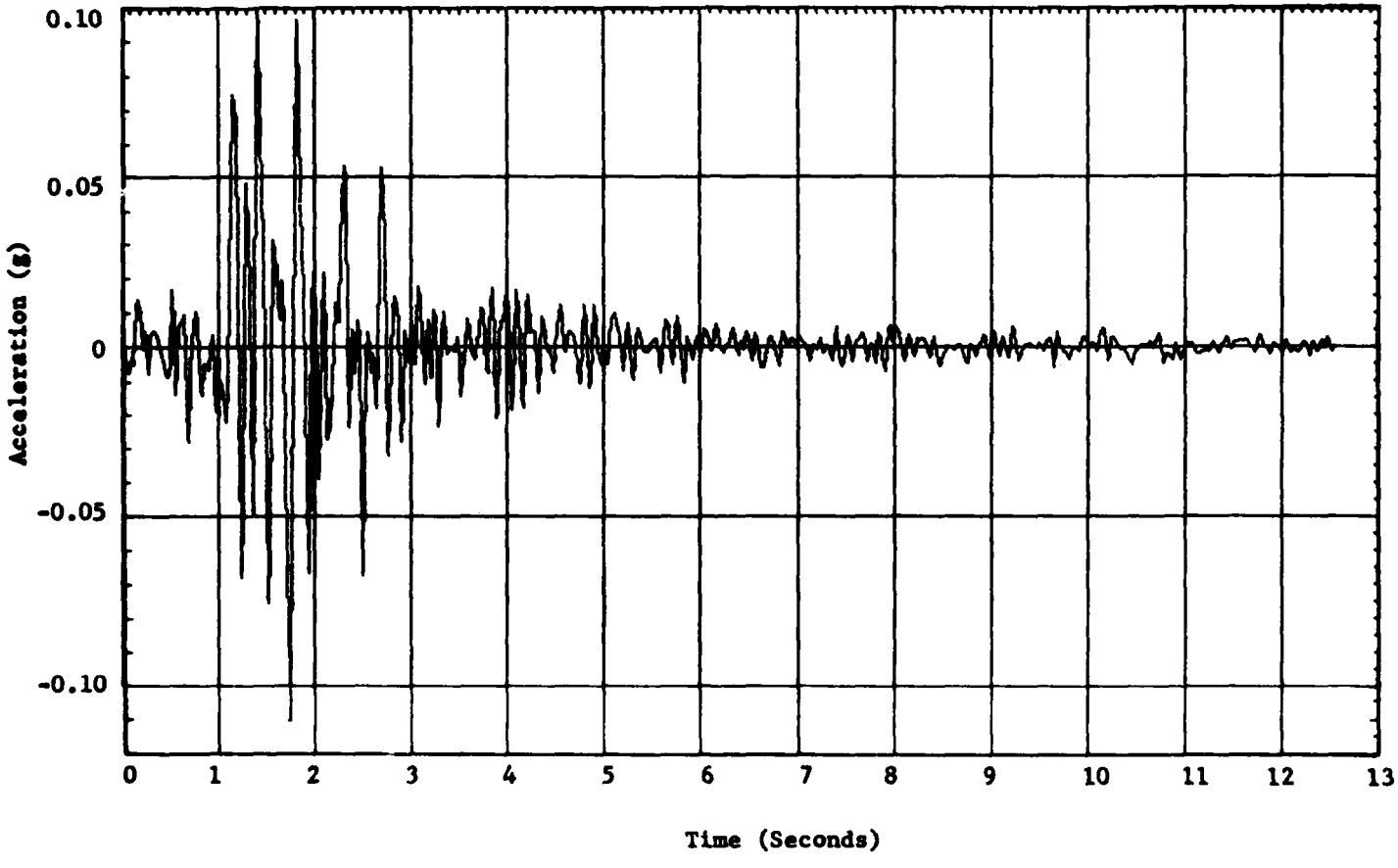

FIG. 4-7 ADJUSTED ACCELEROGRAM USED TO REPRESENT THE SITE ROCK MOTIONS PRODUCED BY A MAGNITUDE 5.25 EARTHQUAKE OCCURRING ON THE NEWPORT-INGLEWOOD FAULT (Based on Golden Gate Park Record, 1957)

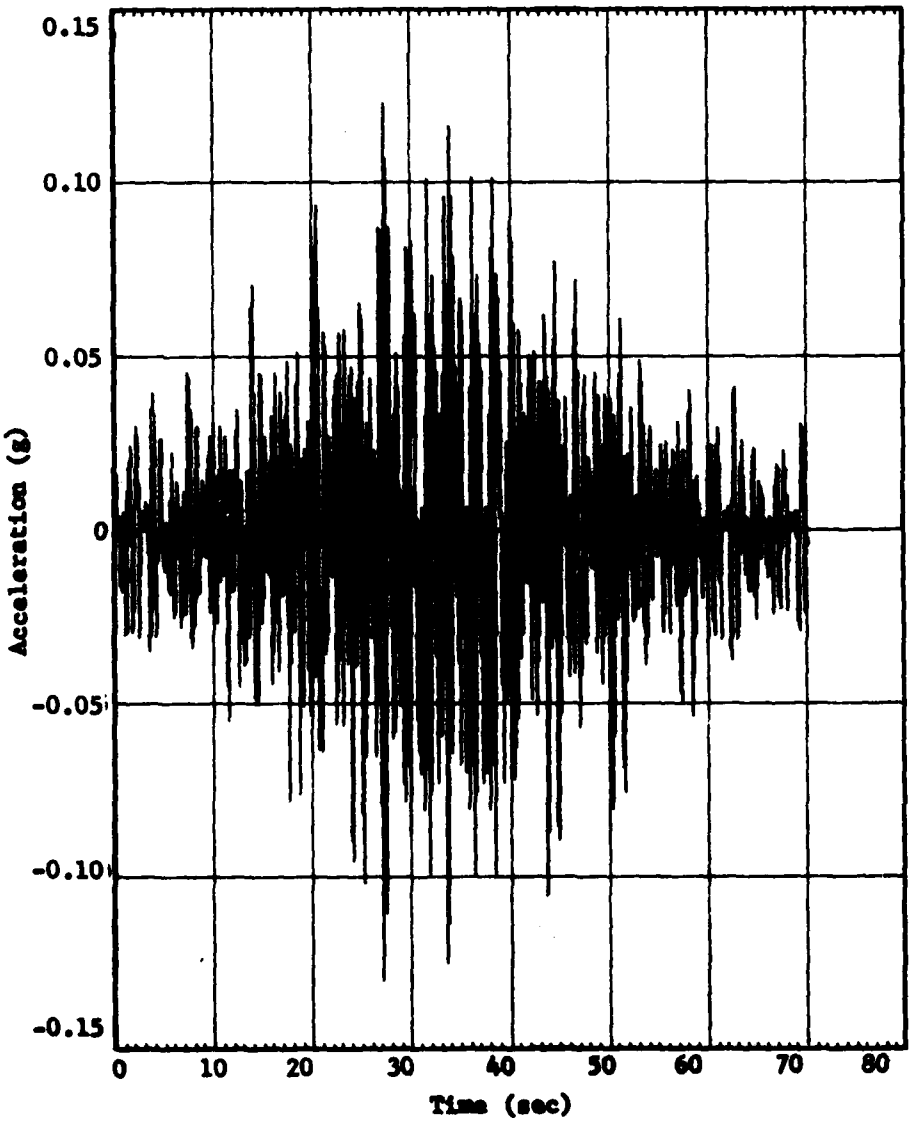

FIG. 4-8 ADJUSTED ACCELEROGRAM USED TO REPRESENT THE SITE ROCK MOTIONS PRODUCED BY A MAGNITUDE 8.25 EARTHQUAKE OCCURRING ON THE SAN ANDREAS FAULT. (Based on Artificial Seed-Idriss Record)

CHAPTER 5

SUBSURFACE MODEL

General

Before a subsurface model for dynamic analysis of the study area could be made, it was necessary to determine or estimate the following information:

a. The order the proposed dredge materials would be placed at the fill site.

b. The shear wave velocities of the geologic formations.

c. The static and dynamic soil parameters of the proposed fill and foundation materials.

Each of these items is discussed in detail in the following sections.

Proposed Construction Techniques

The fill must be constructed in such a manner that all engineering and environmental aspects are met. The environmental requirements require dredging the channels and basins in such a manner that polluted materials are placed above the MLLW level behind an impervious dike.

Frequently dikes are constructed in two or three steps. However, conventional multistep designs may not be particularly effective in controlling the spread of turbid waters from the disposal site. For this reason a special two step design for containment of the spoils is being considered. The first step would include the erection of a stone dike extending from the sea floor to the highest tidal level. The area enclosed by the dike would be filled with the cleaner, less polluted materials dredged from the main channel and outer harbor. After the

first step fill has settled, a second step stone dike would be constructed. The second step fill, consisting of the more polluted sediments from the east and west basins would be placed on top of the first step fill and the polluted materials would then be covered with a blanket of clean imported fill material. Various measures are under consideration for controlling the quality of waste water return flow from diked disposal areas such as; longer retention time for more effective settling, chemical flocculants, aeration, mechanical mixing, and filtering.

This fill design is an estimate as to how the dredge materials will be placed at the fill site and is based solely on engineering and environmental criteria as of December 1973, and is not meant to represent the most economical method of construction.

Shear Wave Velocities

The shear wave velocities were evaluated for the San Pedro and Pico Formations in order to determine the depth at which the base motions would be input during dynamic analysis and for establishing the shear modulus and damping values.

Since actual shear wave measurements were not available at the site, published velocities were utilized. Excellent values of measured shear wave velocities are given in refs. 2, 11, 12, and 13 for various soils and rock formations in the Los Angeles Basin. The shear wave velocities for the San Pedro and Pico Formations, along with the respective depth, density, and source of information is presented in table 5-1.

TABLE 5-1

Published Shear Wave Velocities for the San Pedro and Pico Formations

Geologic Formation	Depth (ft)	SH Velocity (ft/sec)	Density (pcf)	Reference
San Pedro	1,000	3,700	131	12
San Pedro	100	2,100	123	12
San Pedro	130	2,500	125	12
San Pedro	300	1,670	130	2
San Pedro	400	1,980	130	2
San Pedro	200	2,600	130	10
Pico	1,400	4,540	131	12
Pico	1,800	4,200	140	12
Pico	1,000	3,800	140	2
Pico	800	5,300	137	10

These values were adjusted for the overburden pressure effect found at the subject site by means of the following equations after Faust (ref. 12).

$$Vp = 125.3\,(ZT)^{1/6} \qquad (5\text{-}1)$$

Where Vp = Velocity of compressional waves (P-wave)

Z = Depth in feet

T = Geologic age in years

This equation simplified to

$$\frac{V_{z1}}{V_{z2}} = \frac{Z_1^{1/6}}{Z_{z2}^{1/6}} \qquad (5\text{-}2)$$

which allows the direct comparison of shear wave velocity with depth in formations of the same geologic age.

The values given in table 5-1 were adjusted using equation 5-2 which gives the following range in shear wave velocities.

San Pedro Formation	1,700 fps @ 300' to 3,000 fps @ 1,000'
Pico Formation	3,800 fps @ 1,000' to 4,300 fps @ 2,000'

Subsurface Model

In constructing a subsurface model for dynamic analysis, it is necessary to determine the soil profile to a depth which is consistent with the degree of accuracy of the soil parameters to be input and those which are to be calculated. Since the soil parameters used in this study are only well defined in the upper 300 feet, the soil profile was not determined to crystaline bedrock which is at a depth greater than 5,000 feet. Thus, following the present accepted procedures developed by Seed and Idriss (refs. 14, 22) with slight modification, as discussed by Lastrico (ref. 13), the motions at the base of the soil deposit during seismic excitation can be considered those developed in tertiary material which exhibits a relatively high shear wave velocity, even though it does not necessarily exhibit the characteristics associated with sound base rock. Based on this assumption, the soil profile in this study was developed to the approximate top of the Pico Formation which has an estimated range in shear wave velocity of 3,800 to 4,300 fps.

The approximate 900 feet of alluvium above the Pico Formation was divided into 10 layers based on the strata thicknesses indicated by the test hole data shown on figure 2-19. These layers were then subdivided in accordance with the layer thickness criteria discussed in reference 23, providing a total of 26 layers.

The parameters used in the subsurface model to represent the proposed fill were based on pervious evaluations made in Chapter 2 and are summarized in table 5-2. Since the dredge material will form a fill composed predominately of silty sand, only the soil parameters pertinent to these materials are presented.

The dry density and moisture content are based on median values, and the friction angle is taken as a value slightly higher than the lower limit of the available direct shear data. Also presented in table 5-2 are the soil parameters assuming that the materials are placed at a somewhat higher density than is typically found in hydraulic fills. This higher dry density of 99.5 pcf was selected because it may be reasonably obtained in the field with some modified placement procedure and it corresponds to a relative density of 74 percent which is outside the highly susceptable liquefaction range of 40 to 70 percent.

TABLE 5-2

Static Design Values for the Proposed Hydraulic Fill

Soil Parameters	Symbol	Present Construction Procedure	Modified Placement Procedure
Dry unit weight	γ_d (pcf)	94.5	99.5
Relative Density	Dr (%)	59.0	74.0
Moisture content	W (%)	26.0	24.0
Cohesion	C (psf)	—	—
Friction angle	ϕ (Deg.)	32	34

The simplified subsurface model giving the static soil parameters of each soil layer to a depth of approximately 900 feet is shown in figure 5-1. The top 35 feet of the profile is based on the data presented in table 5-2. The soil profile and parameters from an elevation

ELEVATION	SOIL CLASSIFICATION	TOTAL UNIT WEIGHT (γ_T) (PCF)	FRICTION ANGLE (ϕ, DEG.) OR UNDRAINED SHEAR STRENGTH (S_u, PSF)	EARTH PRESSURE AT REST (K_0)	LAYER
+15					
+ 4 MLLW	SP ▽	112.0	32°	0.47	1
- 4	SM	120.0	32°	0.46	2
-12	SM	120.0	32°	0.46	3
-20	SM	120.0	32°	0.46	4
	SP	127.0	35°	0.43	5
-46					
	SM	121.0	36°	0.41	6
-60					
-67	ML	119.5	4000 PSF	0.65	7
	SP	121.0	36°	0.41	8
-80					
-107.5	SP	138.0	43°	0.32	9
-107.5					
	SP	138.0	43°	0.32	10
-135					
	SP	131.0	45°	0.30	11
-171					
	GP	116.5	45°	0.30	12
-187					
	SP-SM	131.0	45°	0.30	13
-243.5					
	SP-SM	131.0	45°	0.30	14

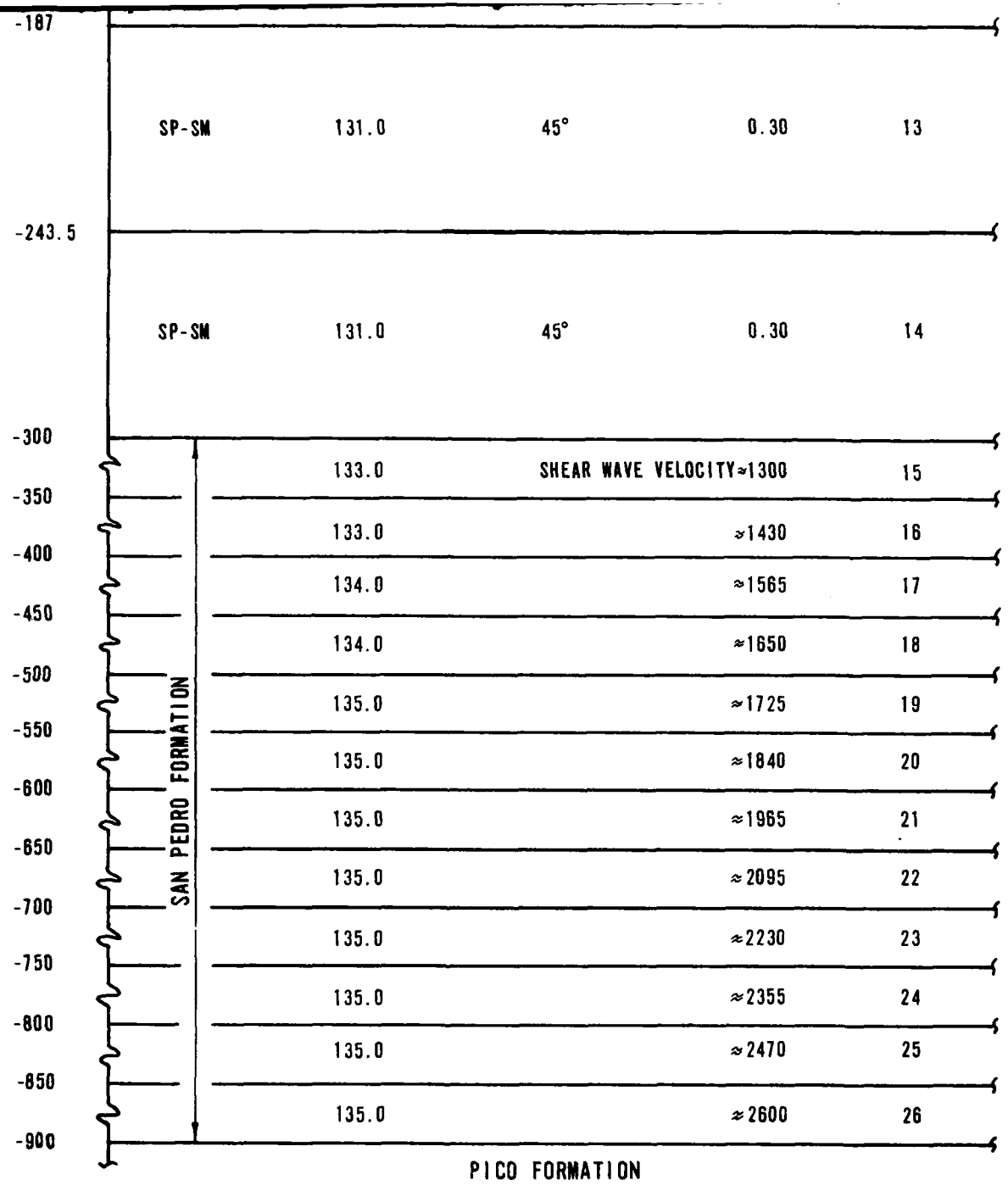

FIG. 5-1 SUBSURFACE MODEL OF THE PROPOSED FILL SITE

of -20 to -300 feet are based on data in figure 2-19. These parameters represent the median density values and the approximate lower limits for the friction angle and shear strength, therefore, some fluctuation in these values can be expected in the actual field situation. At depths greater than 300 feet, it was necessary to rely solely on published data for the San Pedro Formation in order to obtain values of density and shear wave velocity.

The soil shear modulus (G) and damping ratio (λ) for the cohesionless materials, to a depth of 300 feet, were evaluated from the relationships developed by Seed and Idriss (ref. 24). These relationships are presented in figures 5-2a and 5-2b. These figures indicate that the shear modulus varies with the mean effective pressure and strain level and that damping is dependent only on the strain level. The shear modulus for the soil may be expressed by equation (5-3).

$$G = 1000\ K_2\ \sigma_m'^{1/2} \qquad (5\text{-}3)$$

Where G = shear modulus in psf

σ_m' = mean effective pressure in psf

K_2 = a parameter relating G and σ_m' and is primarily a function of relative density and strain.

The shear modulus and damping ratios for saturated cohesive soils have been found to be related to the undrained shear strength and the strain level (ref. 24). These relationships are presented in figure 5-3a and 5-3b.

At depths greater than 300 feet, the values of the shear moduli were determined from the shear wave velocities using the relationship given in equation (5-4).

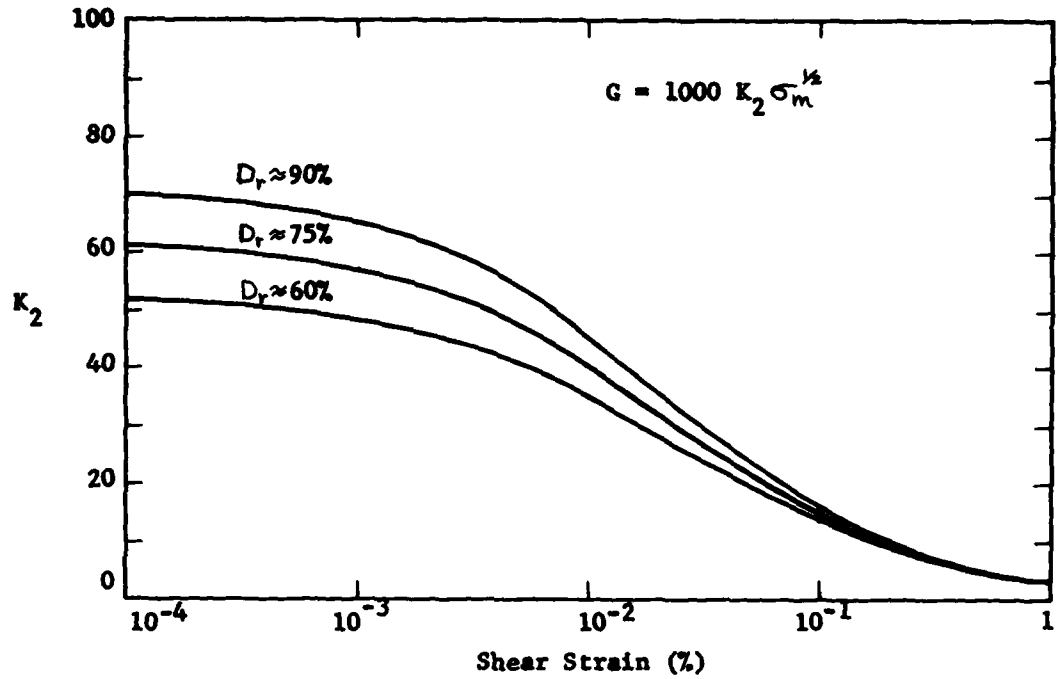

FIG. 5-2a SHEAR MODULI OF SANDS AT DIFFERENT RELATIVE DENSITIES. (Seed and Idriss)

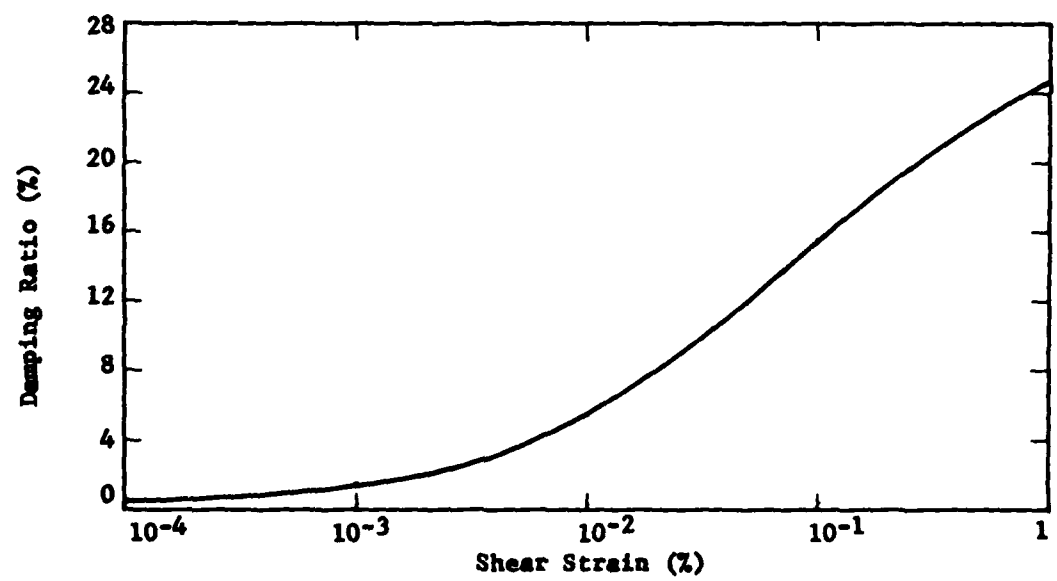

FIG. 5-2b DAMPING RATIOS FOR SANDS. (Seed and Idriss)

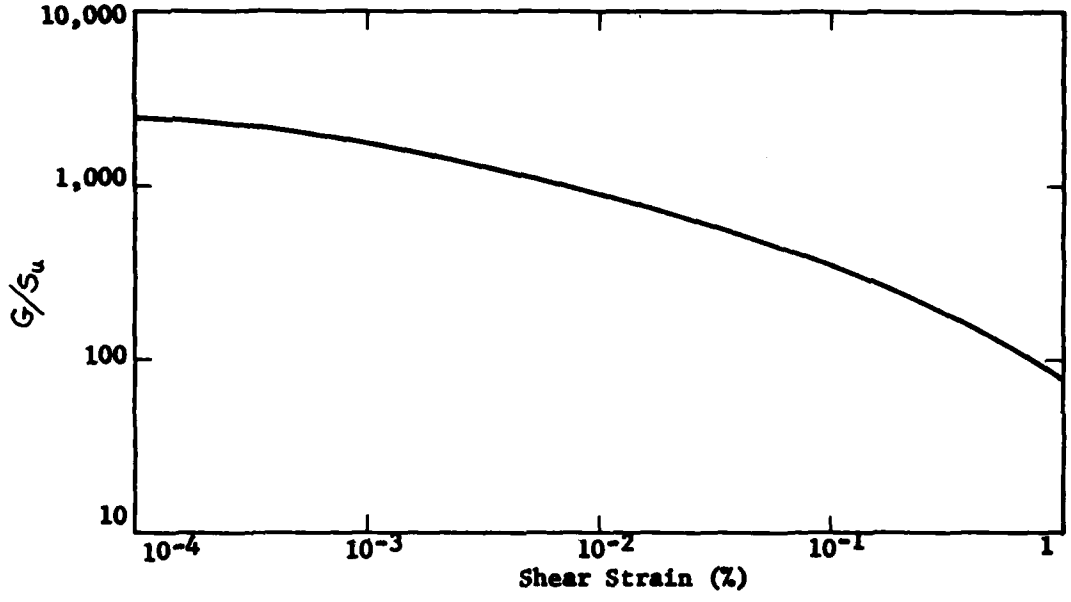

FIG. 5-3a IN-SITU SHEAR MODULI FOR SATURATED CLAYS. (Seed and Idriss)

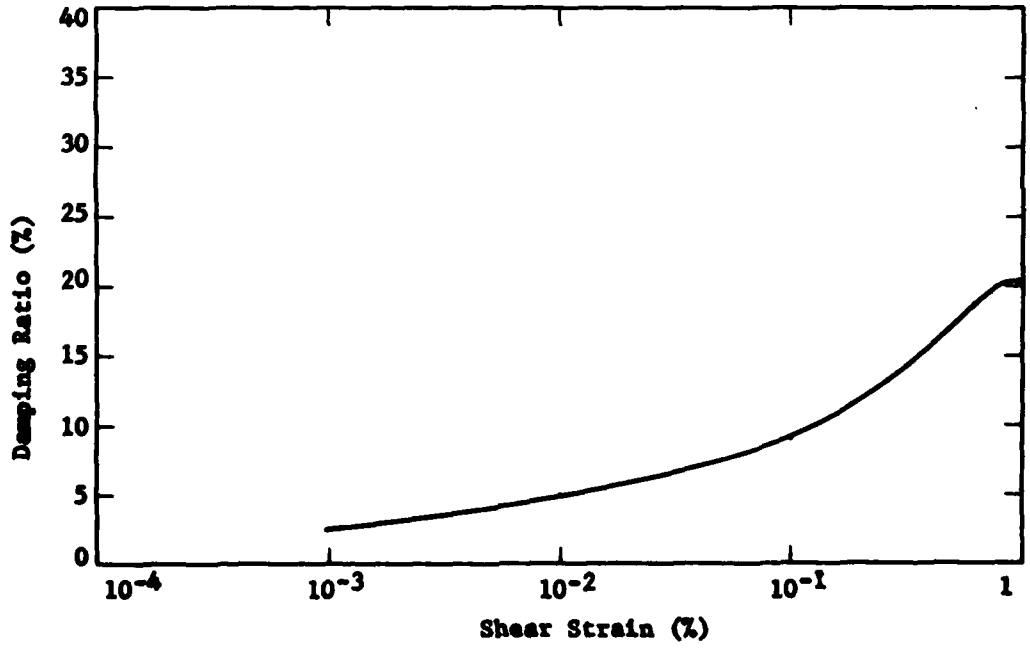

FIG. 5-3b DAMPING RATIOS FOR SATURATED CLAYS. (Seed and Idriss)

$$G = \frac{\gamma V_s^2}{g} \qquad (5\text{-}4)$$

Where G = shear modulus in psf

γ = unit weight of the formation in pcf

V_s = shear wave velocity in fps

g = acceleration due to gravity in ft/sec ^{2}

Should the fill be placed at a higher density, approximately 99.5 pcf, the soil parameters in the top 81 feet of the soil profile would require some adjustment. At depths greater than this, the change in the mean effective pressure is so small that the effects caused by additional overburden pressure on the shear modulus may be neglected.

CHAPTER 6

DYNAMIC ANALYSIS

Method of Analysis

The first step in evaluating the performance of the proposed fill was to compute the response of the fill and underlying foundation materials during the previously selected earthquakes. This computation can readily be made once the following parameters are known:

a. The base motions developed in rock underlying the fill.

b. The dynamic material properties (modulus and damping) of the fill and foundation soils.

The result of this response computation provides values of acceleration, velocity, displacement, strain and stress which are likely to be induced at different depths within the soil profile during the earthquakes. These data can be calculated by means of a lumped mass program which is essentially for level surfaces or a finite element method for sloping irregular boundaries.

The geologic cross section shown on plate 2-3 indicates that the Pico and San Pedro Formations are essentially horizontal. Since the boundaries of the overlying soil layers are also assumed to be horizontal, they may be considered as a series semi-infinite layers. Therefore, using the Pico Formation as the level of base motion input, the lumped mass method of analysis was used to evaluate the overlying soil deposit response to seismic excitation.

Computed Soil Response

The response of the proposed fill and foundation materials to the input base rock motions were calcualted using the Idriss lumped mass program and the Lawrence-Burkely CDC 7600 computer. The results of these computations are presented on plates 6-1 and 6-2 for the foundation material and the proposed fill, assuming a placement dry density of 94.5 pcf, respectively. Plate 6-1 shows the peak acceleration and stress values at various depths within the subsurface model. Plate 6-2 gives the acceleration time histories at the ground surface and the shear stress time histories induced at various depths within the proposed fill during the earthquakes. A summary of the calculated peak surface response characteristics developed by the two earthquake motions are presented in table 6-1.

Also presented in this table are the calculated peak surface response characteristics developed by the magnitude 5.25 earthquake assuming that the fill is constructed at a somewhat higher dry density of 99.5 pcf. As indicated, there is a negligable change in the response characteristics.

TABLE 6-1

Maximum Response Values at the
Surface of the Proposed Fill

Richter Magnitude	Fill Dry Density (pcf)	Relative Density (%)	Acceleration (g)	Velocity (in/sec.)	Relative Displacement (in)	Strain in top layer (%)
5.25	94.5	59	0.17	4.06	0.55	.010
5.25	99.5	74	0.16	3.95	0.54	.010
8.25	94.5	59	0.17	16.99	6.74	.015

The time histories of shear stress, at any level, may be converted to an equivalent series of uniform cyclic stress applications which make the comparison of laboratory and field values meaningful. This conversion was accomplished by appropriate weighting of the ordinates of the time histories based on the methods developed by Lee and Chan (ref. 25). The results of this conversion to equivalent cycles is presented in figures 6-1 through 6-3 where the number of equivalent uniform stress cycles, Neq, is plotted against the ratio R, of the average stress, τave, to the maximum stress, τmax. These figures show the equivalent cycle-stress intensity relationships evaluated at levels 2, 4, and 6 within the hydraulic fill, (see plate 6-2).

This equivalent cycle-stress relationship was used in assessing the stresses developed in the soil, by selecting convient Neq. values of 7 and 26 cycles for the magnitude 5.25 and 8.25 earthquakes respectively. The corresponding average values of the ratio R, were then used to adjust the maximum calculated field induced stresses using equation 6-1, so that a comparison could be made to the laboratory strength values.

$$\tau_{ave} = R\,(\tau_{max}) \qquad (6\text{-}1)$$

Where τ_{ave} = Equivalent average stress

R = Ratio of the average stress to the maximum stress for a given Neq. (see figures 6-1 through 3).

τ_{max} = Maximum calculated field induced stress

A summary of the Neq. and R values used for each earthquake magnitude and fill density is given in table 6-2. The equivalent average earthquake induced stresses within the hydraulic fill, produced by the two earthquake motions being studied are plotted in figure 6-4 with respect to fill density and depth.

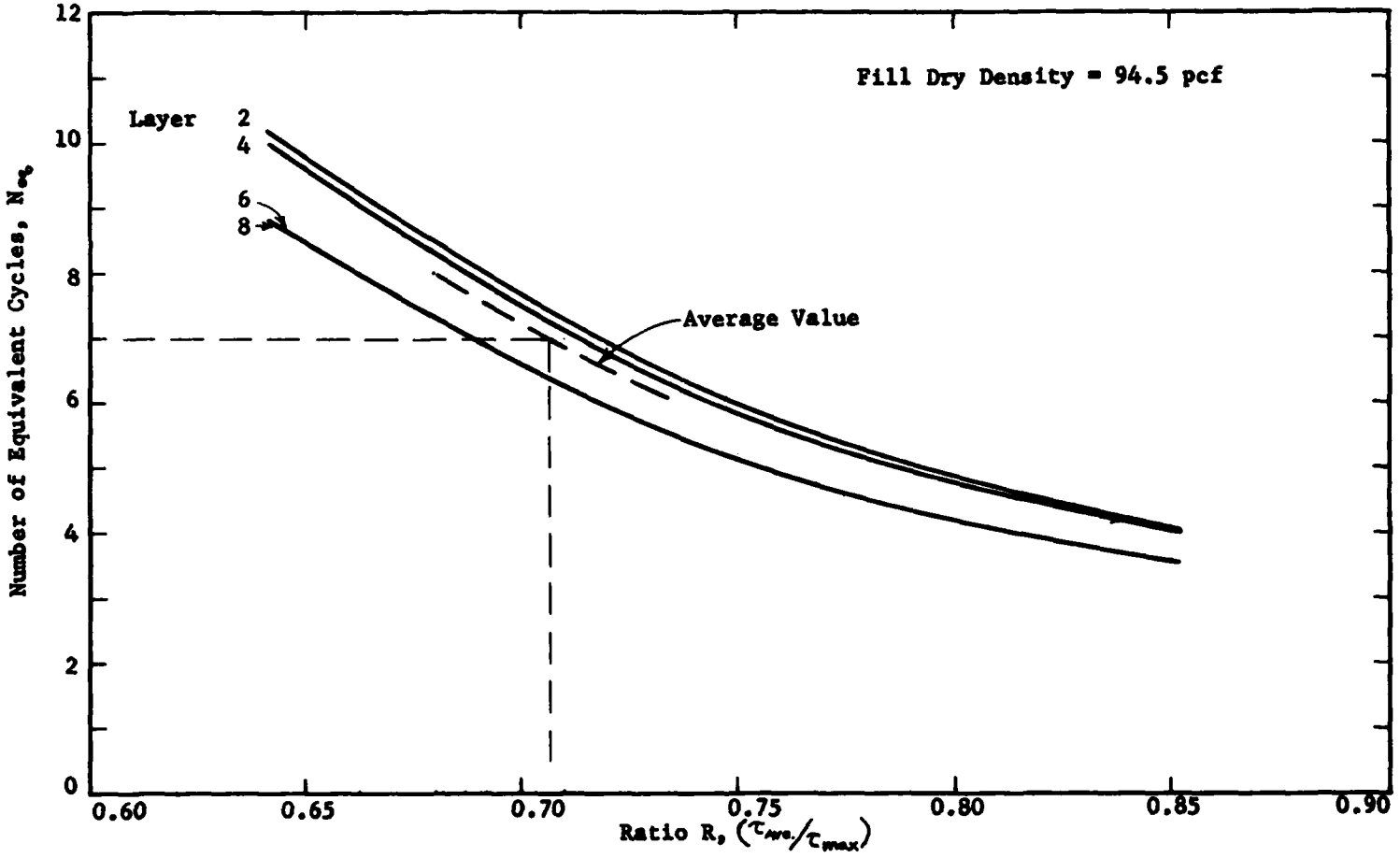

FIG. 6-1 RELATIONSHIP BETWEEN THE RATIO R AND EQUIVALENT CYCLES FOR THE MAGNITUDE 5.25 EARTHQUAKE AND A FILL DENSITY OF 94.5 pcf

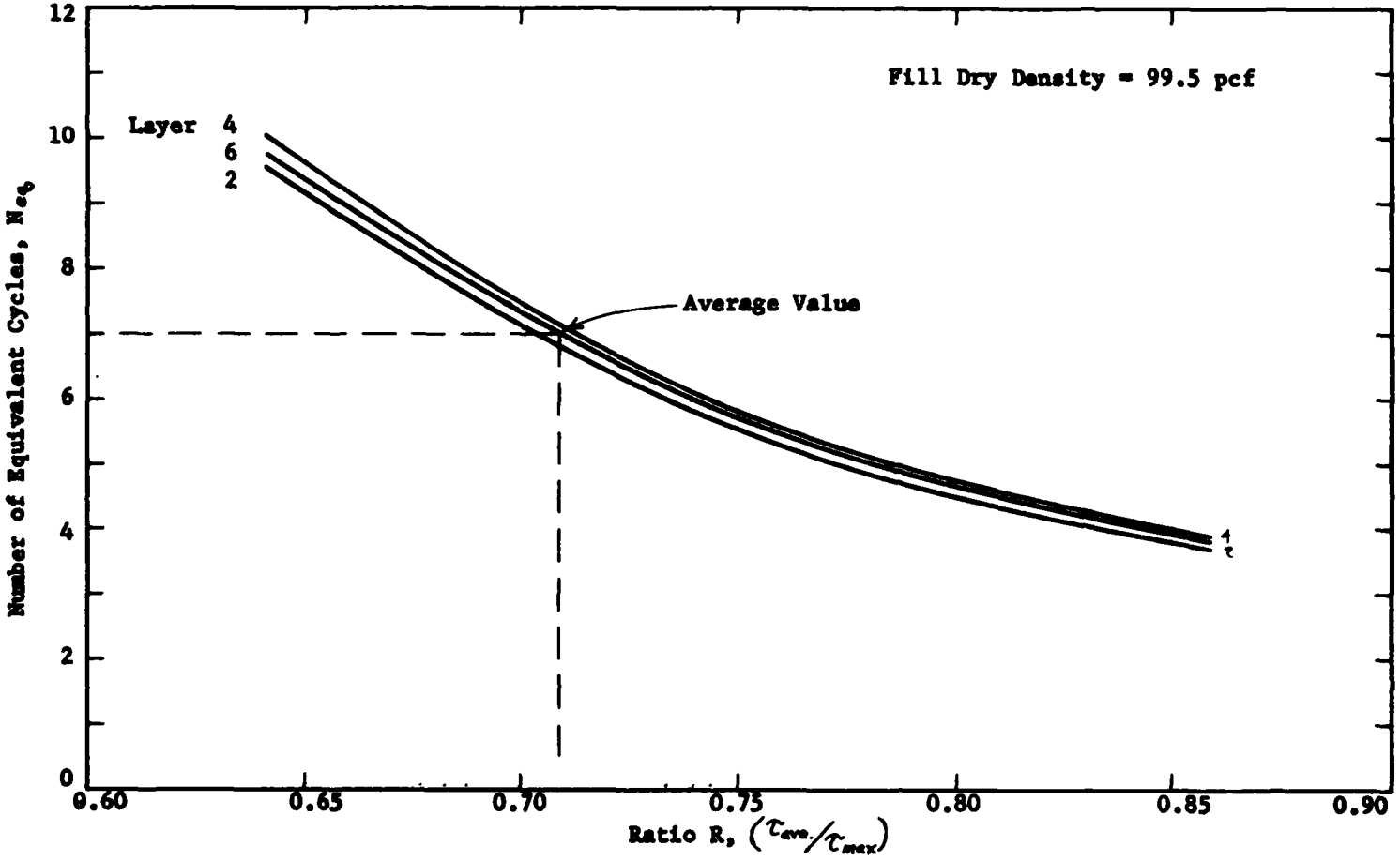

FIG. 6-2 RELATIONSHIP BETWEEN THE RATIO R AND EQUIVALENT CYCLES FOR THE MAGNITUDE 5.25 EARTHQUAKE AND A FILL DENSITY OF 99.5 pcf

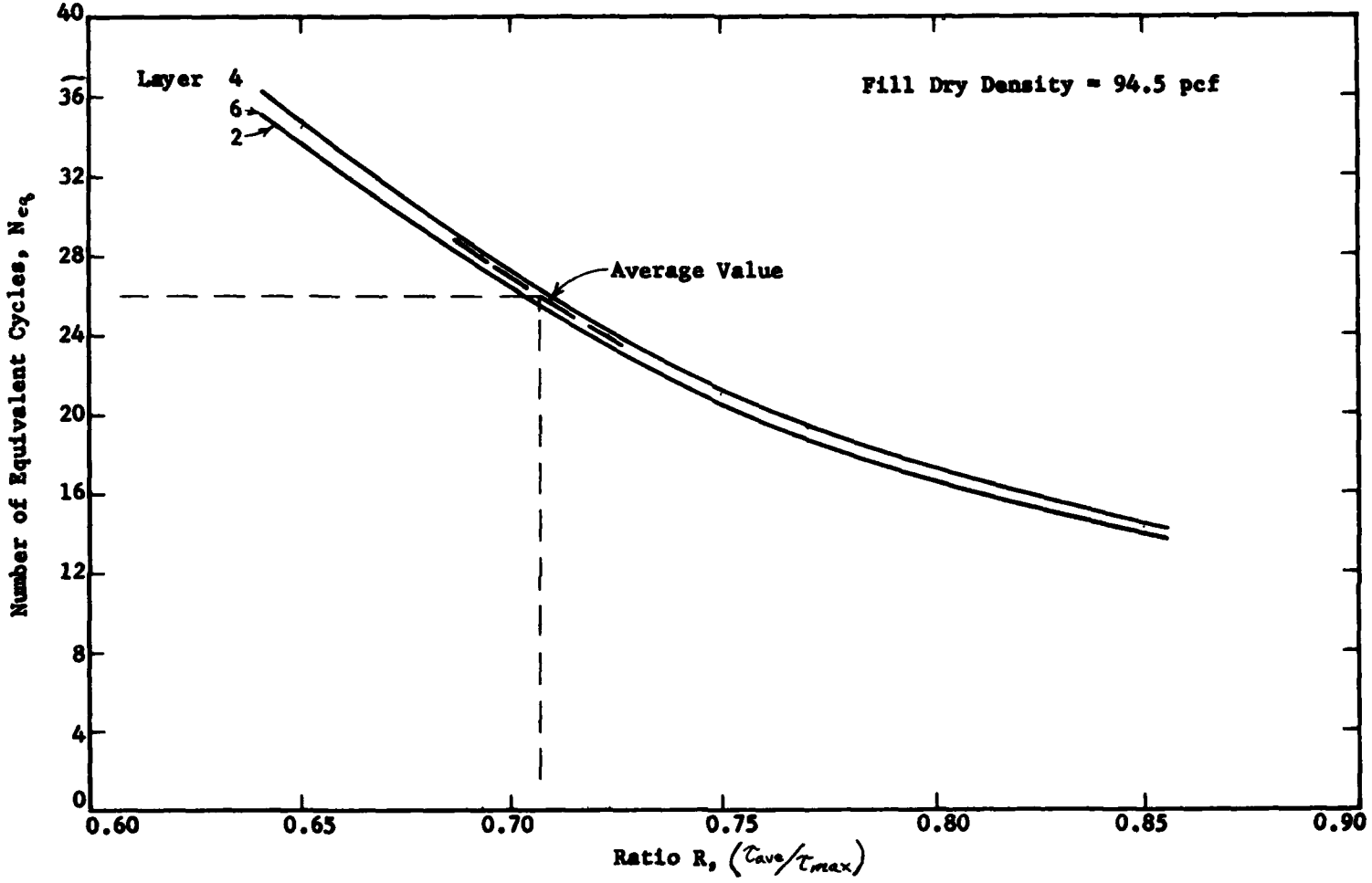

FIG. 6-3 RELATIONSHIP BETWEEN THE RATIO R AND EQUIVALENT CYCLES FOR THE MAGNITUDE 8.25 EARTHQUAKE AND A FILL DENSITY OF 94.5 pcf

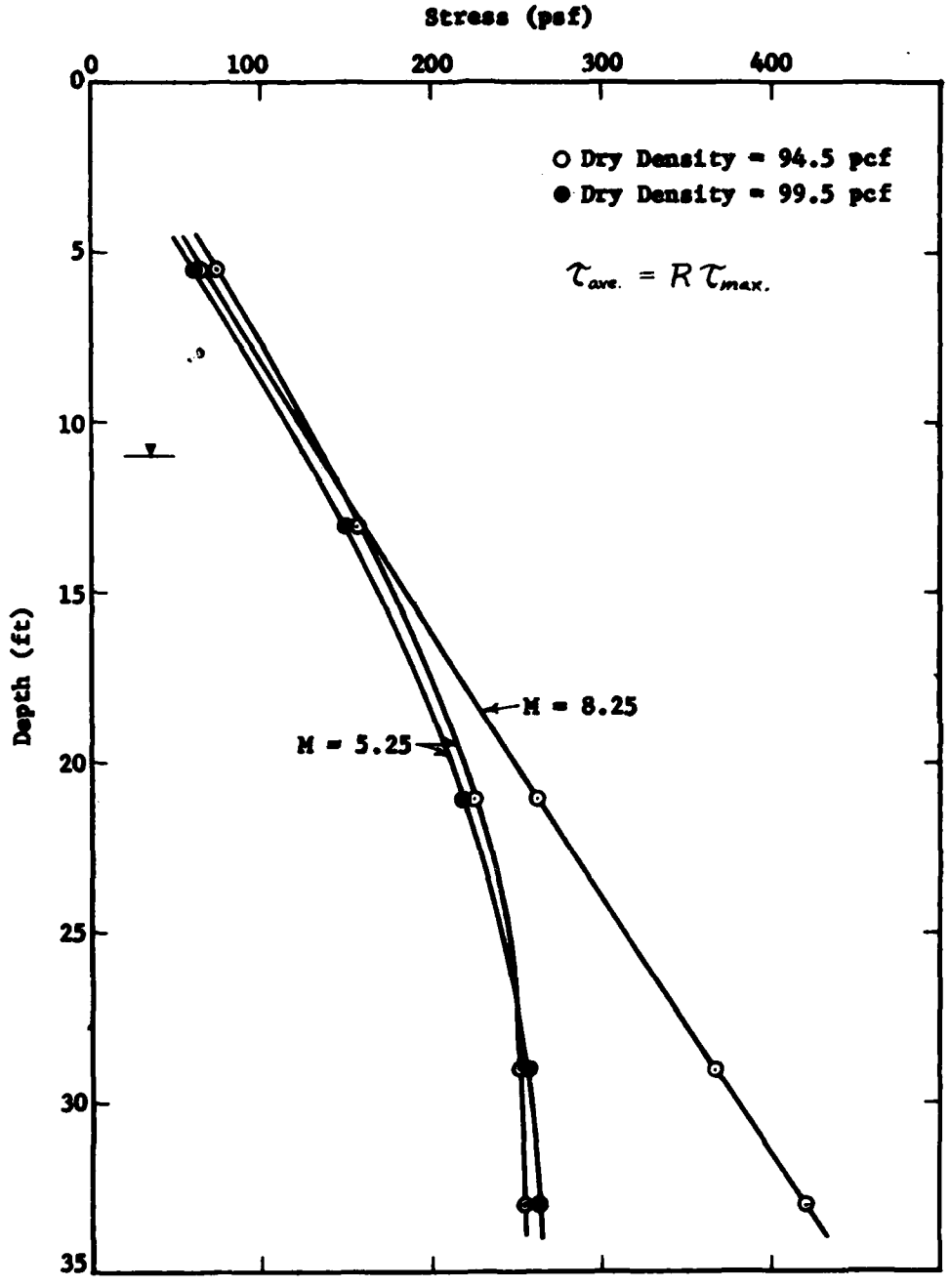

FIG. 6-4 EQUIVALENT AVERAGE EARTHQUAKE INDUCED STRESSES WITH RESPECT TO DEPTH AND FILL DENSITY

TABLE 6-2

Summary of Neq. and R Values Used for Each
Earthquake Magnitude and Fill Density

Earthquake Magnitude	Fill Density	Maximum Fill Surface Acceleration(g)	Neq.	R
5.25	94.5	0.17	7	.71
5.25	99.5	0.16	7	.71
8.25	94.5	0.17	26	.71

Liquefaction Analysis

The strength of the proposed fill material was assessed for both earthquake motions by comparing the calculated average stress, τ_{ave}, induced by the earthquakes to the laboratory evaluated stresses required to cause liquefaction (cyclic strength). The cyclic laboratory strengths of the proposed hydraulic fill soil at 7 and 26 stress cycles are plotted in figure 6-5 for a dry density of 94.5 pcf. These strength curves were determined from the laboratory data presented in figure 3-7. The strengths represented by these two curves were adjusted to represent actual field strengths at different confining pressures and relative densities through the relationship given in equation (6-2), (ref. 8).

$$\left(\frac{\tau}{\sigma}\right)_{field} = C_r \left(\frac{dp}{2\sigma_{3c}}\right)_{triax.} \left(\frac{D_r}{59}\right) \qquad (6\text{-}2)$$

Where τ = Horizontal shear stress required to cause liquefaction in the field at a given depth.

σ = Static vertical effective stress on a horizontal plane.

C_r = Triaxial test correction factor from figure 6-6 (ref. 8).

σ_{dp} = Pulsating deviation stress from figure 6-5.

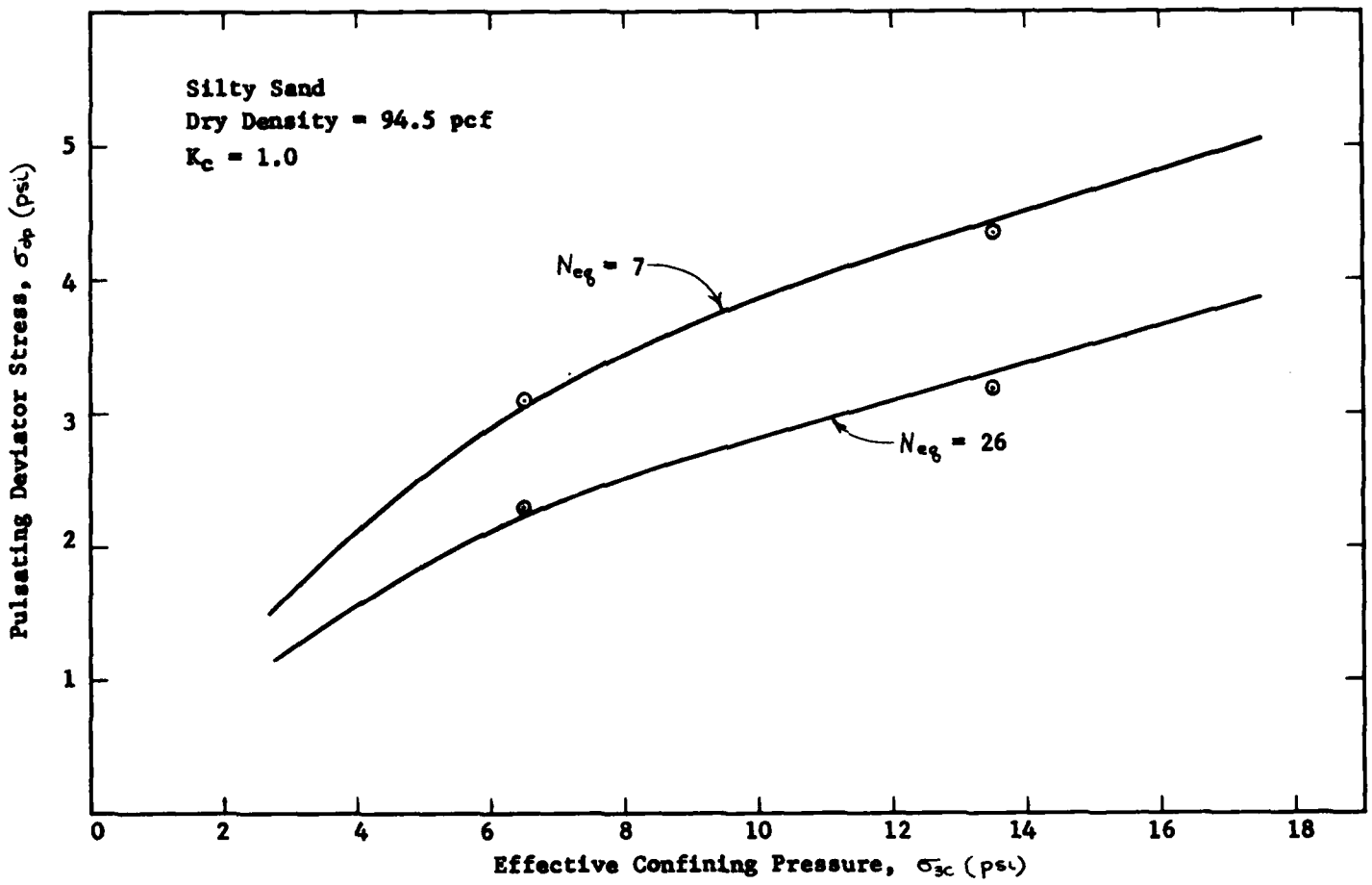

FIG. 6-5 CYCLIC SOIL STRENGTH OF LOS ANGELES HARBOR SILTY SAND AT 7 AND 26 UNIFORM STRESS CYCLES

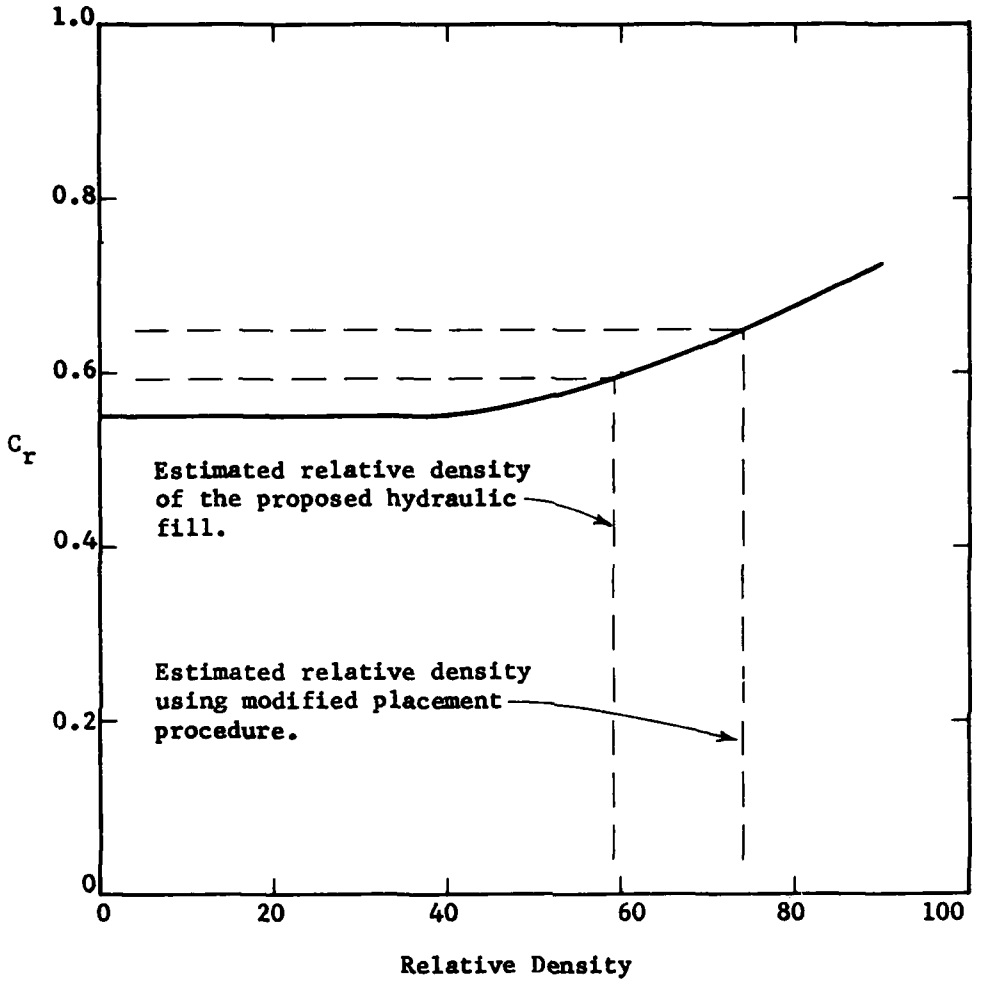

FIG. 6-6 RELATIONSHIP BETWEEN C_r AND RELATIVE DENSITY. (Seed and Peacock)

$\bar{\sigma}_{3c}$ = Effective confining pressure from figure 6-5.

D_r = Relative Density of the hydraulic fill material.

The horizontal shear stresses required to cause liquefaction were calculated for the hydraulic fill at dry densities of 94.5 and 99.5 pcf. The initial values of the parameters used in equation 6-2 and the resulting horizontal shear stresses are tabulated in table 6-3 for three depths within the fill.

TABLE 6-3

Summary of Calculated Horizontal Shear Stresses Required to Cause Liquefaction

Number of Uniform Stress Cycles (Neq)	Depth (ft)	Dry Density (pcf)	Dr (%)	Cr	$\bar{\sigma}_{dp}$ (psi)	$\bar{\sigma}_{3c}$ (psi)	σ_o(psf)	τ(psf)
7	13	94.5	59	.60	3.75	9.33	1344	162
7	21	94.5	59	.60	4.29	12.43	1790	186
7	29	94.5	59	.60	4.75	15.53	2236	205
7	13	99.5	74	.64	3.75	9.38	1350	217
7	21	99.5	74	.64	4.30	12.65	1821	248
7	29	99.5	74	.64	4.85	15.91	2291	280
26	13	94.5	59	.60	2.73	9.33	1344	118
26	21	94.5	59	.60	3.15	12.43	1790	136
26	29	94.5	59	.60	3.60	15.53	2236	155

These cyclic shear strengths are plotted in figures 6-7, 6-8 and 6-9 along with the equivalent average earthquake induced stresses in the proposed fill as shown in figure 6-4. The data in figures 6-7 and 6-8 indicates that the stresses induced by the magnitude 5.25 and 8.25 earthquakes would exceed the cyclic shear strength of the soil, if the fill has a dry density of 94.5 pcf. The data in figure 6-9 is a comparison of the strength and stresses if the

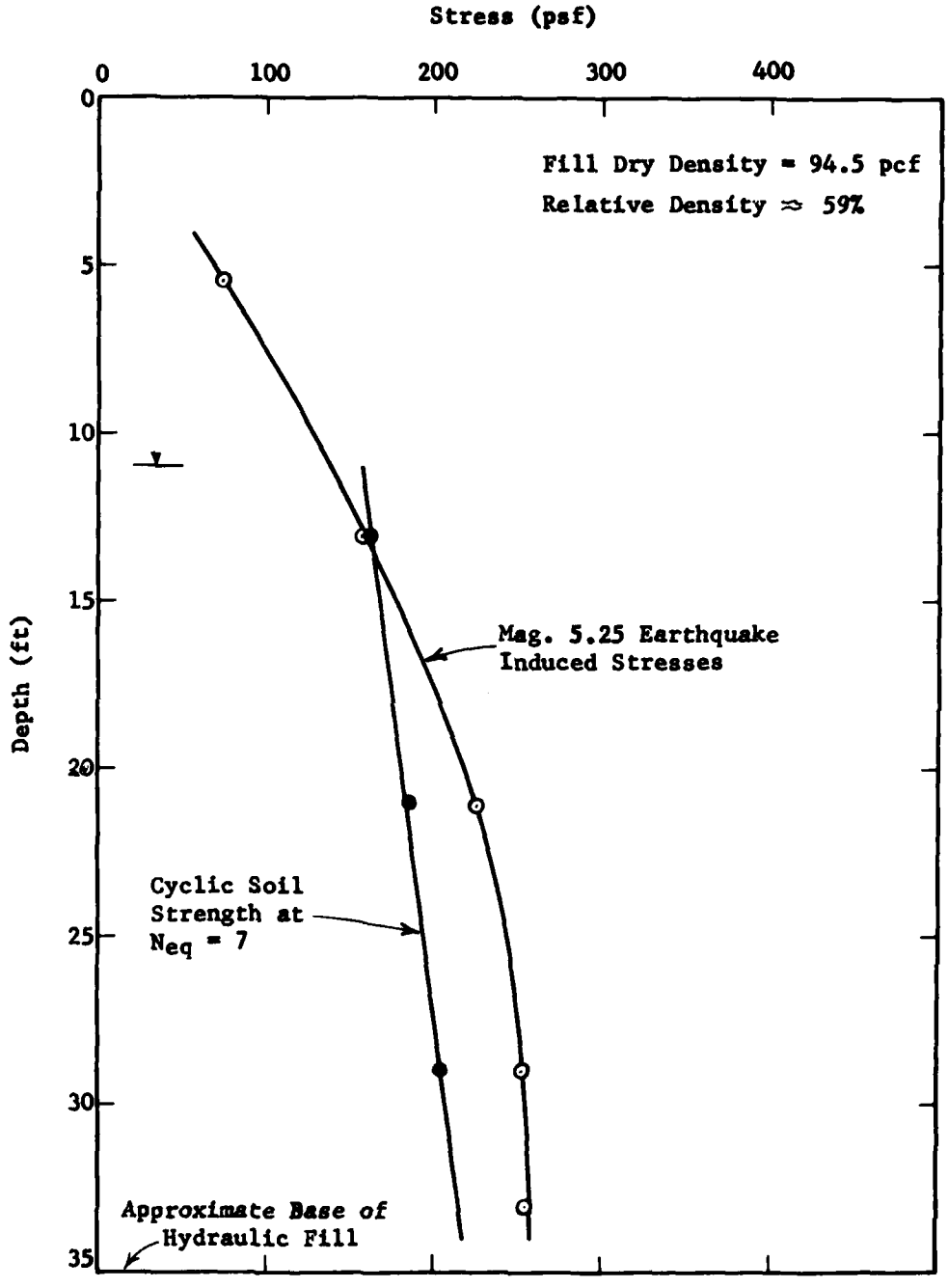

FIG. 6-7 COMPARISON OF CYCLIC SOIL STRENGTH OF SILTY SAND AT A DRY DENSITY OF 94.5 pcf TO THE MAGNITUDE 5.25 EARTHQUAKE INDUCED STRESSES - LOS ANGELES HARBOR

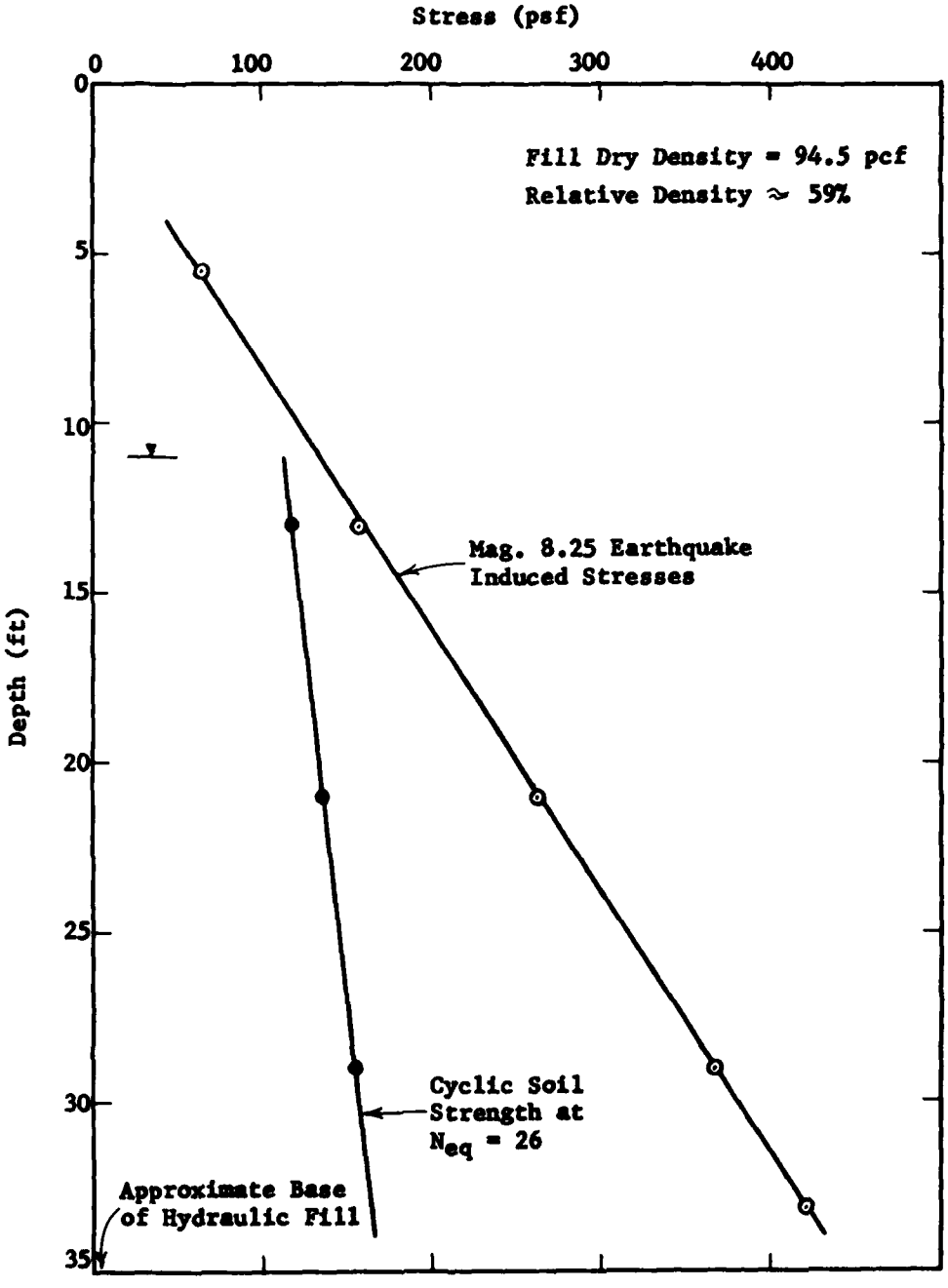

FIG. 6-8 COMPARISON OF THE CYCLIC SOIL STRENGTH OF SILTY SAND AT A DRY DENSITY OF 94.5 pcf TO THE MAGNITUDE 8.25 EARTHQUAKE INDUCED STRESSES - LOS ANGELES HARBOR

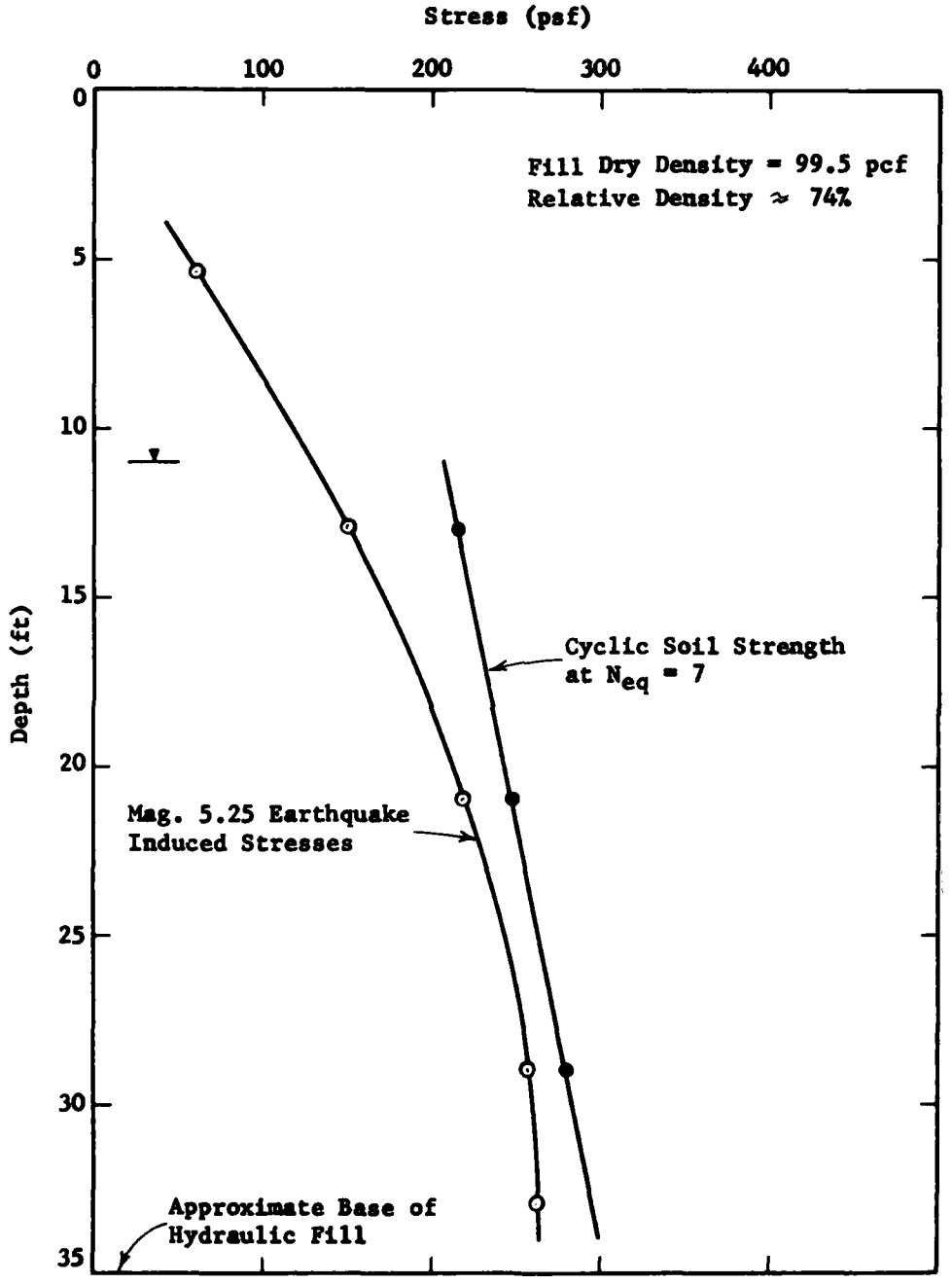

FIG. 6-9 COMPARISON OF THE CYCLIC SOIL STRENGTH OF SILTY SAND AT A DRY DENSITY OF 99.5 pcf TO THE MAGNITUDE 5.25 EARTHQUAKE INDUCED STRESSES - LOS ANGELES HARBOR

proposed fill were constructed at a higher dry density of 99.5 pcf and subjected to the stresses induced by the two earthquake magnitudes. This comparison indicates that the stresses induced by the magnitude 5.25 earthquake are lower than the cyclic shear strength of the soil and the stresses induced by the magnitude 8.25 earthquake are greater than the cyclic shear strength of the soil.

It should be noted that the two probable earthquakes discussed above, give lower accelerations at the site than the maximum probable earthquake (design earthquake) determined in Chapter 4. It would therefore be safe to assume that the stresses induced by the design earthquake would be greater than those of the magnitude 8.25 earthquake and that these stresses would exceed the cyclic strength of the soil.

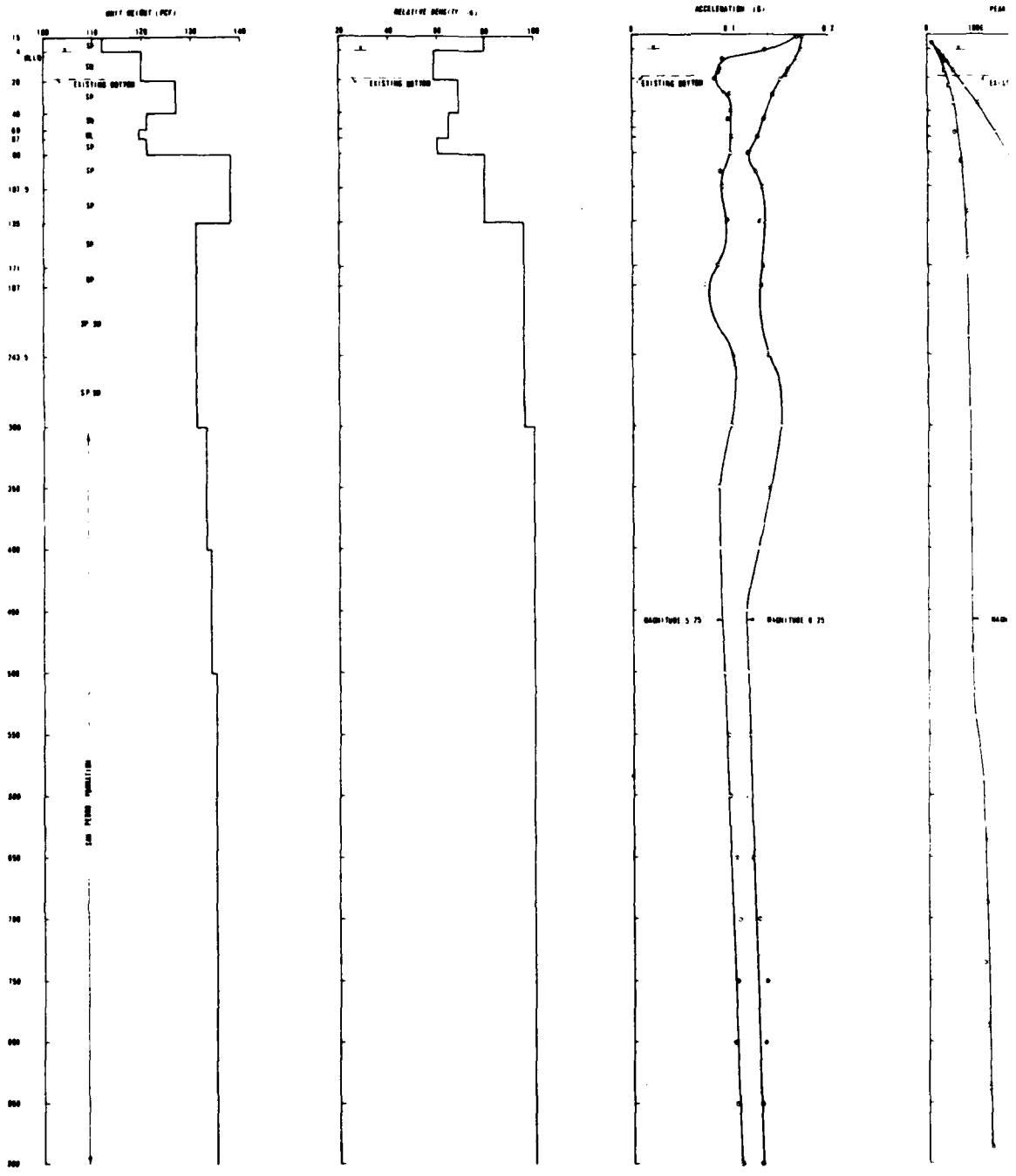

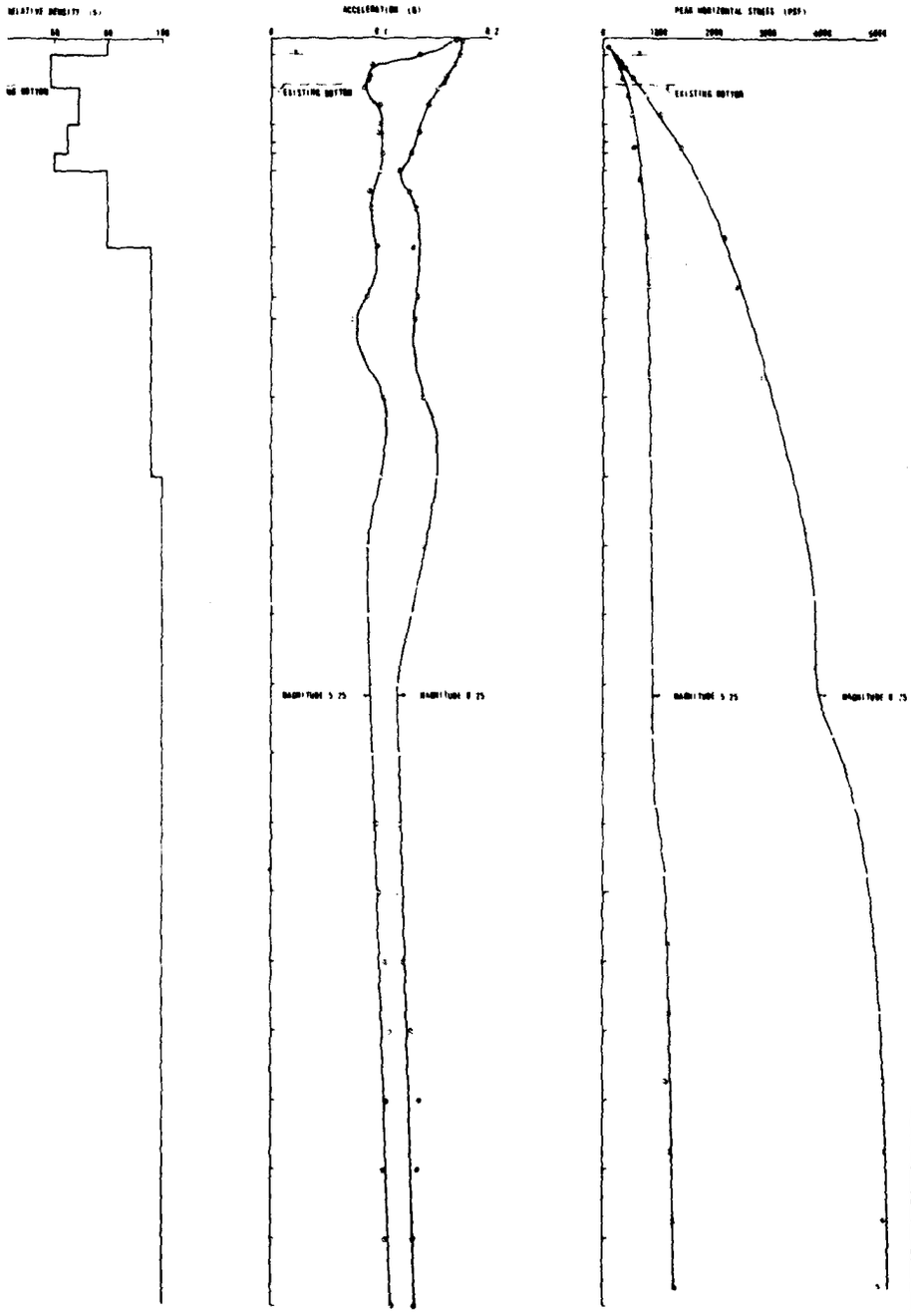

REVISIONS

LOS ANGELES HARBOR

SUBSURFACE RESPONSE
TO EARTHQUAKES OF
RICHTER MAGNITUDE 5.25 AND 8.25

PLATE B-1

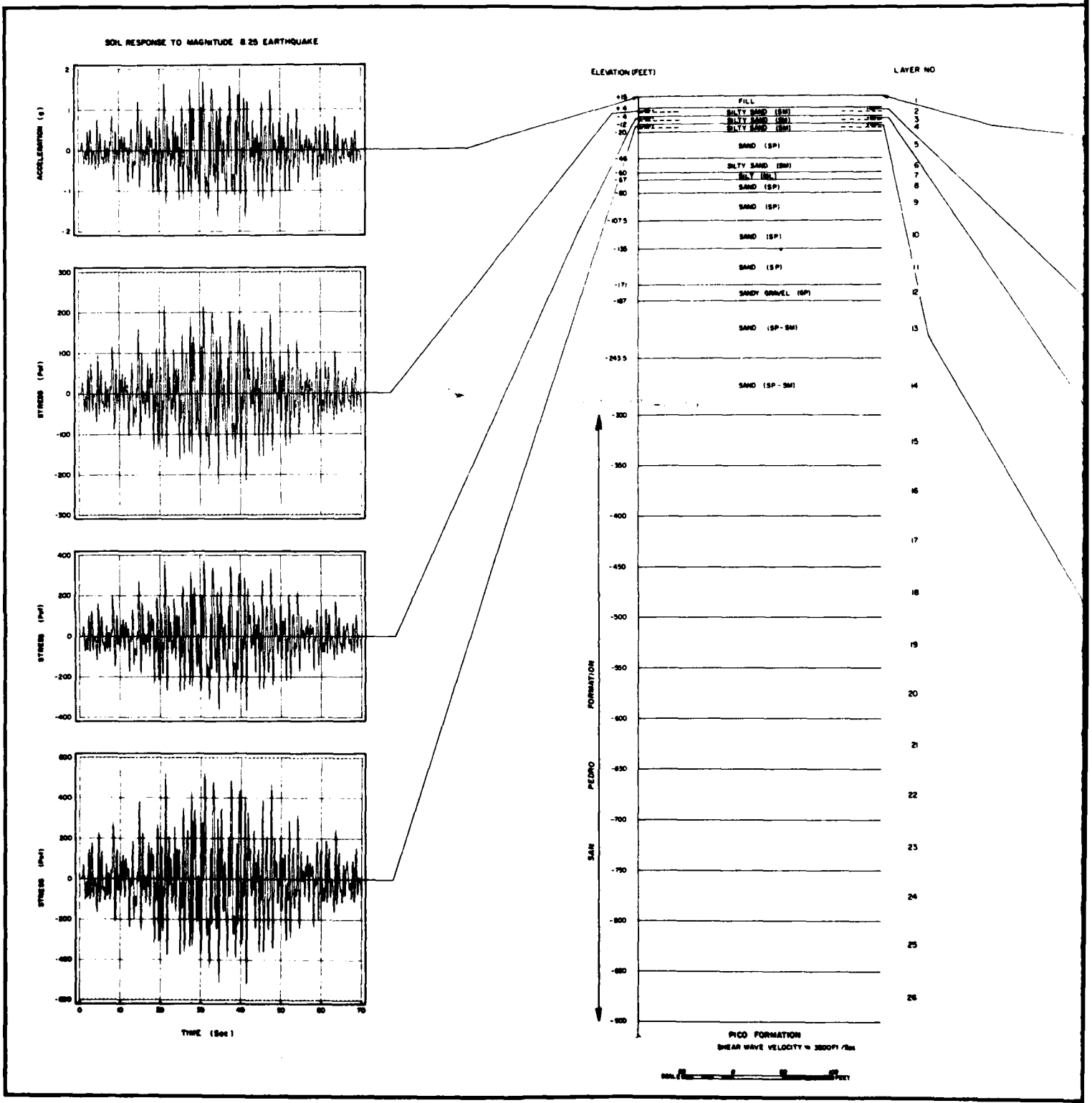
SOIL RESPONSE TO MAGNITUDE 8.25 EARTHQUAKE
ACCELERATION (g)
STRESS (Psf)
STRESS (Psf)
STRESS (Psf)
TIME (Sec)
ELEVATION (FEET)
LAYER NO
FILL
SILTY SAND (SM)
SILTY SAND (SM)
SILTY SAND (SM)
SAND (SP)
SILTY SAND (SM)
SILT (ML)
SAND (SP)
SAND (SP)
SAND (SP)
SAND (SP)
SANDY GRAVEL (GP)
SAND (SP-SM)
SAND (SP-SM)
SAN PEDRO FORMATION
PICO FORMATION
SHEAR WAVE VELOCITY = 3800 FT /Sec

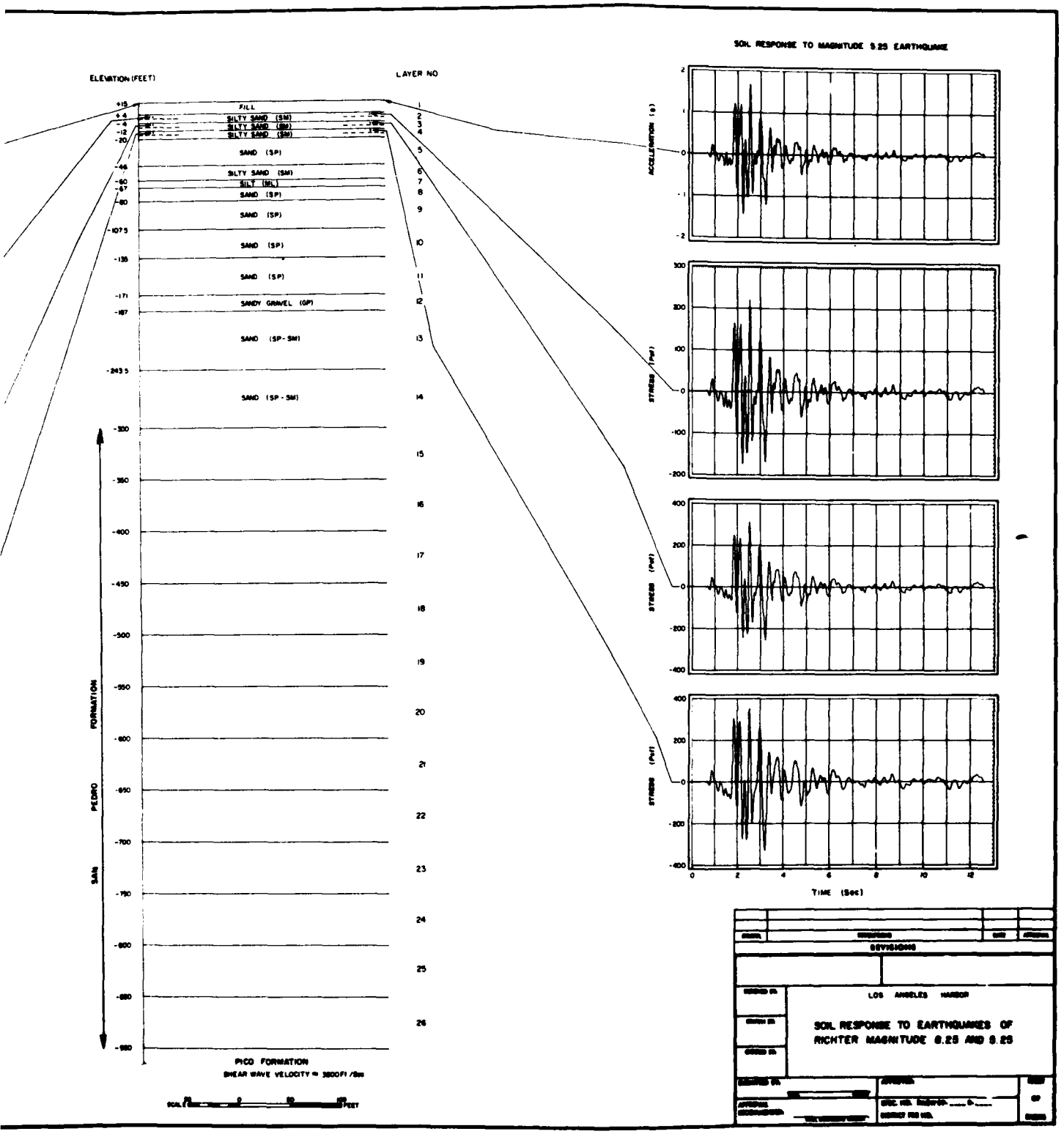
ELEVATION (FEET)
LAYER NO
FILL
SILTY SAND (SM)
SILTY SAND (SM)
SILTY SAND (SM)
SAND (SP)
SILTY SAND (SM)
SILT (ML)
SAND (SP)
SAND (SP)
SAND (SP)
SAND (SP)
SANDY GRAVEL (GP)
SAND (SP-SM)
SAND (SP-SM)
SAN PEDRO FORMATION
PICO FORMATION
SHEAR WAVE VELOCITY = 3800FT/Sec
SOIL RESPONSE TO MAGNITUDE 8.25 EARTHQUAKE
ACCELERATION (g)
STRESS (Psf)
TIME (Sec)
REVISIONS
LOS ANGELES HARBOR
SOIL RESPONSE TO EARTHQUAKES OF RICHTER MAGNITUDE 8.25 AND 8.25

PLATE B-2

2

CHAPTER 7

CONCLUSIONS AND RECOMMENDATIONS

Conclusions

Seismic analyses were conducted on the proposed fill material using two "minor" earthquake motions; a magnitude 5.25 at a distance of 6.5 miles and a magnitude 8.25 at a distance of 52 miles. These seismic events were assumed to occur on the nearest points of the Newport-Inglewood and San Andreas faults, respectively, relative to the Los Angeles Harbor.

The 5.25 magnitude Newport-Inglewood event was determined to have approximately 100 percent probability of occuring within a 100 year design life for the hydraulic fill, and the San Andreas event was assumed to be extremely probable.

A summary of the input base rock acceleration and the computed surface response of the proposed fill is given in table 7-1 for two different fill densities. The dry density of 94.5 pcf corresponds to a relative density of 59 percent and is based on the median dry density value of silty sand data of existing hydraulic fills in the Los Angeles Harbor. The dry density of 99.5 pcf corresponds to a relative density of 74 percent and is used as the median dry density of the proposed fill assuming a construction procedure is developed which produces a fill having a somewhat higher than "typical" density.

TABLE 7-1

Summary of Earthquake Input and Computed Peak Fill Surface Response Motions

Event Location	Richter Magnitude	Dist. to Site (miles)	Max. Rock Accel. (g)	Fill Density (pcf)	Surface Accel. (g)	Surface Vel. (in/sec)	Surface Disp. (in)	Surface Strain (%)
Newport-Inglewood	5.25	6.5	0.11	94.4	0.17	4.06	0.55	0.010
Newport-Inglewood	5.25	6.5	0.11	99.5	0.16	3.95	0.54	0.010
San Andreas	8.25	52.0	0.13	94.5	0.17	16.99	6.75	0.015

The results of laboratory testing and the dynamic analysis revealed that the proposed fill, if constructed in accordance with past procedures, would liquefy under the earthquake motions studied. This instability would constitute a foundation failure for any structure which may be built on the fill.

Should the fill be placed at a higher dry density, approximately 100 pcf, the calculations show that it would be stable if subjected to the motions of the magnitude 5.25 earthquake by a margin of safety of approximately 1.06. However, this higher density material would also liquefy if subjected to the motions of the magnitude 8.25 earthquake.

The maximum probable seismic event, "design earthquake", corresponds to a magnitude 7.0 on the Newport-Inglewood Fault with maximum rock accelerations at the site of approximately 0.5g. This earthquake would cause much more severe shaking at the site than either of the two events studied. Therefore, without further analysis, this maximum probable design earthquake would result in greater stress intensities than those analyzed in this report. These higher stresses would result in liquefaction of the proposed hydraulic fill material at both densities analyzed.

Recommendations

Based on the data collected from various sites throughout the harbor, it is concluded that not only the proposed fill, but also a great many of the existing fills and even some of the natural soil deposits would be highly susceptible to liquefaction, if subjected to strong seismic excitation of the type experienced in the March 10, 1933, Long Beach Earthquake.

Since the Los Angeles-Long Beach Harbor Complex is in a highly seismic region, it is recommended that measures be taken to insure the stability of any new fill and to improve stability or define hazards and risks of existing fills and native materials within the Los Angeles-Long Beach Harbors. These measures should include the following.

a. The main channel and basins should be further investigated by mid-channel drilling in order to substaintiate the soil data presented in this report. The proposed dredge material from these areas should be further tested to determine the effects on strength if the mean gradation were changed by the addition of course grained material.

b. Feasibility of designing and constructing the new fills to withstand the stresses developed by the maximum probable earthquake occuring on the Newport-Inglewood Fault should be investigated.

c. Methods of underwater compaction should be investigated in order to develope an economical and effective construction procedure.

d. An Iso-potential map of liquefaction should be developed for the entire Los Angeles-Long Beach Harbor, delineating areas of high susceptability and risk.

e. Densification procedures should be investigated to determine the feasibility of densifing the existing hydraulic fills and natural soil deposits which exhibit a high susceptability to liquefaction.

BIBLIOGRAPHY

1. Corps of Engineers, "Draft Environmental Statement, Los Angeles-Long Beach Harbors," Office of the Chief of Engineers, Department of the Army, July 1973.

2. Duke, C.M., Johnson, J.A., Kharraz, Y., Campbell, K.W., Malpiede, N.A., "Subsurface Site Conditions and Geology in the San Fernando Earthquake Area." UCLA-ENG-7206, December 1971.

3. United Geophysical Corporation, "A Reflection Seismograph Survey for the City of Los Angeles Harbor Department," Phase I. April 1963.

4. Ivanhoe, L.F., "Geological and Geophysical Interpretation For The Board of Harbor Commissioners", June 1963.

5. Yerkes, Others, "Geology of the Los Angeles Basin, California, Introduction," Geological Survey Professional Paper 420-A, 1965.

6. Sanglerat, G., "The Penetrometer and Soil Exploration," Elsevier Publishing Company, Amsterdam London, New York, 1972.

7. De Mello, V.F.B., "The Standard Penetration Test," Proceedings of the Fourth Panamerican Conference on Soil Mechanics and Foundation Engineering, Volume 1, June 1971.

8. Seed, H.B., and Peacock, W.H., "Precedures for Measuring Soil Liquefaction Characteristics," JSMFD, ASCE, Volume 97, No. SM8, August 1971, pp 1099-1119.

9. Seed, H.B., and Lee, K.L., "Lieuefaction of Saturated Sand During Cyclic Loading," JSMFD, ASCE, Volume 91, No. SM6, November 1966, pp 105-134.

10. Lee, K.L., and Seed, H.B., "Cyclic Stress Conditions Causing Liquefaction of Sand," JSMFD, ASCE, Volume 93, No. SM1, January 1967, pp 57-70.

11. Duke, C.M., Leeds, D.J., "Site Characteristics of Southern California Strong, Motion Earthquake Stations." Report No. 62-55, University of California, Los Angeles, November 1962.

12. Faust, L.Y., "Seismic Velocity as a Funitions of Depth on Geologic Times." Geophysic, 16, 192-206, April 1951.

13. Lastrico, R.M., "Effects of Site and Propagation Path on Recorded Strong Earthquake Motions." Ph.D. Thesis, in Engineering, School of Engineering and Applied Science, University of California, December 1970.

14. Seed, H.B., Idriss, I.M., Kiefer, F.W., "Characteristics of Rock Motions During Earthquakes," JSMFD, ASCE, SM5, September 1969.

15. Schnabel, P.B., Seed, H.B., "Accelerations in Rock for Earthquakes in the Western United States." Report No. 72-2, Earthquake Engineering Research Center, University of California, Berkeley, June 1972.

16. Bennioff, H., 1938, "The Determination of the Extent of Faulting with Application to the Long Beach Earthquake"; Seismological Society of America. Bulletin, Volume 28, pp 77-84.

17. Eaton, J.E., 1933, "Long Beach California Earthquake of March 10, 1933"; Amer. Assoc. of Petroleum Geologists Bull., Volume 17, pp 732-738.

18. Envicom Corp. "Seismic Safety Element, Comprehensive General Plan, City of Torrance. April 1973.

19. Heck, N.H., and Bodle, R.R., "United States Earthquakes, 1928-1934", U.S. Coast and Geodetic Survey, U.S. Government Printing Office, Washington, 1930.

20. Iacopi, R., "Earthquake County", Lane Books, Menlo Park, California.

21. Allen, C.R., Amand, P.St., Richter, C.F., and Nordquest, J.M., 1965, "Relationship Between Seismicity and Geologic Structure in Southern California Region"; Seismological Society of America. Bulletin., Volume 55, pp 753-797.

22. Seed, H.B., Idriss, I.M., "Influence of Soil Conditions on Ground Motions During Earthquake." JSMFD, ASCE, SM1, Janaury 1969.

23. Idriss, I.M., Seed, H.B., "Seismic Response of Horizontal Soil Layers", JSMFD, ASCE, SM4, July 1968.

24. Seed, H.B., Idriss, I.M., "Soil Moduli and Damping Factors for Dynamic Response Analysis," Report No 70-10, Earthquake Engineering Research Center, University of California, Berkeley, December 1970.

25. Lee, K.L., and Chan, K., "Number of Equivalent Significant Cycles in Strong Motion Earthquakes," Proc. International Conf. on Microzonation, Seattle, Washington, Volume II, October 1972, pp 609-627.

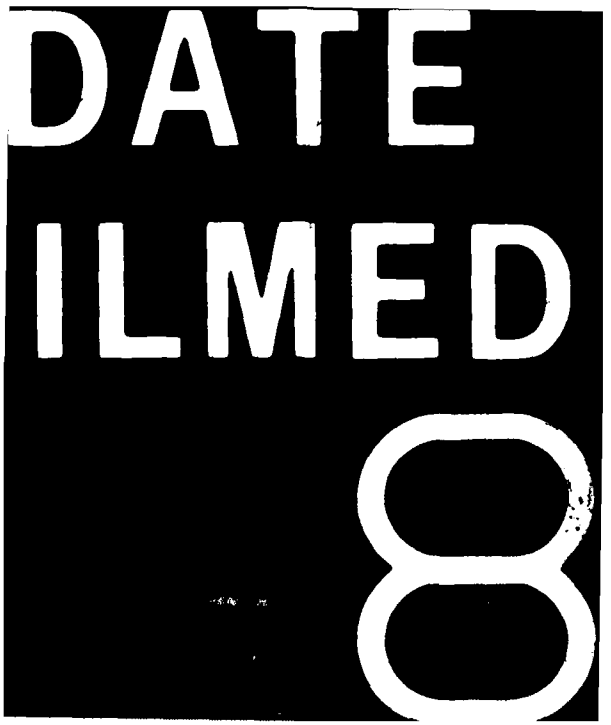
DATE
ILMED
8